

Binuclear Phthalocyanines:
Synthesis, Characterisation and Optical Limiting Properties

Binukleare Phthalocyanine:
Synthese, Charakterisierung und Optical Limiting Eigenschaften

Dissertation

der Fakultät für Chemie und Pharmazie
der Eberhard-Karls-Universität Tübingen

zur Erlangung des Grades eines Doktors
der Naturwissenschaften

2004

vorgelegt von

Mário Calvete

Tag der mündlichen Prüfung: 22. Januar 2004

Dekan: Prof. Dr. H. Probst

1. Berichterstatter: Prof. Dr. h. c. M. Hanack

2. Berichterstatter: Prof. Dr. G. Häfeling

Die vorliegende Arbeit wurde am Institut für Organische Chemie der Eberhard-Karls-Universität Tübingen unter der Anleitung von Prof. Dr. Dr. h. c. M. Hanack durchgeführt, dem ich für seine Unterstützung und sein Interesse herzlich danke.

Für meine Eltern, immer.

Index

I General part	9
1. Introduction	10
2. Phthalocyanines and related macrocycles	10
2.1 Historical parenthesis	10
2.2 Absorption spectra of phthalocyanines	11
2.3 General synthesis of phthalocyanines	12
2.4 Solubilization of phthalocyanines	13
2.5 Expansion of the π -system: benzoannulated phthalocyanines	15
3. Optical limiting: A nonlinear optical effect	17
3.1 Nonlinearity of the Optical Limiting Effect	18
3.2 Optical limiting: mechanisms and models	20
3.3. Phthalocyanines and optical limiting	21
3.4. Naphthalocyanines and optical limiting	27
3.5. Z-scan technique	28
3.5.1. Some examples	29
II Aim of the work	32
III - Results and discussion	34
1. Synthesis of binuclear phthalocyanines	34
1.1. Synthesis of [2,3,9,10,16,17-hexa-2-ethylhexyloxy-25,26- dicyano] phthalocyaninato nickel 11	39
1.1.1. Synthesis and spectroscopic characterization of phthalocyanine 4	40
1.1.2. Synthesis and spectroscopic characterization of phthalocyanine 9	41
1.1.3. Synthesis and spectroscopic characterization of phthalocyanine 10	41
1.1.4. Synthesis and spectroscopic characterization of phthalocyanine 11	42
1.2. Ni/Ni binuclear metal-phthalocyanines 12 and 13	42
1.2.1. Synthesis and spectroscopic characterization of binuclear phthalocyanines 12 and 13	42
1.3. Compounds (14 and 15) - Ni/Cu binuclear metal-phthalocyanines	47
1.3.1. Synthesis and spectroscopic characterization of binuclear phthalocyanines 14 and 15	47
1.3.1.1. Atomic Absorption Spectroscopy - a simple and effective method for qualitative and quantitative determination of metals	48
2. Binuclear metal phthalocyanines for optical limiting purposes	51
2.1. Synthesis of an unsymmetric functionalized magnesium phthalocyanine [2,3,9, 10,16,17-hexa-2-ethylhexyloxy-25,26-dicyano] magnesium phthalocyanine 19	52
2.1.1. Synthesis and spectroscopic characterization of phthalocyanine 16	53
2.1.2. Synthesis and spectroscopic characterization of phthalocyanine 17	54
2.1.3. Synthesis and spectroscopic characterization of phthalocyanine 18	55
2.1.4. Synthesis and spectroscopic characterization of phthalocyanine 19	55
2.2. Binuclear metal phthalocyanines with InCl and GaCl as central moieties	56
2.2.1. Synthesis of binuclear phthalocyanines 20-23	56
2.2.2. Spectroscopic characterization of binuclear phthalocyanines 20-23	58
3. Synthesis of octaalkoxy substituted Ga, In and Tl Pc's	62
3.1. Isolation and spectroscopic characterization of Mg phthalocyanine 24	63
3.2. Synthesis and spectroscopic characterization of metal free phthalocyanine 25	63
3.3. Indium (26), gallium (27) and thallium (28) octasubstituted Pc's	64
3.3.1. Synthesis and spectroscopic characterization of phthalocyanines 26 and 27	64

3.3.2. Synthesis and spectroscopic characterization of phthalocyanine 28	66
4. Optical limiting measurements for the In/In binuclear Pc 22	68
IV - SUMMARY	72
V - EXPERIMENTAL PART	75
1. General comments	75
2. Synthesis	76
2.1. Synthesis of precursors	76
2.1.1. 4,5-bis(2-ethyl-hexyloxy)-1,2-phthalonitrile 1	76
2.1.1.1 1,2-bis(2-ethyl-hexyloxy)benzene	76
2.1.1.2 1,2-dibromo-4,5-bis(2-ethyl-hexyloxy)benzene	77
2.1.1.3 4,5-Bis(ethylhexyloxy)-1,2-phthalonitrile 1	78
2.1.2. 1,4-Epoxy-1,4-dihydronaphthalene-6,7-nitrile 2	78
2.1.2.1 6,7-dibromo-1,4-epoxy-1,4-dihydronaphthalene	78
2.1.2.2. 1,4-Epoxy-1,4-dihydronaphthalene-6,7-nitrile 2	79
2.2. Synthesis of the benzoannulated unsymmetrically substituted nickel phthalocyanine 11	80
2.2.1. [2,3,9,10,16,17-hexa(2-ethylhexyloxy)-23,26 - dehydro-23,26-epoxybenzo-phthalocyaninato]nickel (4)	80
2.2.2. [2,3,9,10,16,17-hexa(2-ethylhexyloxy)-23,26-dihydro-23,26-epoxybenzo-24,25-tetracyclone-phthalocyaninato]nickel adduct 9	81
2.2.3. [2,3,9,10,16,17-hexa(2-ethylhexyloxy)-23,26-dihydro-23,26-epoxybenzo-25,26-fumaronitrile-phthalocyaninato]nickel adduct 10	82
2.2.4. [2,3,9,10,16,17-hexa(2-ethylhexyloxy)-25,26-dicyano-phthalocyaninato] nickel (11)	82
2.3. Synthesis of the Ni/Ni and Ni/Cu binuclear metal-phthalocyanines	83
2.3.1. Unsymmetrically substituted Ni/Ni binuclear metal-phthalocyanine 12	83
2.3.2. Symmetrically substituted Ni/Ni binuclear metal-phthalocyanine 13	84
2.3.3. Unsymmetrically substituted Ni/Cu binuclear metal-phthalocyanine 14	85
2.3.4. Symmetrically substituted Ni/Cu binuclear metal-phthalocyanine 15	86
2.4. Synthesis of the benzoannulated unsymmetrically substituted magnesium phthalocyanine 19	88
2.4.1. [2,3,9,10,16,17-hexa(2-ethylhexyloxy)-23,26-dihydro-23,26-epoxybenzo-phthalocyaninato]magnesium (16)	88
2.4.2. [2,3,9,10,16,17-hexa(2-ethylhexyloxy)-23,26-dihydro-23,26-epoxybenzo-24,25-tetracyclone-phthalocyaninato]magnesium adduct 17	89
2.4.3. [2,3,9,10,16,17-hexa(2-ethylhexyloxy)-23,26-dihydro-23,26-epoxybenzo-25,26-fumaronitrile-phthalocyaninato]magnesium adduct 18	90
2.4.4. [2,3,9,10,16,17-hexa(2-ethylhexyloxy)-25,26-dicyano-phthalocyaninato] magnesium 19	90
2.4.5. Binuclear Mg/Mg phthalocyanine 20	91
2.4.6. Binuclear Mg/Mg phthalocyanine 21	92
2.4.7. Binuclear Mg/Mg phthalocyanine 22	93
2.4.8. Binuclear Mg/Mg phthalocyanine 23	94
2.5. Synthesis of octa-substituted In, Ga and Tl phthalocyanines	95
2.5.1. [2,3,9,10,16,17,24,25 - octa - (2-ethylhexyloxy)] magnesium phthalocyanine (24)	95
2.5.2. [2,3,9,10,16,17,24,25]-octa-(2-ethylhexyloxy)phthalocyanine (25)	96
2.5.3. [2,3,9,10,16,17,24,25-octa-(2-ethylhexyloxy)] In (III) phthalocyanine-chloride (26)	97
2.5.4. [2,3,9,10,16,17,24,25-octa-(2-ethylhexyloxy)] Ga (III) phthalocyanine-chloride (27)	98

2.5.5. [2,3,9,10,16,17,24,25-octa-(2-ethylhexyloxy)] Tl (III) phthalocyanine- chloride (28)	99
VI - LITERATURE	100

Abbreviations:

δ	chemical shift
λ	wavelength
br	broad
cm	centimeter
°C	Degree Celsius
C	Coulomb
CH ₂ Cl ₂	dichloromethane
CDCl ₃	chloroform
DBU	1,8-diazabicyclo[5.4.0]-undec-7-ene
DCM	dichloromethane
DMF	<i>N,N</i> -dimethylformamide
E.I.	Electron Ionisation
ESA	Excited State Absorption
F	Faraday
FAB	Fast Atom Bombardement
FD	Field Desorption
HOMO	Highest Occupied Molecular Orbital
IR	Infra Red
LUMO	Lowest Unoccupied Molecular Orbital
m	meter
MS	Mass spectroscopy
NLO	Non linear optics
NMR	Nuclear Magnetic Resonance
OL	Optical Limiting
Pc	Phthalocyanine
ppm	parts per million
Nc	Naphthalocyanine
RSA	Revere Saturable Absorption
Tetracyclone	tetraphenylcyclopentadien-1-one
THF	Tetrahydrofurane
THF-d ₈	octa deuterated tetrahydrofurane
TLC	Thin layer chromatography
UV/Vis	Ultra-violet/Visible
V	Volt

1. Introduction

In the area of materials chemistry, the growth of interest in using all-optical, electro-optical and opto-mechanical devices in modern technology has been very high, especially in the last few years. For example, the substitution of electronic by optical devices in communication technology, showed to be an impressive accelerator for proceeding, transport and storage of data. Manipulation of amplitude, polarization, direction or phase of the optical beam is of unique significance. In order to carry out these manipulations, an understanding of the nonlinear optical phenomena is essential.

The structural prerequisite for the verification of NLO phenomena^[1] in organic compounds is the presence of a network of delocalized π -conjugated electrons, which infer high polarizability and fast charge redistribution when the conjugated molecule interacts with rapidly variable intense electromagnetic fields like those of laser radiations.^[2] Among the conjugated organic molecules possessing NLO properties, the class of phthalocyanines (Pc's) and related species like naphthalocyanines, occupy a prominent position due to their high thermal and chemical stability and the ease of preparation and purification.^[3]

Phthalocyanines offer great structural flexibility, and can host ~ 70 different elements in the central phthalocyanine cavity. Moreover a large range of peripheral substituents of phthalocyanines is known, which were introduced in order to improve the poor solubility of unsubstituted phthalocyanine.

Several mechanisms can give rise to NLO response. NLO properties of phthalocyanines are of great interest, since these compounds combine several physical and chemical properties favourable for the development of effective optics devices into a single compound.^[4] The intention of developing optical limiting (which will be discussed later) devices for eye and sensor protection from aggressive energetic light pulses motivated researchers in the quest of better materials for this purpose.^[5,6] Pc's show optical limiting (OL) effect through the mechanism of excited state absorption (ESA). This means the OL effect generated by Pcs is an accumulative nonlinearity because it is produced through the polarization of the electronic ground state and the successive absorption from this polarized state as determined by the intensity of the applied electric field.^[7]

The following paragraphs will demonstrate the potential of phthalocyanines in the field of materials science, and specially for optical limiting applications.

2. Phthalocyanines and related macrocycles

Phthalocyanines are widely used as pigments in textiles, polymers and paints.^[8] They exhibit remarkable qualities like lightfastness, brightness and stability towards environmental influences. Pc's consist of a planar macrocycle with an 18 π -electron system, which mainly confers this known stability. For many years, these macrocycles have been the target of meticulous investigation,^[3,8] particularly considering their properties as dyes.^[9,10] In recent times, research has been retargeted for applications in materials science,^[11-15] including, phthalocyanines as liquid crystals,^[16-18] as Langmuir-Blodgett films,^[19-23] as molecular semi-conductors,^[24] in electrophotographic applications,^[25-28] in optical-data storage,^[29-31] in cancer therapy,^[32-34] in fuel cells,^[35] in photoelectrochemical cells,^[36] in photovoltaic cells,^[37] in gas-sensing devices,^[38-45] as organic semi-conductors,^[11-13,46,47] as photosensitizers,^[48] and in nonlinear optics.^[4,49,50] Phthalocyanines do not occur in nature, but they are structurally related to porphyrins such as haemoglobin, vitamin B₁₂ and chlorophyll (see Figure 1).

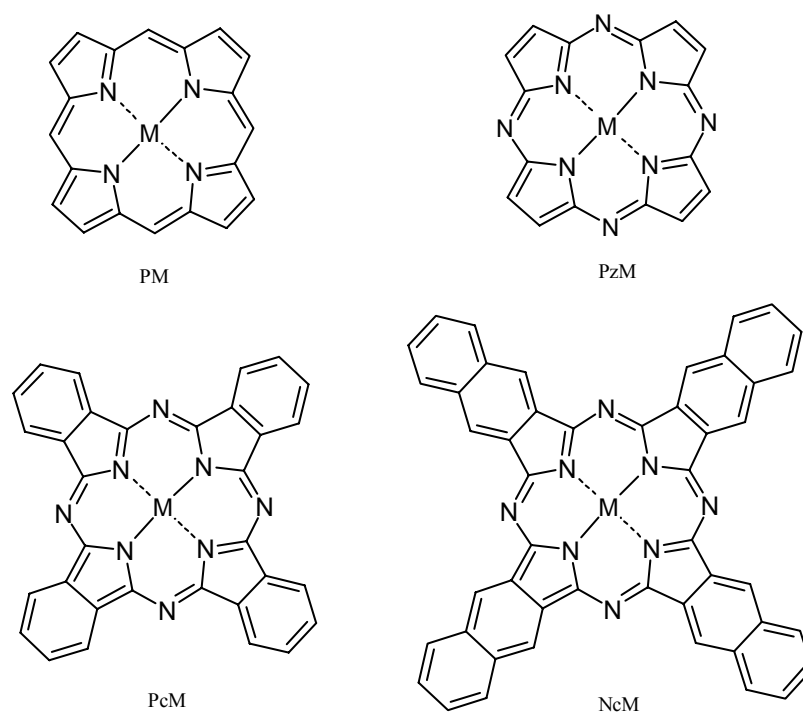


Figure 1: Porphyrine (PM), porphyrazine (PzM), phthalocyanine (Pc) and naphthalocyanine (Nc) complexes

2.1 Historical parenthesis

A metal-free phthalocyanine was found for the first time in 1907 as by-product during the preparation of 2-cyanobenzamide.^[51] However, not much importance was given to the discovery at that time. Later, in 1927, a copper phthalocyanine was prepared in 23% yield by reacting 1,2-dibromobenzene with copper(I) cyanide in pyridine.^[52] The structure of this substance was investigated meticulously by Linstead. He was the first to use the term phthalocyanine,^[53] deriving the name from the Greek words *naphtha* (rock oil) and *cyanine* (blue). In the subsequent years he elucidated the structure of phthalocyanines as well as procedures for obtaining several metal phthalocyanines and the metal free Pc's.^[54-62]

As mentioned before, nowadays, phthalocyanines have numerous applications. This extensive use of phthalocyanines is due to their remarkable structural flexibility.^[63] The coordination number of the square-planar phthalocyanine is four, and therefore many of the metals, having higher coordination numbers, can bond with a variety of axial ligands.^[3]

2.2 Absorption spectra of phthalocyanines

Purity and intensity of phthalocyanine's colour arises from an isolated and intense band (Q-band) at the red end of the visible spectrum of light, between 650 and 720 nm approximately. A second band (B-Band) appears between 300 and 400 nm, being generally less intense (Figure 2). In the spectra of metal phthalocyanine solutions, the intense Q-band arises from a doubly degenerate π - π^* -transition between the A_{1g} (a_{1u}^2) ground state to the first excited singlet state, which has E_u ($a_{1u}^1 e_g^1$) symmetry. The second allowed π - π^* -transition (B-band) is caused by a transition between either an a_{2u} or a b_{2u} orbital to the e_g orbital (LUMO).^[64]

In the case of metal free phthalocyanines all states are non-degenerated, due to the reduced D_{2h} molecular symmetry. The Q-band transition is polarized in either the x or y direction, and is therefore splitted in two bands.^[5]

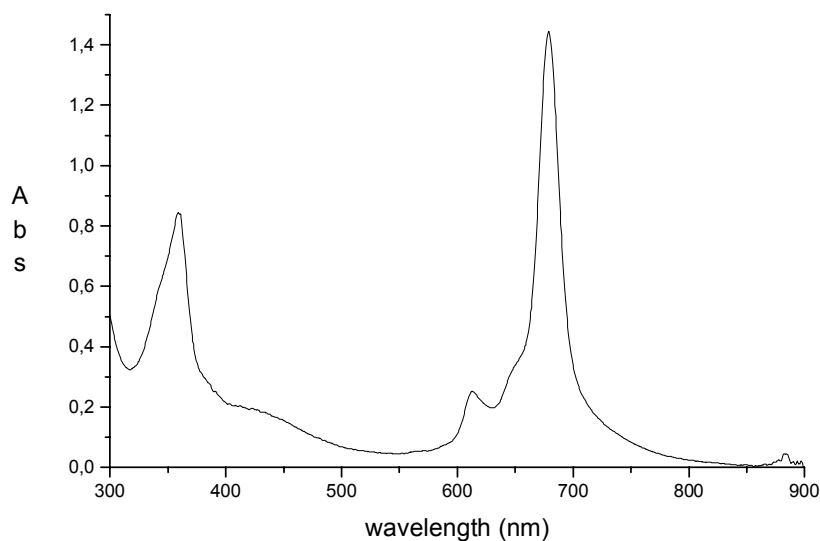


Figure 2: UV/Vis spectra of $(RO)_8PcMg$ (R = 2-ethylhexyl)

Additional bands, which appear in the spectra of certain molecules can be assigned to metal-ligand or ligand-metal charge transfer or even to exciton coupling between the π -systems of dimeric complexes.^[3]

2.3 General synthesis of phthalocyanines

In general, the synthesis of phthalocyanines proceeds from a single step reaction, normally denominated cyclotetramerization of benzoic acid or its derivatives, e.g. phthalic anhydride, phthalimide, *o*-cyanobenzamide, phthalonitrile or isoindolinediimine^[3,65] (see Figure 3).

The most used precursor for substituted phthalocyanine synthesis is the substituted phthalonitrile, or in some cases, when the low reactivity of the precursor inhibits the macrocycle formation, isoindolinediimines can be used as well. Nucleophilic hindered bases like 1,8-diazabicyclo-[5,4,0]-undec-7-ene (DBU) can be used as powerful catalysts for the cyclotetramerization of phthalonitriles in solution (e.g. pentanol, octanol), with the metal ion as template for the formation of metal phthalocyanines.^[3]

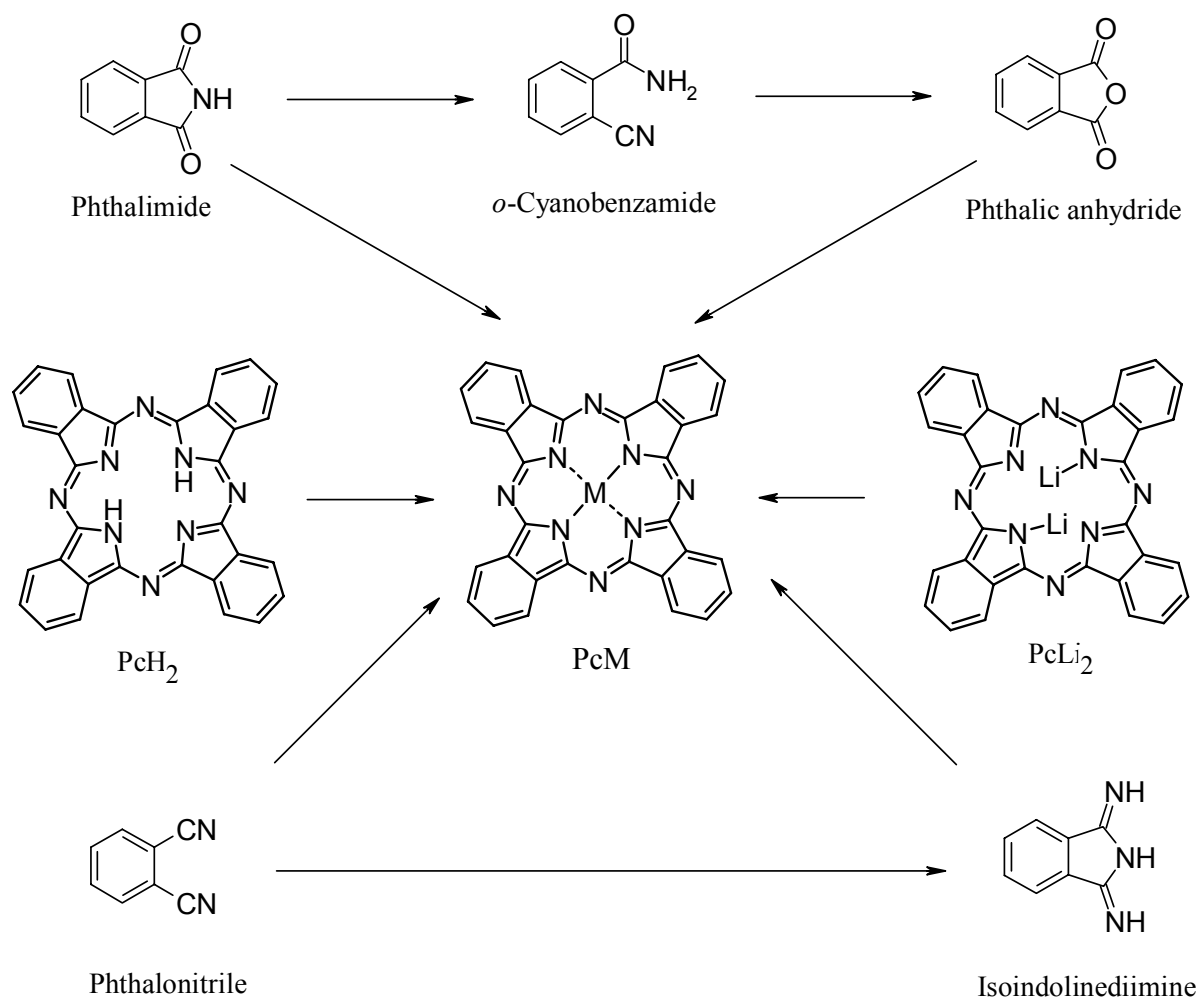


Figure 3: Phthalocyanine synthesis scheme

2.4 Solubilization of phthalocyanines

The solubility of phthalocyanines in common organic solvents can be increased by introduction of bulky or long chain substituents in the periphery of macrocycle (peripheral substitution) and/or, in case of possibility, by coordination of the central metal with additional axial ligands (axial substitution).^[66-68] Depending on the position of the substituents in the precursor, different structural isomers are formed during the preparation of phthalocyanines. Asymmetric precursors, like 3-, 4-, 3,4-, 3,5- substituted phthalonitriles, form a mixture of structural isomers during the tetracyclomerization. As an example, the four isomers of 2,(3)-tetrasubstituted phthalocyanine are shown in Figure 4. The single isomers are (C_{4h}) 2,9,16,23-, (D_{2h}) 2,10,16,24-, (C_{2v}) 2,9,17,24- and (C_s) 2,9,16,24- tetrasubstituted complexes.

Symmetrically disubstituted precursors, due to their location, form either the 2,3,9,10,16,17,23,24-^[69] or the 1,4,8,11,15,18,22,25-^[3] octasubstituted phthalocyanines

(Figure 5). Also the 1,2,3,4,8,9,10,11,15,16,17,18,22,23,24,25-hexadecasubstituted have been prepared.^[70]

Substituents enable phthalocyanine solvation because they increase the distance between the stacked molecules.^[3,11] The peripherally substituted phthalocyanines studied in more detail are the tetra- and octa- substituted ones.^[11] Generally, the solubility of tetra-substituted phthalocyanines is higher than the octasubstituted analogues, mainly due to the fact that the tetrasubstituted phthalocyanines are prepared as a mixture of isomers (see Figure 4), and therefore, leading to a lower degree of order in the solid state, when compared to the symmetrically octasubstituted phthalocyanines.

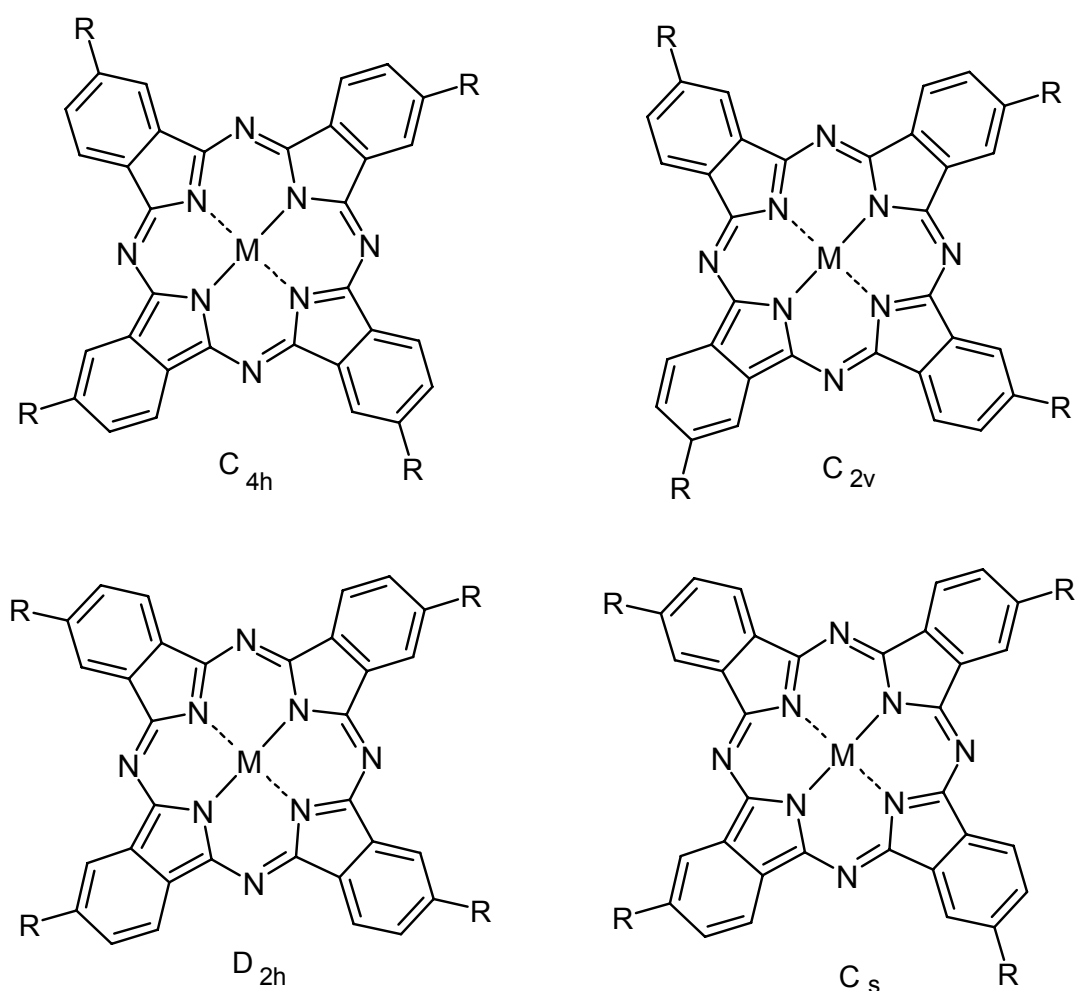


Figure 4: Constitutional isomers from 2,(3)-tetrasubstituted phthalocyanines

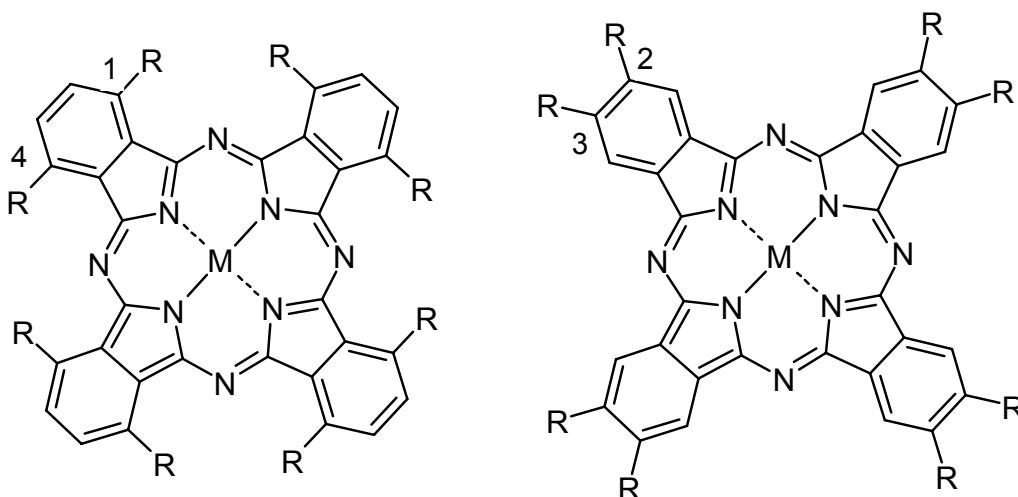


Figure 5: 1,4- and 2,3- octasubstituted phthalocyanines

Furthermore, the less symmetrical isomers have a higher dipole moment derived from the more unsymmetrical arrangement of the substituents in the periphery of the macrocycle. This was proven by Hanack *et al.* after complete separation of the four structural isomers for the first time.^[71-73]

2.5 Expansion of the π -system: benzoannulated phthalocyanines

Preparation of benzoannulated phthalocyanines such as 1,2-naphthalocyanine (Nc), 2,3-naphthalocyanine, anthracenocyanine (Ac) or 9,10 phenanthrenocyanine (Phc), from the corresponding benzoannulated phthalonitriles, is carried out under similar conditions to those of general phthalocyanine synthesis (Figure 6).

The characteristic properties of these complexes are mainly due to their extended π -electron systems. In the electronic absorption spectra going from 2,3-naphthalocyanine to 2,3-anthracenocyanine, an increasing bathochromic shift of the Q-band compared to phthalocyanines is observed.^[74] The HOMO-LUMO energy gap generally decreases in systems with larger π -electron delocalization. This increasingly larger π -electron system enhances intermolecular π - π interactions, favouring stronger aggregation and lower solubility.^[75]

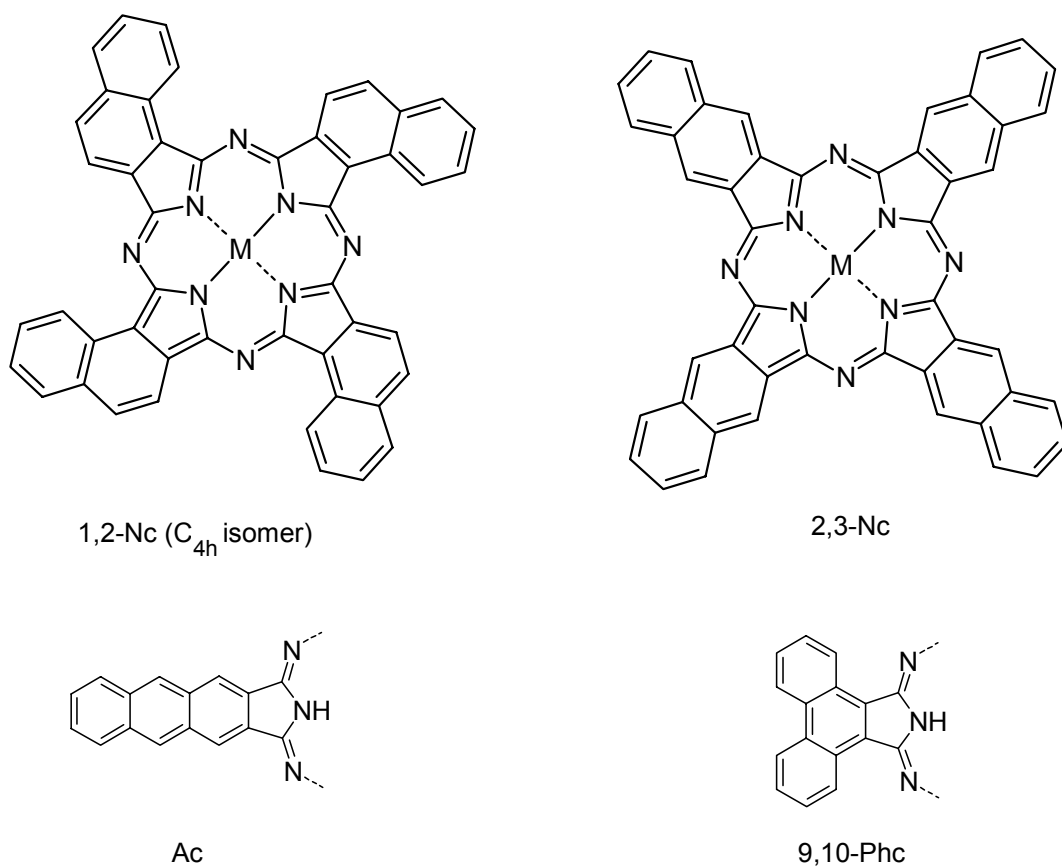


Figure 6: Benzoannulated phthalocyanines

Electronically, 1,2-naphthalocyanines are similar to phthalocyanines. There is only a small bathochromic shift of the Q-band.^[76] Angular annulation of the benzo moieties has a smaller effect on the HOMO-LUMO energy gap than the linear annulation^[75,76] (Figure 7).

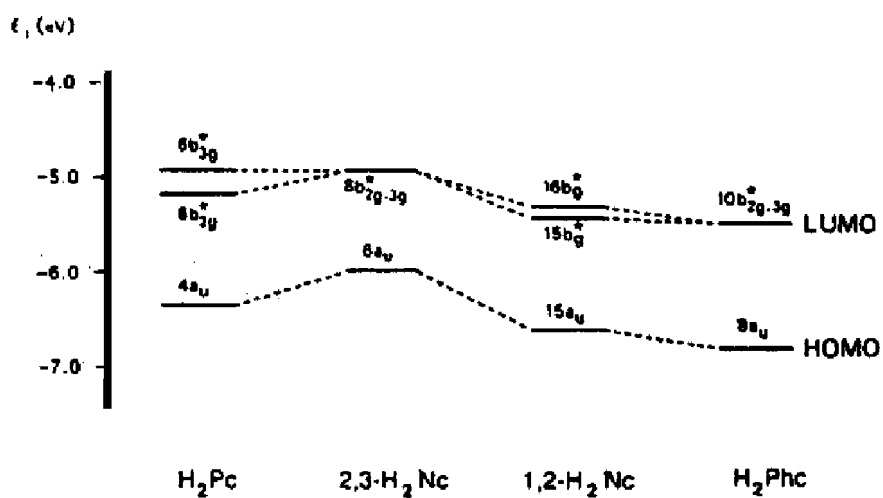


Figure 7: HOMO-LUMO energy gap between H_2Pc , $2,3-H_2Nc$, $1,2-H_2Nc$ and H_2Phc

3. Optical limiting: A nonlinear optical effect

Some special materials have the particular property of changing reversibly their optical properties with the variation of the radiation intensity I during their irradiation with intense light-sources. These effects are verified when I reaches a material-specific critical value (here denoted as I_{lim}), at which the material undergoes a physical and/or chemical transition leading to the reversible modification of the optical properties of the material itself.^[78] In general, light intensity modifies the absorptive, refractive and scattering properties of the illuminated system once $I > I_{lim}$. In the case of molecular species, the extinction coefficient k can vary with the intensity I according to a relationship:

$$k = k_0 [1/ 1+(I/I_{lim})] \quad (1)$$

with k_0 corresponding to the low intensity limit value of k . Equation (1) describes the optical behaviour of a saturable absorber and expresses the fact that the extinction coefficient k decreases with the increase of the incident intensity. In doing so, the optical system gets more transparent at higher incident intensities, and behaves like an intensity-activated optical switch. On the other hand, in the case of optical limiting (OL) systems the opposite situation is verified, i.e. the optical system has an extinction coefficient which increases reversibly with the augmentation of the incident radiation intensity.^[79,80] This phenomenon constitutes the so-called reverse saturable absorption (RSA), and takes mostly place with the irradiation of organic dyes, donor-acceptor molecules, fullerenes and, in less extent, inorganic semiconductors. The OL effect can be produced also by means of several other mechanisms based on fundamental optical processes different to absorption, e.g. refraction and/or scattering. In fact, OL effect based on radiation diffraction or scattering does not allow the formation of a well-resolved image once the incident light rays have interacted with the optical limiter system. As a consequence, optical limiters based on phenomena other than absorption have the practical limitation of not being useful for the protection of those complex light-sensitive elements, e.g. the eye, employed in direct viewing operations which require a clear vision of the surrounding environment. For this reason among the available systems for the limiting of intense radiations, those based upon the phenomenon of absorption are preferable.

3.1 Nonlinearity of the Optical Limiting Effect

In the practice, the occurrence of the OL effect is verified when a constant output intensity I_{out} (in $J\ cm^{-2}\ s^{-1}$) is transmitted through the limiter once the incident intensity I_{in} exceeds the system-characteristic threshold value I_{lim} . This means that no matter of how many photons per unit of time will impinge the system, the flux of photons passing through the system remains constant when the irradiation of the system has levels of photonic fluxes corresponding to the situation $I_{in} > I_{lim}$. The optical response of an ideal optical limiter is presented in Figure 8.

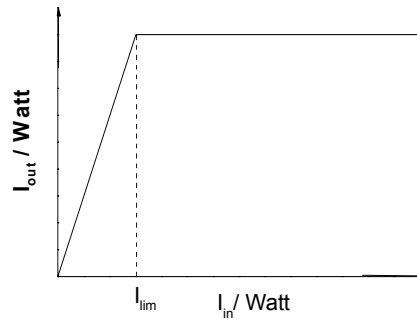


Figure 8: Trend of the light intensity I_{out} transmitted by an ideal optical limiter versus the incoming light intensity I_{in} . In the abscissae axis the threshold intensity I_{lim} at which I_{out} saturates is indicated.

The transmittance T [$= d(I_{out}) / d(I_{in})$] of an ideal optical limiter is not constant within the whole regime of irradiation and T becomes a function of I_{in} with $T \rightarrow 0$ for $I_{in} \gg I_{lim}$. A useful parameter for the evaluation of the OL effectiveness of different systems is the intensity threshold defined as the incident intensity value at which the transmittance of the system is equal to the 50% of the linear transmittance.

As nonlinear optical (NLO) phenomenon, the effect of OL can be also analyzed in terms of the vector polarization \vec{P} defined as the number of dipole moments per unit volume of material (in $C\ m^{-2}$), and its variations with the applied electric field \vec{E} (in $V\ m^{-1}$) of the interacting electromagnetic wave. In the weak field regime, the polarization and the electric field of the applied radiation are directly related according to:

$$\vec{P} = \epsilon_0 \chi \vec{E} \quad (2)$$

where χ is the generalized macroscopic susceptibility (a tensorial property), and ϵ_0 the dielectric constant of the vacuum ($8.85 \times 10^{-12} \text{ F m}^{-1}$). In the case of strong field regime, the susceptibility becomes itself a function of the applied electric field, thus giving rise to a nonlinear dependence of polarization on applied electric field. In a system of non-interacting molecules, the macroscopic susceptibility χ is given by the product of the molecular polarizability α' and the density number N (in m^{-3}) of the molecules:

$$\chi = N \alpha' \quad (3)$$

At low light intensities, the polarization \vec{P} is only dependent on the frequency of the light. Nevertheless, in an intense electric field of a laser beam, the polarization cannot follow the oscillations of the electric field linearly and the macroscopic polarization \vec{P} varies with the amplitude of the electric field \vec{E} :

$$\begin{aligned} P_i(\omega_1) = & \sum_J \chi_{ij}^{(1)}(-\omega_1; \omega_2) E_j(\omega_2) + \sum_{JK} \chi_{ijk}^{(2)}(-\omega_1; \omega_2, \omega_3) E_j(\omega_2) E_k(\omega_3) + \\ & \sum_{JKL} \chi_{ijkl}^{(3)}(-\omega_1; \omega_2, \omega_3, \omega_4) E_j(\omega_2) E_k(\omega_3) E_l(\omega_4) \end{aligned} \quad (4)$$

In equation (4) $\chi^{(1)}$, $\chi^{(2)}$ and $\chi^{(3)}$ describe the linear, the second and third order optical susceptibilities, respectively.

An important mechanism for the occurrence of NLO effects like OL is optical pumping. In this case the incident laser frequency approaches a transition frequency in the molecule. The light is absorbed, causing transitions to the excited state. The optical properties of the excited state differ considerably from those of the ground state and the higher the population in the excited state, the larger the changes in the optical properties of the material. Optical pumping involves real transitions to the excited state, and this phenomenon is quite different from the small perturbations of the electronic cloud which are verified in the regime of linear polarization. Optical pumping can induce both saturable and reverse saturable absorption depending on the difference of the absorption properties of the system between the ground and excited states at the wavelength of irradiation.

3.2 Optical limiting: mechanisms and models

It is usually convenient to describe a molecular optical limiter as a system possessing four relevant electronic energy levels for the analysis of NLO absorption produced by these species (Figure 9). In a four-level system like the one depicted in Figure 9, the absorption of the photon can take place for both transitions [1→3] and [2→4] with σ_{13} and σ_{24} as absorption cross-sections, respectively. Assuming the lifetimes of the states with the energies values corresponding to the levels 3 and 4 are short (this implies fast intersystem crossing (ISC) [3→2] and fast fluorescence decay [4→2]), then the only significantly populated levels will be 1 and 2 during the irradiation process.

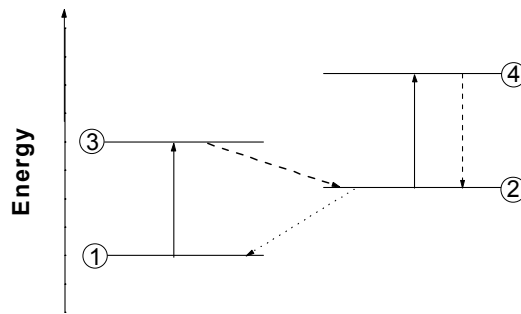


Figure 9: Energy diagram of a four-level system. Full lines indicate absorption from ground [1→3] and excited states [2→4]; dashed lines represent intersystem crossing [3→2] and excited state fluorescence [4→2] (fast processes); dotted line indicates phosphorescence [2→1] (slow process)

The kinetics representing the time variations of the different levels in a four-level model during irradiation are given by the following equations:

$$dN_1/dt = -\sigma_{13} \Phi_{in} N_1 + N_3/\tau_{31} + N_2/\tau_{21} \quad (5)$$

$$dN_2/dt = -\sigma_{24} \Phi_{in} N_2 + N_3/\tau_{32} + N_4/\tau_{42} - N_2/\tau_{21} \quad (6)$$

where N_i , τ_{jk} and Φ_{in} represent the population in the i -level, the time required for the transition [j →k] and the flux of incident photons (in: number of photons / cm² s),

respectively. The steady state solutions for the populations at the level 1 and 2 are given by:

$$N_1(\text{Steady state}) = N_{\text{tot}}(1 + \Phi_{\text{in}}/\Phi_{\text{sat}})^{-1} \quad (7)$$

$$N_2(\text{Steady state}) = N_{\text{tot}}(\Phi_{\text{in}}/\Phi_{\text{sat}})/(1 + \Phi_{\text{in}}/\Phi_{\text{sat}}) \quad (8)$$

being $N_{\text{tot}} = N_1 + N_2$ (N_3 and N_4 are considered negligible), and $\Phi_{\text{sat}} = 1/(\sigma_{13}\tau_{21})$. At this point is convenient to define an effective absorption cross-section σ_{eff} through the Lambert-Beer equation:

$$(d\Phi_{\text{in}}/dz) = -\Phi_{\text{in}} \sigma_{\text{eff}} N'_{\text{tot}} \quad (9)$$

in which N'_{tot} is the number of absorbers per unit of volume and z is the direction of light propagation, in order to obtain the steady-state dependence of σ_{eff} on Φ_{in} (statement of nonlinearity of the optical absorption of a four-level system):

$$\sigma_{\text{eff}} = \sigma_{24} + \{(\sigma_{13} - \sigma_{24})/[1+(\Phi_{\text{in}}/\Phi_{\text{sat}})]\} \quad (10)$$

In a saturable absorber $\sigma_{13} > \sigma_{24}$ and strong irradiation achieved when $\Phi_{\text{in}} > \Phi_{\text{sat}}$, brings about a bleaching of the system, i.e. the ratio $\Phi_{\text{out}}/\Phi_{\text{in}}$ tends to increase with increasing irradiation. Such a phenomenon doesn't produce OL purposes because this requires the decrease of the ratio $\Phi_{\text{out}}/\Phi_{\text{in}}$ upon Φ_{in} increase. On the other hand, the OL will be achieved when the four-level system fulfills the condition $\sigma_{24} > \sigma_{13}$, i.e. the system in the excited state has a larger absorption cross-section with respect to the ground state at the wavelength of irradiation.

The behaviour of the four-level system will then correspond to the operation accomplished by an optical limiter based on NLO absorption and the four-level system is recognized as a reverse saturable absorber. Equation (6) shows the effectiveness of the nonlinear absorption produced with excited state absorptive systems, which relies upon the value of the excited state absorption cross-section σ_{24} at the wavelength of irradiation. From this analysis the OL effect generated by molecular systems like Pc's is an accumulative nonlinearity because it is produced through the polarization of the electronic ground state and the successive absorption from this polarized state as determined by the intensity of the applied electric field. An important characteristic associated with the accumulative feature of

the operation mode in reverse saturable absorbers is the scarce dependence of the absorption kinetics on the incident pulse duration. Consequently, the response of the optical limiter based on reverse saturable absorbers is mainly dependent on the radiation fluence (in photons per irradiated area), instead of the radiation intensity (in photons per irradiated area per unit time).

The excited state absorption is not the sole mechanism with which optical limiting effects can be achieved. In fact other mechanisms can intervene in processes of optical limiting like thermal refractive beam spreading,^[82] non-linear refraction^[83] or optical breakdown-induced scattering.^[84,85] In the latter case, a perturbation of the electronic distribution with the electric field associated with the incident light, or an directional rearrangement of polar molecules with intensity-dependent changes of the refractive index represent the active mechanisms for the occurrence of optical limiting.

The values of $\chi^{(3)}$ attainable through electron-cloud deformation or molecular alignment fall in the range 10^{-34} – 10^{-29} C m V⁻³ with transition time in the order of 10^{-15} – 10^{-9} s.^[86,87] On the other hand the mechanism of multiple absorption originated by optical pumping,^[88] can result in values of $\chi^{(3)}$ as high as 10^{-19} C m V⁻³.^[89] Such relevant differences are basically due to an electronic transition to excited states and not simply an electronic redistribution is involved in the process of optical limiting.

The response-time in optical pumping can vary quite extensively in a range from 10^{-13} to 10^{-3} s, being directly proportional with the lifetime of the first upper excited state.^[90] This can affect radically the values of I_{lim} at which saturation occurs. The involvement of excited states in the mechanism of optical pumping brings about not only intensity-dependent absorption, but also intensity-dependent refraction.^[81]

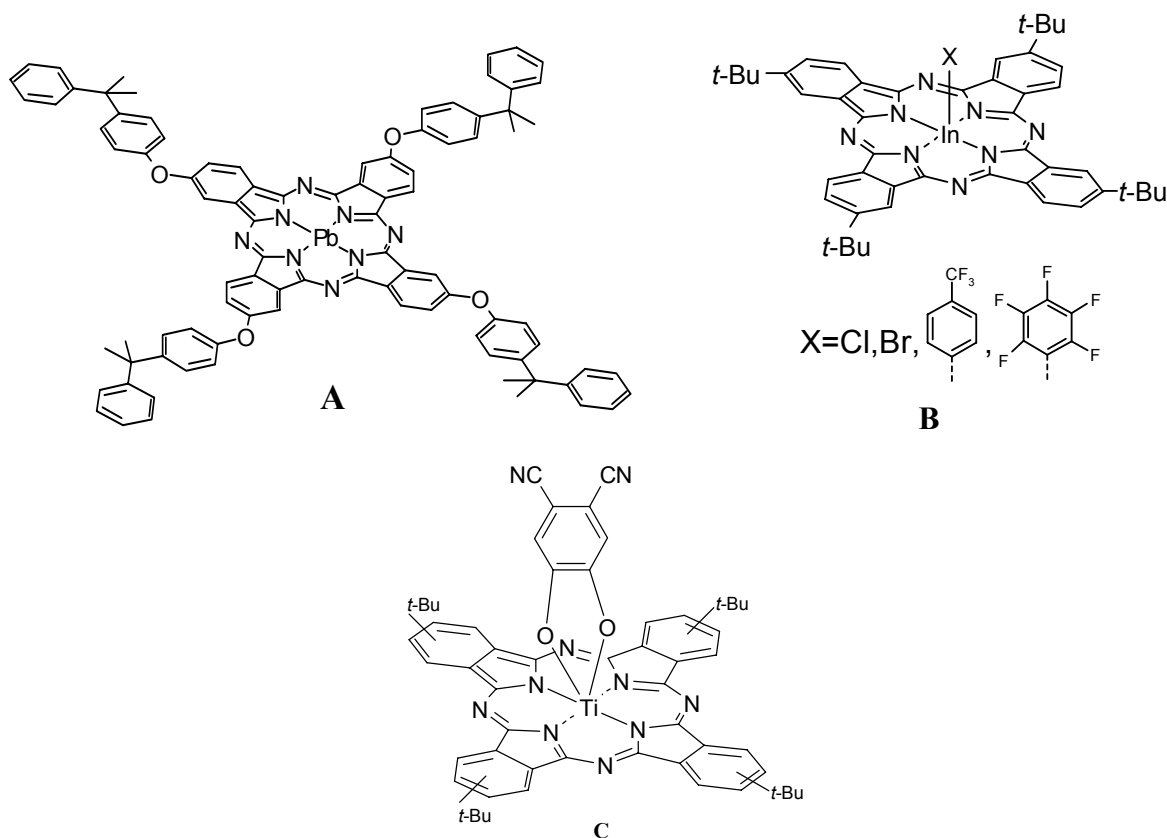
3.3. Phthalocyanines and optical limiting

As already pointed before, the structural prerequisite for the verification of NLO phenomena^[1] in organic compounds, such as optical limiting, is the presence of a network of conjugated π -electrons, which infer high polarizability and fast charge redistribution when the conjugated molecule interacts with rapidly variable intense electromagnetic fields like those of laser radiations.^[2] In the variety of conjugated organic molecules possessing NLO properties, the class of phthalocyanines (Pc's) and related species like naphthalocyanines, porphyrins or tetraazaporphyrins (see Figure 1), occupy a prominent position for the high thermal and chemical stability and the ease of preparation.^[3]

Pc's show OL effects through the mechanism of excited state absorption (ESA). This means the OL effect generated by Pcs is an accumulative nonlinearity because it is produced through the polarization of the electronic ground state and the successive absorption from this polarized state as determined by the intensity of the applied electric field.^[7]

Phthalocyanines are a class of materials which is most extensively investigated, due to the remarkable ability of modulation of phthalocyanine's physical properties as required, through suitable chemical derivatization of the phthalocyanine frame^[36,91a-d] or variation of the central metals.^[91-109]

To be used as optical limiters, phthalocyanines must show a high level of linear transmission and large nonlinear absorption over a broad spectral bandwidth, as well as a high threshold for damage. Moreover, the nonlinear absorption must appear within a sub-nanosecond response time.^[4] Among the phthalocyanine based nonlinear absorbers that have been used as optical limiting materials and approach the necessary characteristics for a practical device some examples can be cited: (β -cumylphenoxy)₄PcPb (**A**),^[91e-h] (*tert*-butyl)₄PcInX compounds (**B**),^[4,90,92a,92b] (*tert*-butyl)₄PcTi[O₂C₆H₂](CN)₂ (**C**).^[92c]



There are several structural factors that can influence the optical limiting properties of phthalocyanines. In general, the appropriate changes in the structure by chemical modification are mostly enough to change significantly the OL properties of the phthalocyanine. This

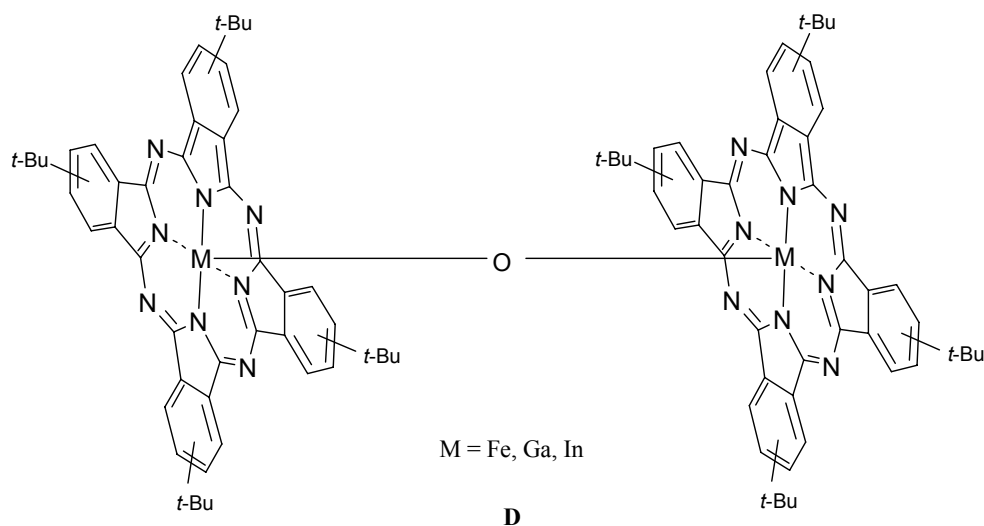
chemical modification can change positively or negatively several aspects of electronic, molecular and supramolecular properties of the material. Consequently, all the factors discussed below must be taken in account for the achievement of an effective optical limiter.

Varying the central atom (metal) in a phthalocyanine can cause a change in the performance of the material as an optical limiter. Central moieties, such as VO, TiO, GaCl or InCl, have the ability of introducing high dipole moments perpendicularly oriented to the Pc or Nc ring, which alter the electronic structure of the macrocycle,^[93a] and introduce new steric effects that modify the packing properties of PcMX's.^[90]

The introduction and variation of peripheral substituents in phthalocyanines can also modify the structural arrangement of the molecule or the spatial relationship between neighbouring molecules. The use of unsymmetrically substituted phthalocyanines are another approach to enhance the OL properties of phthalocyanines, since the introduction of non-symmetry in structural arrangement can change the electronic structure of the macrocycle.^[93b]

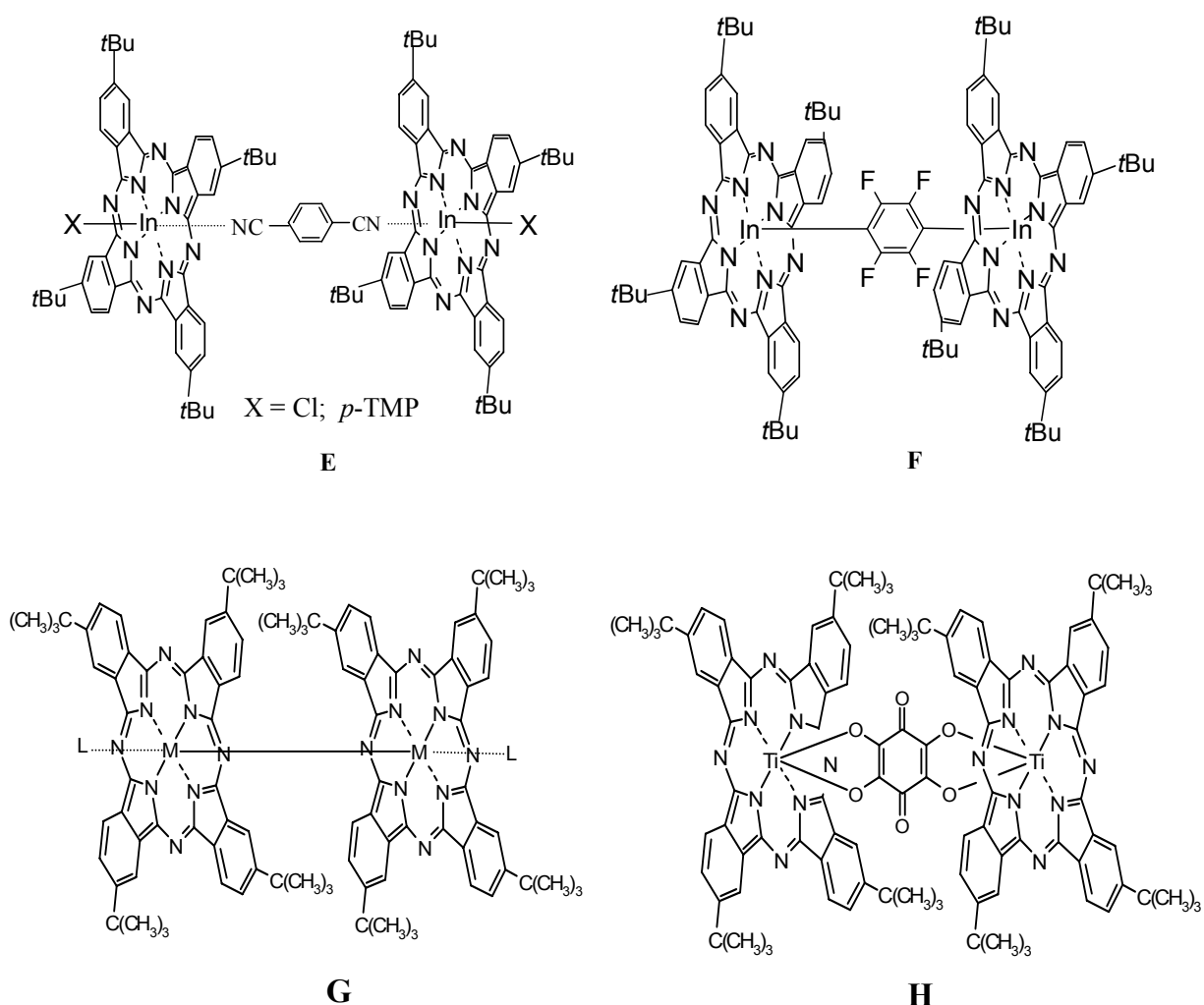
Our working group has been very much interested the in last few years on the improvement of the Pc's structural characteristics in order to achieve OL properties enhancement.^[90,92a,94-108]

Optical limiting properties have been mainly studied for monomeric Pc's. Only few studies have been carried out for dimeric or binuclear Pc's.



Among dimeric Pc's, the NLO properties of μ -oxo bridged Pc dimers with the general structure Pc(X)M-O-M(X)Pc [M = Fe, Ga and In (compound **D**), diisocyanobenzene (dib) (compound **E**) and 2,3,5,6 tetrafluorophenylene(TFP) (coumpound **F**), X= Cl and TMP]^[97,108,109h] have been studied, mostly in our group. The larger OL effect generated by the

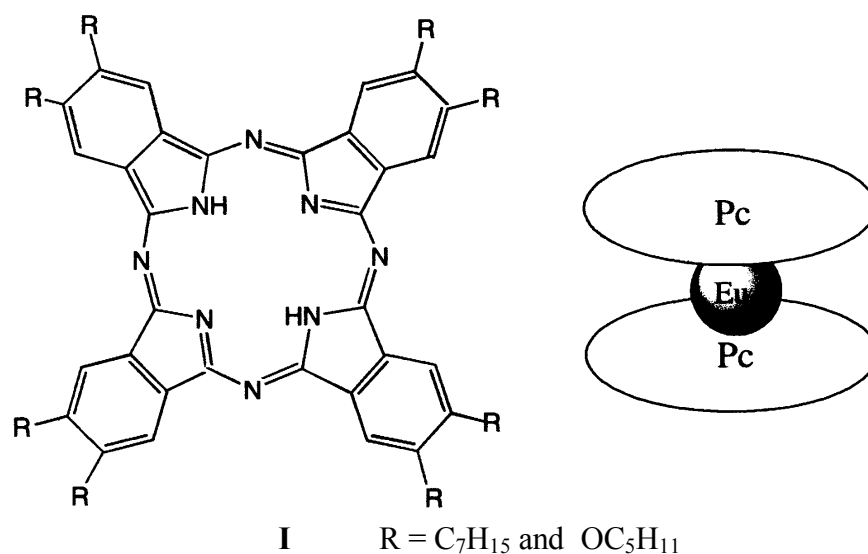
dimers PcInX-dib-InPc as bridging ligand with respect to the bridged dimers PcIn-TFP-InPc , indicates the sharing of the common axial ligand TFP in PcIn-TFP-InPc reduces the excited absorption cross-section of the lower triplet excited state which is responsible for the nonlinear optical absorption. On the other hand, the similarity of the Z-scan profiles (see page 20) for $[\text{tBu}_4\text{PcInCl}]_2\text{.dib}$ and $[\text{tBu}_4\text{PcIn}(p\text{-TMP})]_2\text{.dib}$ combined with their better OL performance, is indicative of the favorable effect associated with the presence of the additional axial electron-withdrawing groups Cl and TMP in their structures.^[108]



A newly synthesized dimer with a direct M-M bond $[\text{tBu}_4\text{PcM}]_2$ 2L with $\text{M} = \text{In}$ and $\text{L} = \text{tmed}$ ($\text{tmed} = \text{N}, \text{N}, \text{N}', \text{N}'\text{-tetramethylethylenediamine}$) (compound **G**) display OL properties with improved features with respect to the single Pc ring coordinated by one single metal atom.^[102,109h] Similarly, the Pc dimer with central Ti atoms bridged by tetrahydroxy-p-benzoquinone (compound **H**) also displays an OL effect with improved characteristics if compared with the parent monomer.

The above referred optical limiting measurements were only carried out for these type of dimers. Directly conjugated binuclear Pc's, as we will explain later (see page 24), were not used for OL studies, so far.

The NLO properties of dimeric Pc's constituted by sandwiched bis(phthalocyaninato)lanthanides have been studied and analyzed by several groups.^{109a-c]} Modifications of the energy levels scheme involved in the NLO processes are usually taken into account due to the existence of cofacial interactions between the two Pc rings.^[109d] The main structural limitation associated with the use of lanthanide Pc's is the impossibility of varying the electronic properties of the sandwiched coordinating atom through, e.g. axial substitution, due to the fixed valence of the lanthanides. The OL properties of sandwich-type lanthanides diphtalocyanines were also investigated.^{109e,109f]} In one of these studies, it was demonstrated that $\text{Eu}[\text{Pc}(\text{OC}_5\text{H}_{11})_8]_2$ exhibited better optical limiting behavior than $\text{Eu}[\text{Pc}(\text{C}_7\text{H}_{15})_8]_2$ (compound **I**).^[109e]

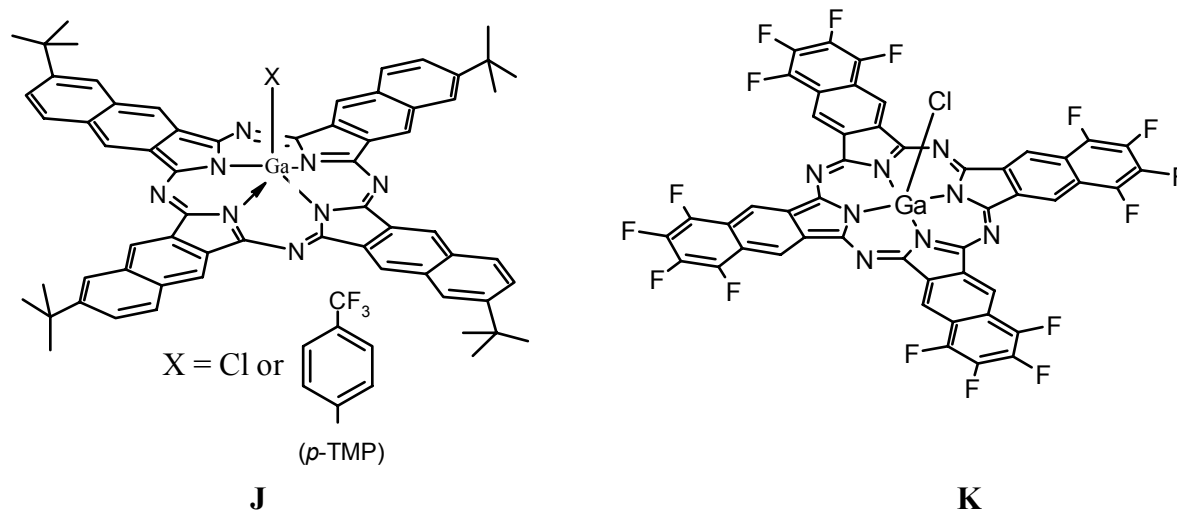


3.4. Naphthalocyanines and optical limiting

As pointed out before, being analogues of phthalocyanines, naphthalocyanines have a more extended conjugated π -system due to the additional tetra-benzo-annulation (Figure 1). Such a structural modification is reflected in case of 2,3-naphthalocyanines in their UV-Vis spectra as a strong bathochromic shift of the Q-band and as the enlargement of the highly transparent window between the Q- and B-bands, desirable for optical limiting. To the

contrary, UV-Vis spectra of 1,2-naphthalocyanines do not differ very much from those of Pc's: the position of the Q-band is almost not affected by 1,2-annulation indicating no strong conjugation of the annulated benzo-rings with the phthalocyanine macrocycle.^[75,76]

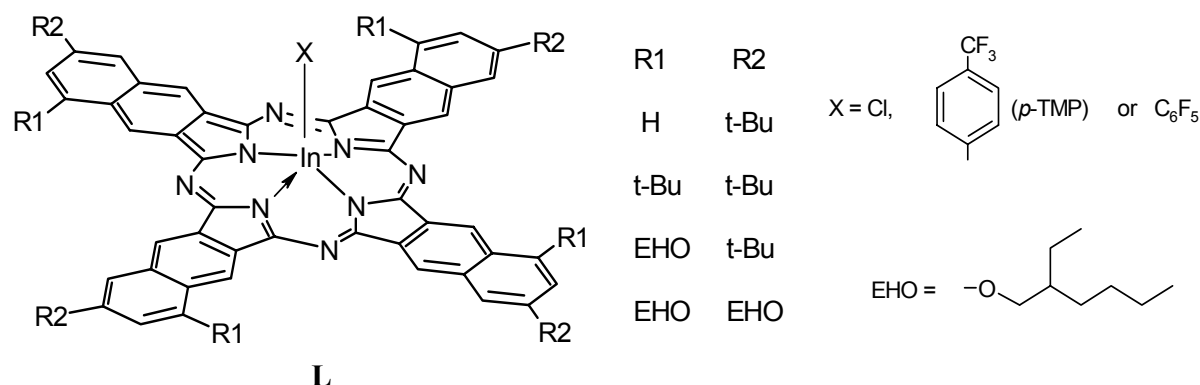
Therefore, only 2,3-naphthalocyanines received an attention in connection with their optical limiting properties. No OL studies on 1,2-naphthalocyanines were reported till now. The approaches for the fine tuning of OL properties of naphthalocyanines are quite similar to those used for the modification of OL properties in phthalocyanines, e.g. peripheral and/or axial ligand substitution, variation of the central atom, etc. However, one should take into account that the negative effects connected with their tendency to aggregate and/or to decompose photochemically are stronger than in case of phthalocyanines.



OL measurements were carried out in our group for the first time on axially substituted gallium tetra-*tert*-butyl naphthalocyanines $t\text{-Bu}_4\text{NcGaCl}$, $t\text{-Bu}_4\text{NcGa}(p\text{-TMP})$ (compound **J**) and the μ -oxo-dimer $[t\text{-Bu}_4\text{NcGa}]_2\text{O}$ in chloroform solutions.^[98] An hexadecafluorinated gallium-2,3-naphthalocyanine $\text{F}_{16}\text{NcGaCl}$ (compound **K**) and a μ -oxo-dimer $[\text{F}_{16}\text{NcGa}]_2\text{O}$ were also prepared and studied recently by us.^[103] Although the solubility of the monomeric species appeared to be too low for OL-studies, the optical limiting properties of the dimeric $[\text{F}_{16}\text{NcGa}]_2\text{O}$ were studied in THF and compared with those of $t\text{-Bu}_4\text{NcGaCl}$, $[t\text{-Bu}_4\text{NcGa}]_2\text{O}$ and C_{60} at 532 nm irradiation, exhibiting the best results for $(\text{F}_{16}\text{NcGa})_2\text{O}$.

Through the appropriate peripheral substitution, the Nc's can give an increased transmitting window, shifted to the red, which is desirable for the fabrication of optical limiters effective in the broad visible-light range including the red-light region. Some substitution patterns which provoke absorption in the near-IR and infer high solubility to indium-naphthalocyanines as materials for OL were also realized (compound **L**).^[110] Among

these octa-substituted Nc's the mixed substituent derivative $(t\text{-Bu})_4(\text{EHO})_4\text{NcInCl}$, where EHO is 2-ethylhexyloxy, and its axially substituted analogue $(t\text{-Bu})_4(\text{EHO})_4\text{NcIn}(p\text{-TMP})$ have shown high solubility and no aggregation at 2×10^{-3} M concentration in chloroform.



3.5. Z-scan technique

The measurement techniques used in the studies of these materials are third-harmonic generation (THG),^[87] degenerate four-wave mixing (DFWM),^[111-114] electric field induced second harmonic generation (EFISH),^[115] and Z-scan methods.^[116-118] This last referred method will be discussed in more detail, also in connection with the measurements of the OL effect generated by the compounds whose synthesis is reported in this thesis (page 60).

The Z-scan technique^[117] allows the experimental determination of nonlinear transmission and nonlinear refraction. In the Z-scan technique the sample under investigation moves along the optical axis of a focused Gaussian beam. The sample experiences a large variations of the incident intensity along its path and nonlinear optical effects can be then induced.

3.5.1. Some examples

Considering a Gaussian beam in a tight focus geometry as shown in Figure 10, the transmittance of a nonlinear medium is recorded through an open or closed aperture as a function of the sample position z measured with respect to the focal plane ($z = 0$). The sample for a Z-scan determination must have a thickness smaller than the diffraction length $w_0^2 \pi / \lambda$ (w_0 is the beam waist radius at the focus and λ is the laser wavelength) of the focused beam (thin medium condition).

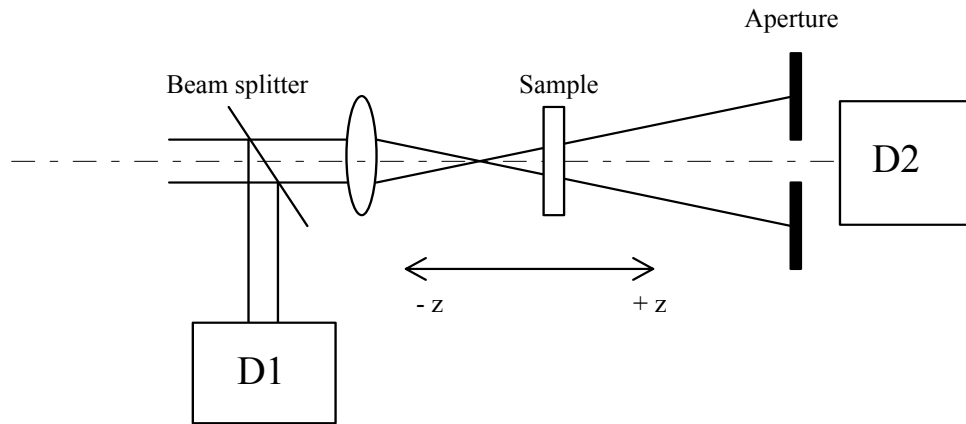


Figure 10: Typical Z-scan set-up. The ratio of the signal measured by the photo diodes D2/D1 is recorded as a function of sample position Z

In the simple case of positive nonlinear refractive index and absence of nonlinear absorption in the far field region, the beam irradiance is low and negligible nonlinear refraction occurs. Consequently the transmittance remains constant. As the sample is brought closer to the focus, the beam irradiance increases, leading to self-lensing effects in the sample. A positive self-lensing prior to focus will tend to broaden the beam, as shown in Figure 11-b, causing a beam broadening in correspondence of the closed aperture which results in a decrease of the measured transmittance. As the scan in Z continues and the sample passes the focal plane to the right (positive Z), the same self-defocusing decreases the beam divergence, leading to beam narrowing in correspondence of the closed aperture, and thus transmittance increases, as represented in Figure 11-c. This is analogous to placing a thin lens at or near the focus, resulting in a minimal change of the far-field pattern of the beam. The Z-scan is completed as the sample is moved away from focus (positive z) such that the transmittance becomes linear since the irradiance is again low. Therefore, a prefocal transmittance minimum (valley) followed by a postfocal transmittance maximum (peak) is the Z-scan signature of the sole positive refractive nonlinearity as shown in Figure 12 when a Z-scan closed aperture configuration is adopted (presence of a spatial filter in front of D2 with an aperture smaller than the beam diameter in Figure 10). Negative nonlinear refraction, following the same analogy, gives rise to an opposite peak-valley pattern. The sign of the nonlinear index is then immediately obvious from these patterns (Figure 12).

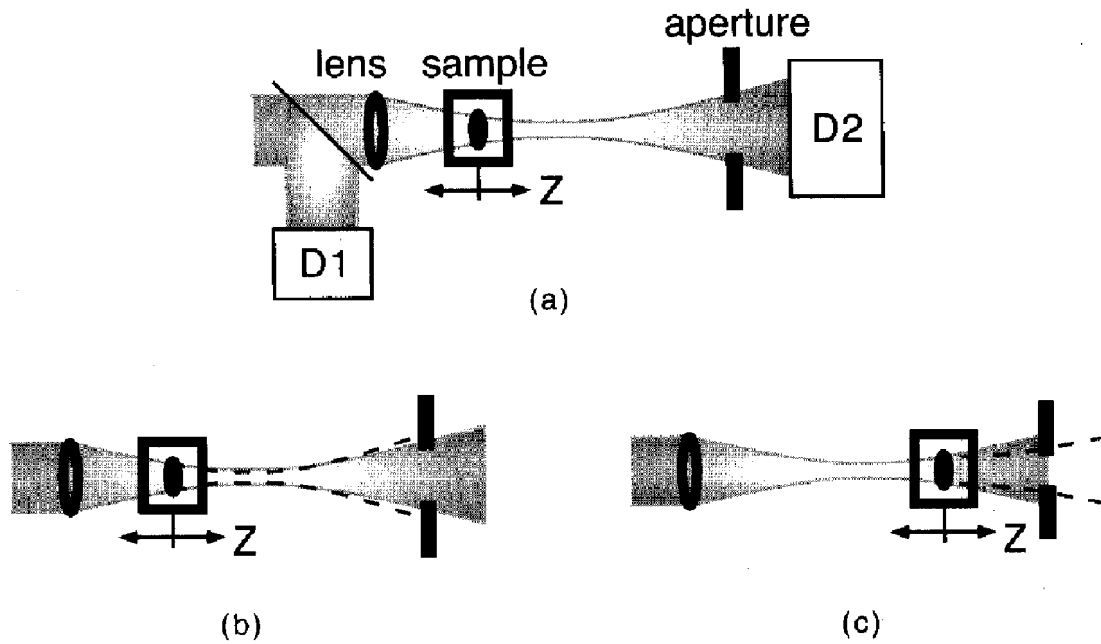


Figure 11: (a) Linear and (b,c) nonlinear optical behavior of a refracting system with $n_2 > 0$ (b) before and (c) after the passage through the Gaussian beam focus in a Z-scan experiment.

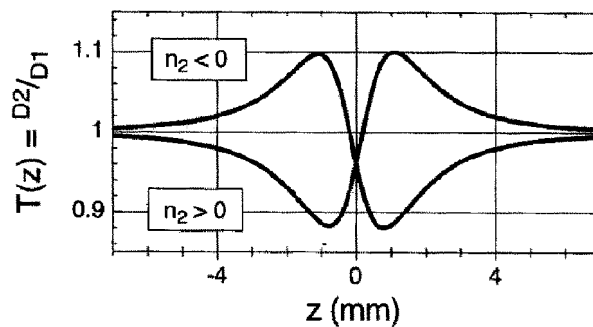


Figure 12: Z-scan signature for the sole occurrence of negative (positive) refraction nonlinearity resulting from a prefocal beam narrowing (broadening) followed by a postfocal beam broadening (narrowing). In case of $n_2 > 0$, the optical effects originating the Z-scan pattern of this figure are shown in Figure 11 (b) and (c).

In case of positive nonlinear absorption, i.e. occurrence of RSA, then in the open aperture configuration (presence of a spatial filter in front of D2 with an aperture larger than the beam diameter in Figure 10), the typical Z-scan pattern is that presented in Figure 13. As the sample approaches the beam focus the increase of beam intensity promotes changes in the sample in such a way that the overall absorption coefficient of the sample increases and, consequently, the transmission decreases. In the far field region, i.e. $Z \gg 0$ or $\ll 0$, which

corresponds to the linear optical regime, the transmittance value of the system reaches reversibly the pristine value.

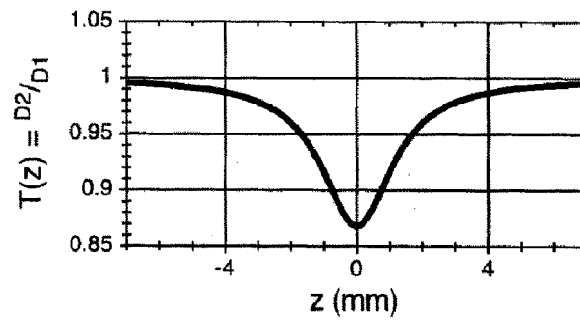


Figure 13: Z-scan pattern of a positive nonlinear absorber (RSA occurrence).

II - Aim of the work

The objective of this work is a systematic study on the synthesis and an investigation of optical limiting (OL) properties of binuclear metal phthalocyanines based on the structure type as represented in Figures 14 and 15.

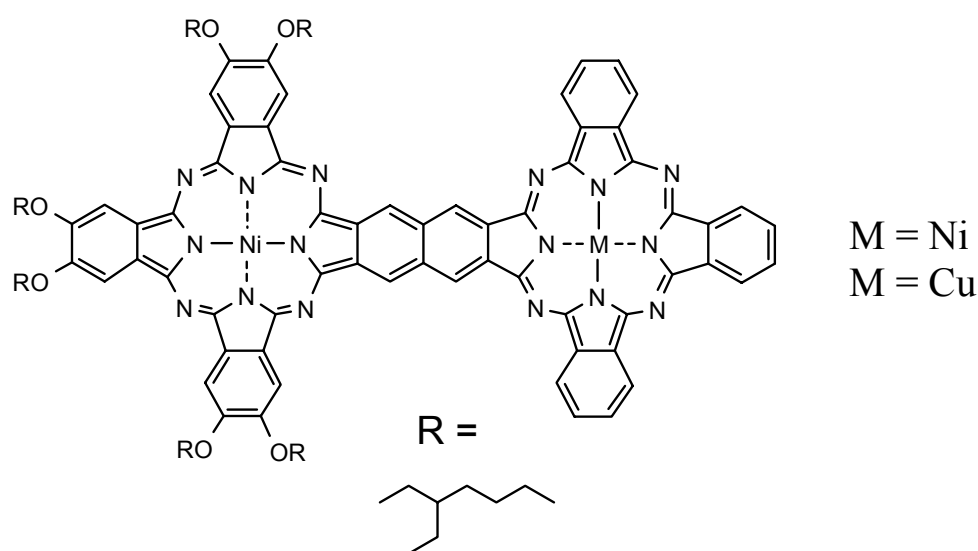


Figure 14: Unsymmetrically substituted binuclear metal phthalocyanines

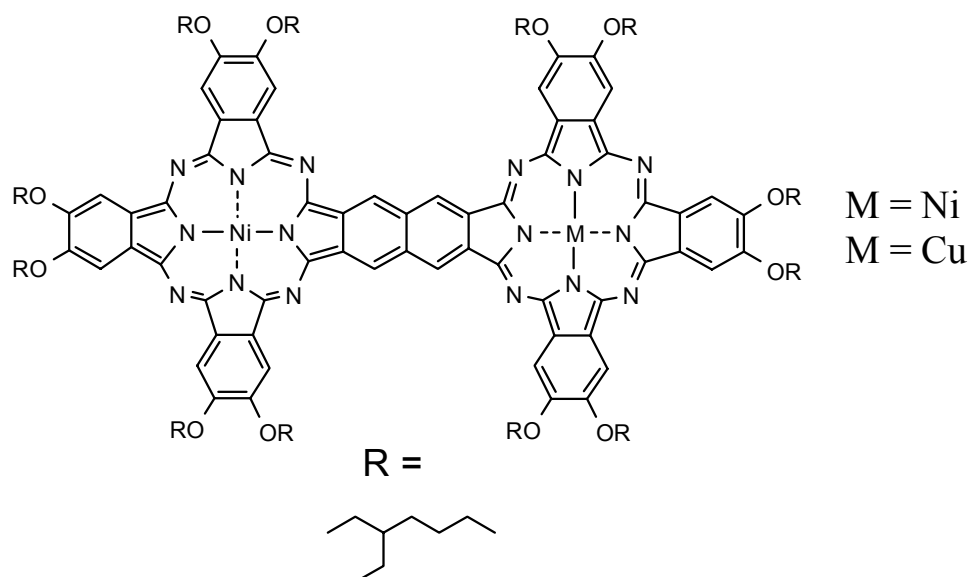


Figure 15: Symmetrically substituted binuclear metal phthalocyanines

The intention of our work at first is synthetic, since we plan to synthesize the binuclear metal phthalocyanines shown in Figures 14 and 15 with the same metals but also with different metals.^[120] In a primary approach, copper and nickel seem to be convenient for the

later purpose, since both have good chelating and stabilizing properties for the formed phthalocyanines.^[11,120,121] Afterwards, indium and gallium are planned to be examined (Figure 16), in a way that optical limiting could be investigated, since phthalocyanines with metals from this group, as pointed out before, possess enhanced OL properties.^[4,95,109] Another important feature is that the planned synthetic pathway (see below) permits to introduce asymmetry in the binuclear metal phthalocyanines, due to an asymmetric substitution pattern (see Figure 14).

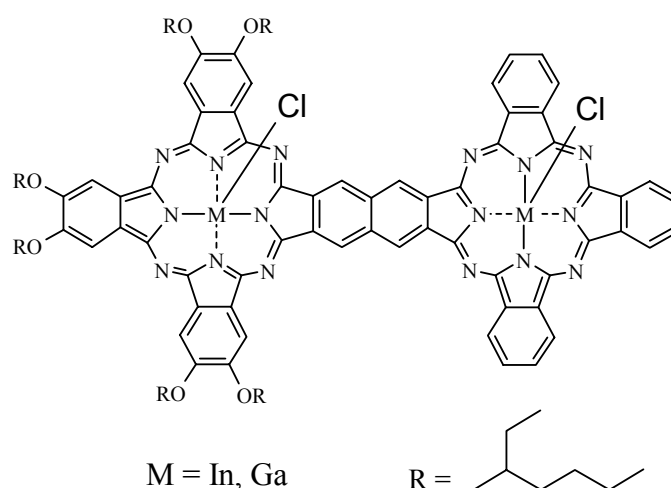


Figure 16: Binuclear phthalocyanines designed for optical limiting

The synthesis of the binuclear metal phthalocyanines shown in Figure 14 and 15 will follow the procedure from Scheme 1 (page 31). The binuclear In and Ga phthalocyanines given in Figure 16 were synthesized via the corresponding Mg compounds according to Scheme 5 and Scheme 10 on page 45 and 48, respectively, representing the first approach to obtain these compounds through a direct synthesis.

The measurements of the OL properties of the synthesized compounds is also part of the work. Emphasis will be put on the performance of the synthesized complexes as optical limiters. These investigations were carried out at Trinity College in Dublin, Ireland, in cooperation with the group of Prof. Dr. Werner Blau, supported by an E.U. network scientific project, and with Prof. Dr. James Shirk, at U. S. Naval Research Laboratory, in Washington, D.C. U.S.A.

III - Results and discussion

1. Synthesis of binuclear phthalocyanines

Planar or nearly planar binuclear Pcs, binuclear Pc-triazolehemiporphyrates (Thp)^[123,124] (Figure 17) and phthalocyanine based dimers^[124-135] are known. As an example, a dimer in which two Pcs are linked with bis(acetylene) bridges^[125] (Figure 18) was obtained by coupling the Pc derivatives having two acetylene units in the presence of a copper salt in pyridine. Another example is an oligo(phenylenevinylene)-bridged Pc dimer^[127] (Figure 19), obtained by our group through the reaction of 2 equivalents of a modified Pc-monoaldehyde with 1 equivalent of p-xylylene bis(triphenylphosphonium)bromide. Also a Pc dimer fused with anthraquinone was reported recently by our group^[126] (Figure 20). Torres et al. reported the preparation of heterodimetallic binuclear Pc-derivatives, having Ni and Zn as different metals (Figure 21).^[124] Preparation of heterodimetallic binuclear Pc-Thp-compounds with Ni and Zn have also been reported by the same authors.^[123]

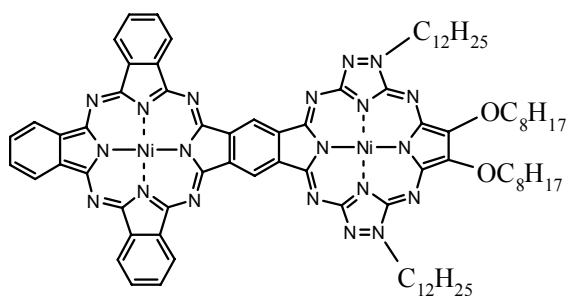


Figure 17: Binuclear Pc-triazolehemiporphyrinate (Thp)^[123,124]

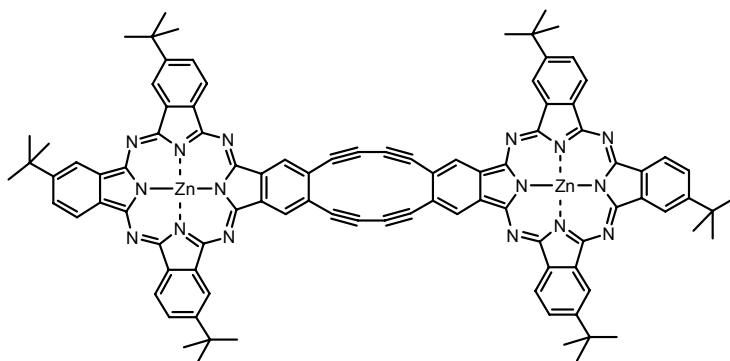


Figure 18: Dimer linked by bis(acetylene) bridges^[125]

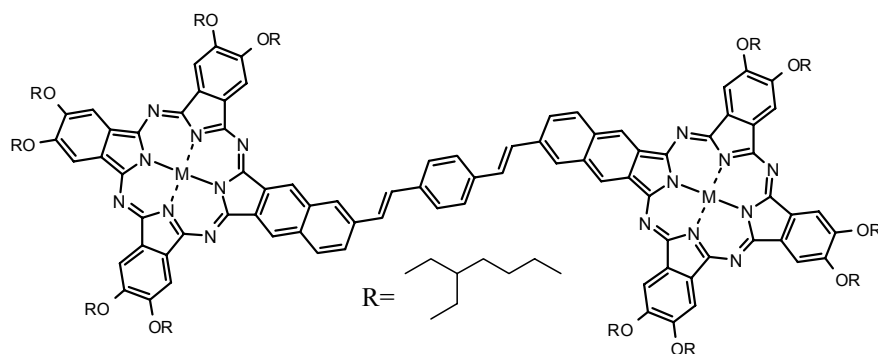


Figure 19: Oligo(phenylenevinylene) bridged Pc dimer^[127]

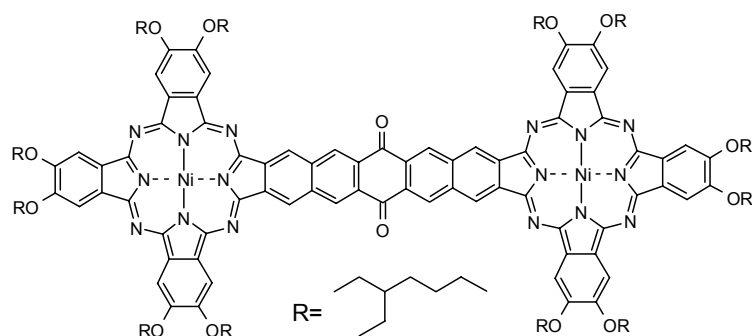


Figure 20: Pc dimer fused with anthraquinone^[126]

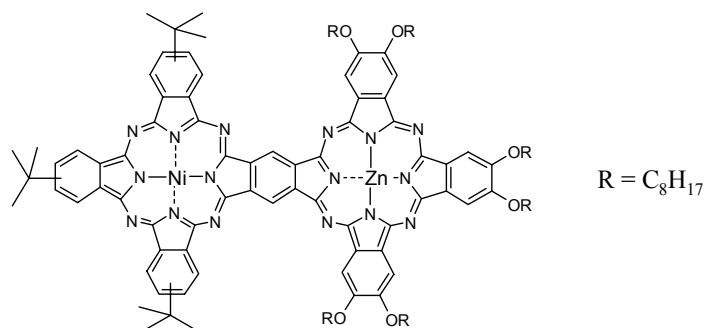


Figure 21: Heterodimetallic binuclear Pc^[124]

Among the reported binuclear Pcs, the metal free compound with the structure given in Figure 22 with twelve dodecyloxy substituents was synthesized by mixed condensation of didodecyloxydiiminoisoindoline with naphthalene-bis(diiminoisoindoline).^[129] The reaction was carried out in one step, producing the mononuclear octadodecyloxy phthalocyanine and other statistical products, among the desired binuclear Pc, which was isolated in a comparable low yield. A corresponding binuclear metal phthalocyanine was not prepared. In contrast to the binuclear Pc shown in Figure 21,^[124] which can also be considered as an unsymmetrically

substituted mononuclear Pc, two complete Pc's are linked together in the phthalocyanine shown in Figure 22.

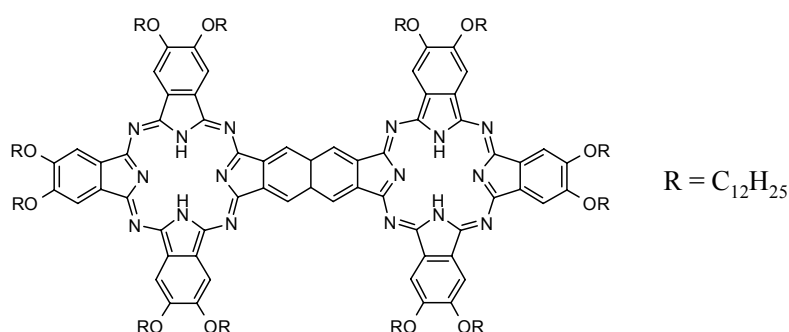
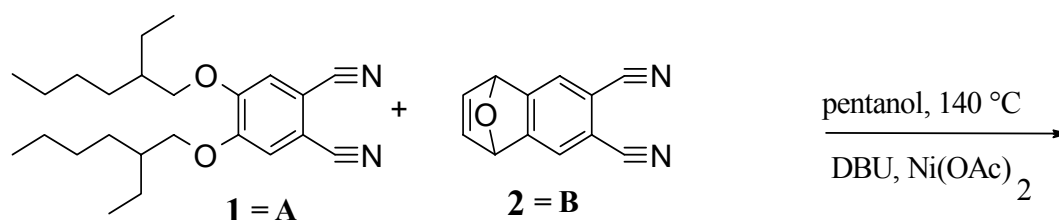


Figure 22: Metal-free binuclear Pc^[129]

We have developed now a new synthesis of binuclear Pc's (Scheme 1, page 31/32) of the type shown in Figure 22, which allows us to obtain the binuclear Pcs **12-15** containing the same metals, Ni, and also different metals e. g. Ni and Cu in the same molecule (**14, 15**), as well as to obtain unsymmetrically substituted binuclear PcM's (**12, 14**).^[120]

The new synthesis starts with the Pc **11**, (page 31), containing two cyano groups. These benzoannulated unsymmetrically substituted PcMs are desirable building blocks for the preparation of polymers,^[127] for the linkage of PcMs with other materials, e.g. poly *p*-(phenylenevinylene) (PPV),^[127,138] or in our case as the starting material for the synthesis of binuclear PcMs.

The combination of two different phthalonitriles permits the preparation of phthalocyanines with high functionality. In principle, two different phthalonitriles **A** and **B** can be condensed to give six different phthalocyanines, in a statistical distribution (Figure 23).



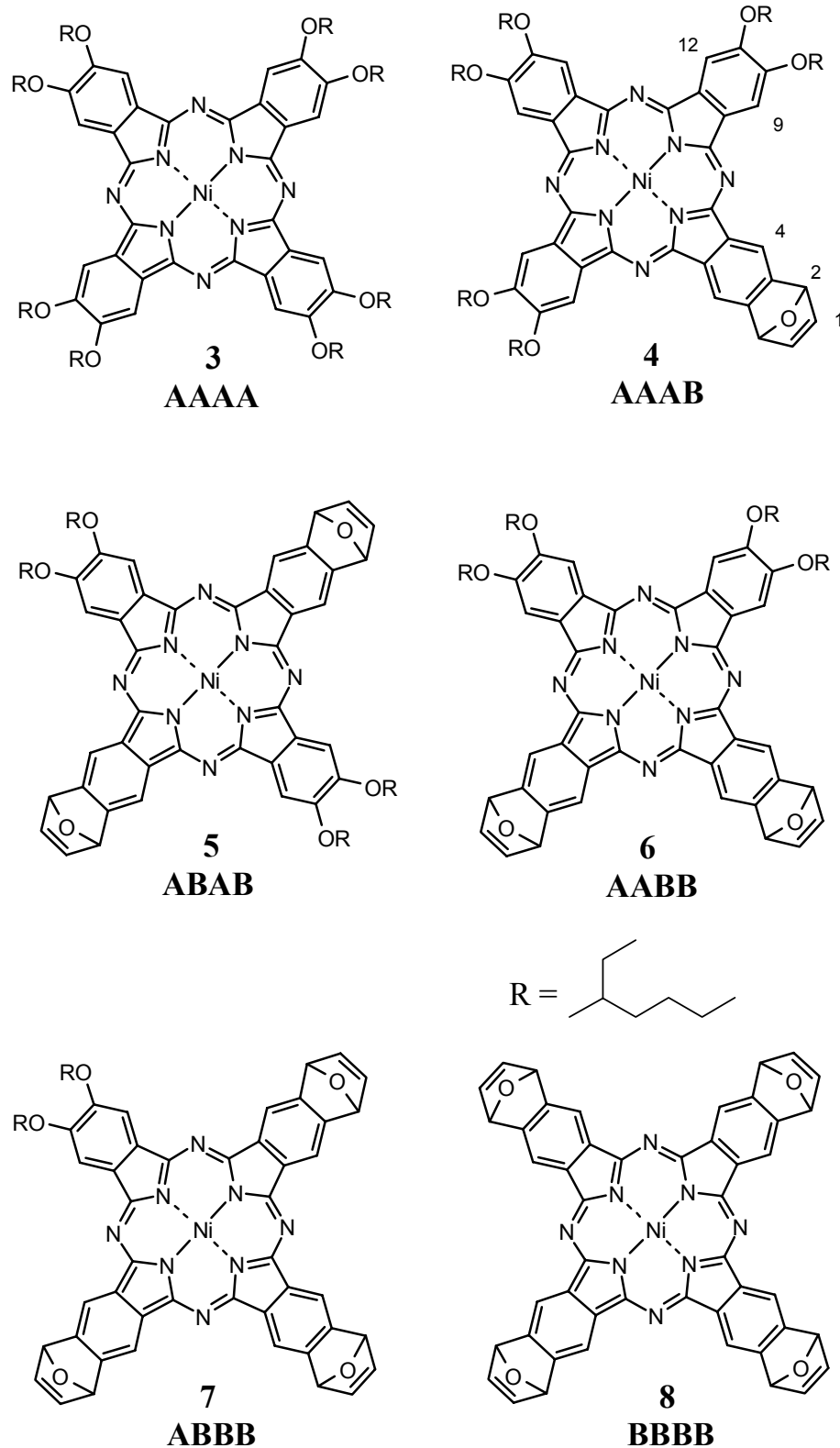


Figure 23: Possible products from a statistical condensation

From the six possible isomers shown in Figure 23, which are formed by the reaction of **1** and **2**, the one which is the necessary compound to carry out a straightforward synthesis of **12–15** is the unsymmetrically substituted phthalocyanine **4** (see Scheme 1). By changing the

ratio between the two dinitriles **1** and **2** in the statistical synthesis, the resulting amount of each isomer can be varied, so that the required isomer **4** is obtained in good yield. In the following, we describe which relative portions of the six phthalocyanines **3-8** in the product mixture are to be expected by varying the stoichiometry of **1** and **2**, assuming a simple model, with the same kinetics for all the condensation steps. When the ratio between the dinitriles **A** (**1**) and **B** (**2**) is 1:1 (i.e. 50%), the probability of obtaining **AA**, **AB** and **AB** is approximately $(0.5)^2 = 0.25$. However, for **AB** it must be considered that **BA** makes the same contribution, because there are two permutations of the elements **A** and **B** at two places. Thus, for all six specified Pcs **3-8**, the probability is $(0.5)^4 = 0.0625$. This number, however, must be still multiplied by the number of permutations. This simple model does not consider the template and/or steric or electronic effects. In addition, it does not consider that the particle reservoir decreases during the reaction. However, this can be neglected, to the good approximation of the large particle number.^[136]

In Table 1 an example with the number of permutations and the relative portions of products **3-8** for different reactions stoichiometry used in the model of Cook et al.^[136,137] is given.

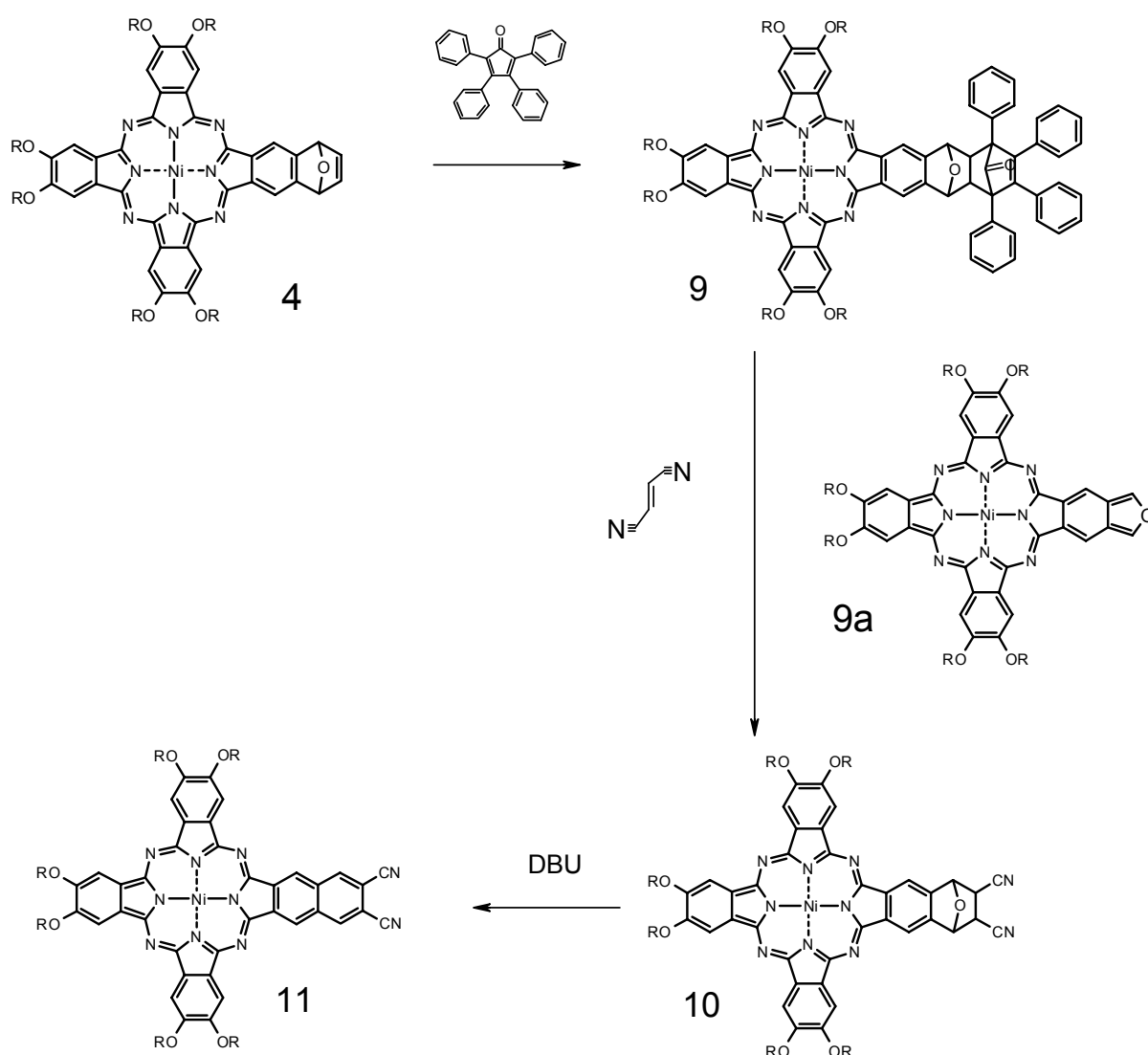
Table 1: Expected relative portions from the statistical condensation mixture of products.

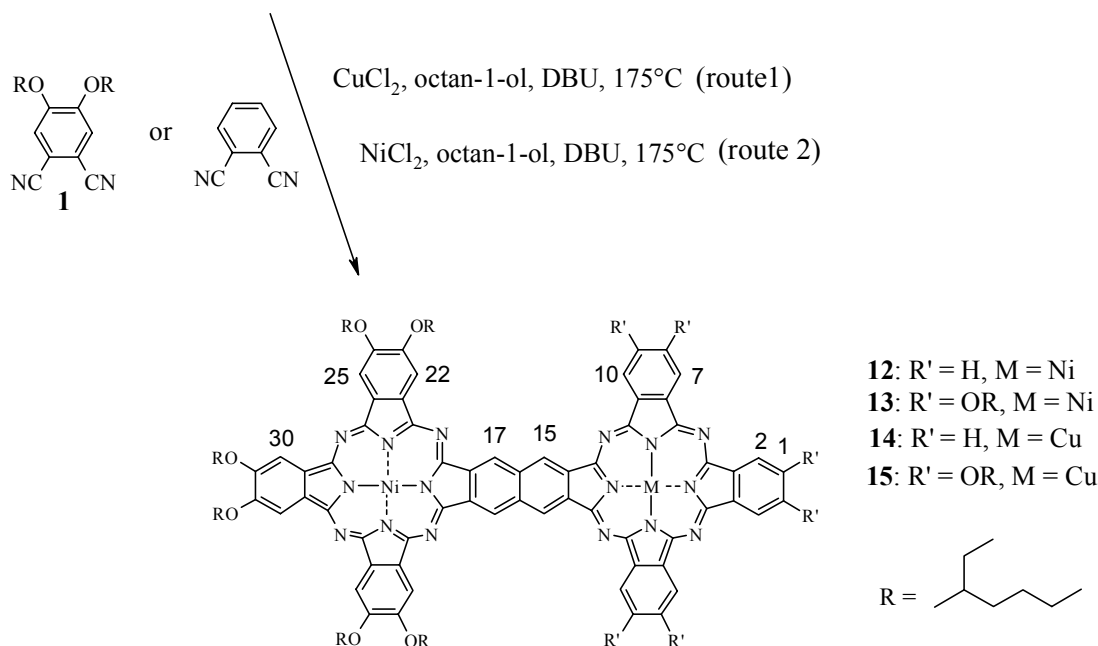
A:B	3 (AAAA)	4 (AAAB)	5 (ABAB)	6 (AABB)	7 (ABBB)	8 (BBBB)
1:1	6.25	25	12.5	25	25	6.25
3:1	31.6	42.2	7.0	14.1	4.7	0.4
9:1	65.6	29.2	1.6	3.2	0.4	0.01
Permutations	1	4	2	4	4	1

From Table 1 it is evident that the relative portions obtained from a statistical condensation can be modulated by changing the concentrations of **A** and **B**, in order to obtain an excess of the desired phthalocyanine. In the present case the stoichiometry used was 3:1, since the desired product is the **AAAB** product **4**, in which the theoretical yield is approximately 42%.

1.1. Synthesis of [2,3,9,10,16,17-hexa-2-ethyl-hexyloxy-25,26-dicyano-phthalocyaninato] nickel (11)

As described, the synthesis shown in Scheme 1 allows us to obtain the binuclear Pcs **12-15** containing the same metal as well as different metals e. g. Ni and Cu in the same molecule **14** and **15**, as well as to obtain unsymmetrically substituted binuclear PcM's **12** and **14**.^[120] Compounds **12** and **13** were synthesized with Ni as central metal in both cavities, while **14** and **15** containing Ni and Cu in their cavities. Both Ni and Cu were chosen as central metals mainly due to their good chelating and stabilizing properties of the formed Pc rings.^[11,120,121]





Scheme 1: Overall synthesis of compounds **12-15**

According to Scheme 1, first we had to synthesize and isolate considerable amounts of Pc **4**. The subsequent steps shown in the Scheme are explained in detail in the following.

1.1.1. Synthesis and spectroscopic characterization of phthalocyanine **4**^[137,138]
(c.f. Scheme 1)

To obtain the phthalocyanine **4** a statistical condensation with a 3:1 stoichiometry was carried out, by reacting 3 equivalents of dinitrile **1** and 1 equivalent of dinitrile **2** with Nickel(II)-acetate in *n*-pentanol at 140 °C for 18 hours, in the presence of catalytic amounts of DBU, as shown in Figure 23.

The products shown in Figure 23 were separated by chromatography over silica gel. The first fraction, which was the **AAAA**-isomer **3**, was eluted with dichloromethane (DCM). After the collection of the first fraction, the second, which was the desired fraction, was eluted (compound **4**), using the same solvent. Chromatography was continued, but the subsequent fractions were eluted all together with a mixture of DCM:ethyl acetate (4:1), since the rest of the products were not necessary for our purpose.

The ¹H-NMR spectrum of phthalocyanine **4** show the expected aggregation and broadening of the signals. The multiplets of the 2-ethylhexyloxy substituents present an unstructured signal between 1.05 and 2.08 ppm. The aromatic signals, in spite of the broadening, appear as singlets. The protons of the epoxynaphthalene bridge are found at 6.24

ppm, while the protons from carbons 9 and 12 appear at 8.23 ppm, and the protons from carbon 4 at 8.80 ppm (see Figure 23, compound **4**).

The ^{13}C -NMR spectrum shows all the characteristic signals, especially the epoxynaphthalene fragment at 82.7 ppm (see experimental, page 72).

In the UV/Vis spectra of phthalocyanines, besides the intense Q-bands (650-750 nm), the Soret-band appears between 300 and 400 nm. Both bands are due to π - π^* transitions in the 18- π electron systems of the macrocycle.^[140,141] The Q-bands are assigned to HOMO-LUMO transitions (Q_{0-0}). Near this Q-band other transitions, with lower intensity, of vibrational levels can also be found (Q_{1-0} , Q_{2-0} , etc...). In the case of **4**, the UV/Vis spectrum shows the Q-bands (Q_{0-0}) at 665 nm, and Q_{1-0} at 601 nm. The typical B-band appears at 401 nm.

1.1.2. Synthesis and spectroscopic characterization of phthalocyanine **9**^[137,138]

(c.f. Scheme 1)

Compound **4** and tetraphenylcyclopentadien-1-one (tetracyclone) were dissolved in dry toluene and stirred at 70°C for 4 days. Compound **9** was obtained in 89% yield after chromatographic work-up. The ^1H -NMR spectrum of **9** shows the characteristic signals from the phenyl protons in the aromatic region between 6.33 and 7.68 ppm, as well as the alkyloxy chains in the non aromatic region, between 1.00 and 2.06 ppm. The ^{13}C -NMR shows also the characteristic C=O signal at 196.6 ppm, among the other assigned signals (see experimental, page 73). The IR spectrum of **9** shows clearly the C=O band at 1780 cm^{-1} . The UV/Vis spectrum, when compared to its precursor, **4**, shows a five nm red-shift, from 665.0 nm in **4** to 670.0 nm in **9**, for the Q-band.

1.1.3. Synthesis and spectroscopic characterization of phthalocyanine **10**^[137,138]

(c.f. Scheme1)

The reaction of **9** with fumaronitrile in *o*-xylene at 140° C afforded compound **10** in 93% yield. The reaction proceeds via the intermediate **9a** (see Scheme 1) which is formed from **9** (with formation of tetraphenylbenzene), reacting then with fumaronitrile to give **10**. The ^1H -NMR spectrum of **10** shows the loss of the phenyl protons from the previous step, which were replaced by the protons that are adjacent to the cyano groups on the nonaromatic ring, at 3.76 ppm. The ^{13}C -NMR shows also the characteristic CN signal at 116.3 ppm, among the other assigned signals (see experimental, page 74). The UV/Vis spectrum exhibits a five nm red-shift, to 676.0 nm, when compared to its precursor, **9**, for the Q-band.

1.1.4. Synthesis and spectroscopic characterization of phthalocyanine **11**^[137,138]

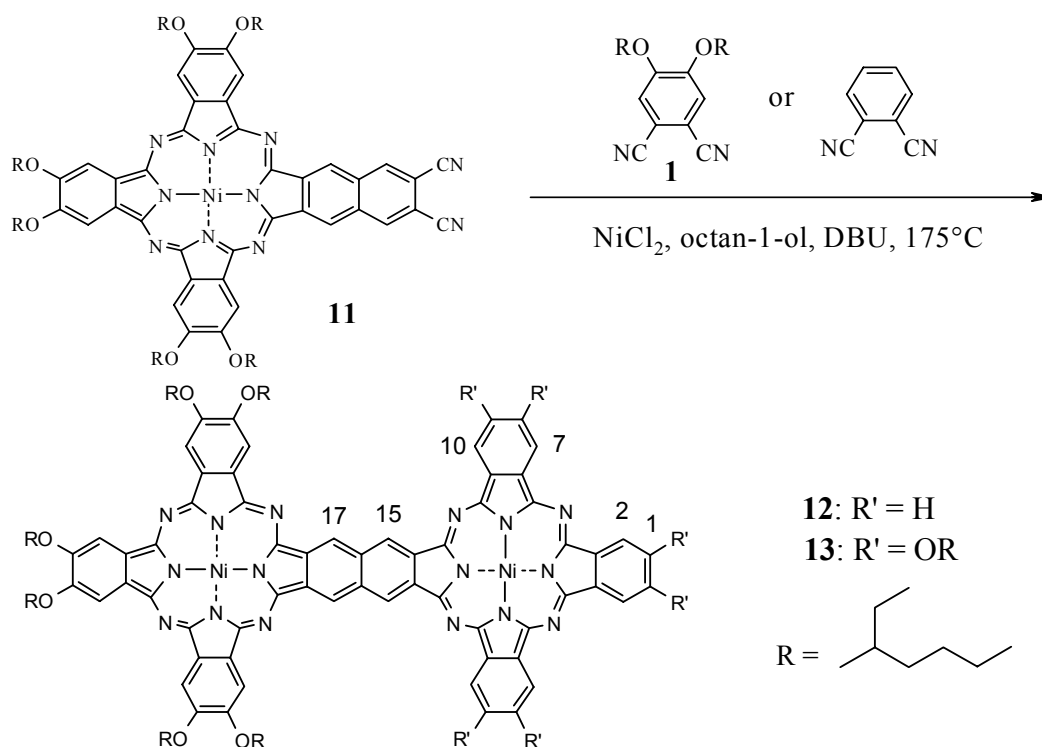
(c.f. Scheme1)

Dehydration of **10** with DBU in anhydrous toluene leads to **11** in 94% yield. A downfield shifted singlet for the protons from the epoxy bridge is observed (see experimental, page 74). The UV/Vis spectrum has a bathochromic shift of 25 nm, to 700.5 nm for the Q-band, due to an increased conjugation of the molecule, when compared to its precursor, **10**.

1.2. Ni/Ni binuclear metal-phthalocyanines **12** and **13**

1.2.1. Synthesis and spectroscopic characterization of the binuclear phthalocyanines **12** and **13**

Pc **11** was reacted with the appropriate dinitrile [phthalonitrile or 4,5-bis(2-ethylhexyloxy)-1,2-phthalonitrile (**1**)] in a statistical condensation approach in order to form the “second phthalocyanine ring” in **12** and **13** (Scheme 2).



Scheme 2: Binuclear phthalocyanines **12** and **13**

In general, as previously discussed (page 28), in a reaction of two different dinitriles **A** and **B**, six different products can be expected. However, in the reaction of one equivalent of **11**, with four equivalents of phthalonitrile or phthalonitrile **1** and NiCl₂ in octanol in the presence of catalytic amounts of 1,8-diazabicyclo[5.4.0]-undec-7-ene (DBU), only the **AAAB** and **AAAA** products were formed. The other isomers, e.g. **AABB** or **ABAB** are not obtained due to the high steric demand of dinitrile **11** (**B**) in the process of the chelating ring formation. Pure **11** does not form any **BBBB**-product in presence of NiCl₂. Force field calculations carried out on the hypothetical **BBBB**-isomer (Hyper Chem 5.0) showed very high steric crowding of this isomer, as depicted in Figures 24 and 25. Separation of the **AAAB** and **AAAA** isomers, in case of **12** and **13**, was performed by column chromatography on silica gel,^[73] with further purification by extracting the **AAAB** products (**12** or **13**) with methanol several times. Were obtained yields of 23% and 20% for **12** and **13**, respectively.

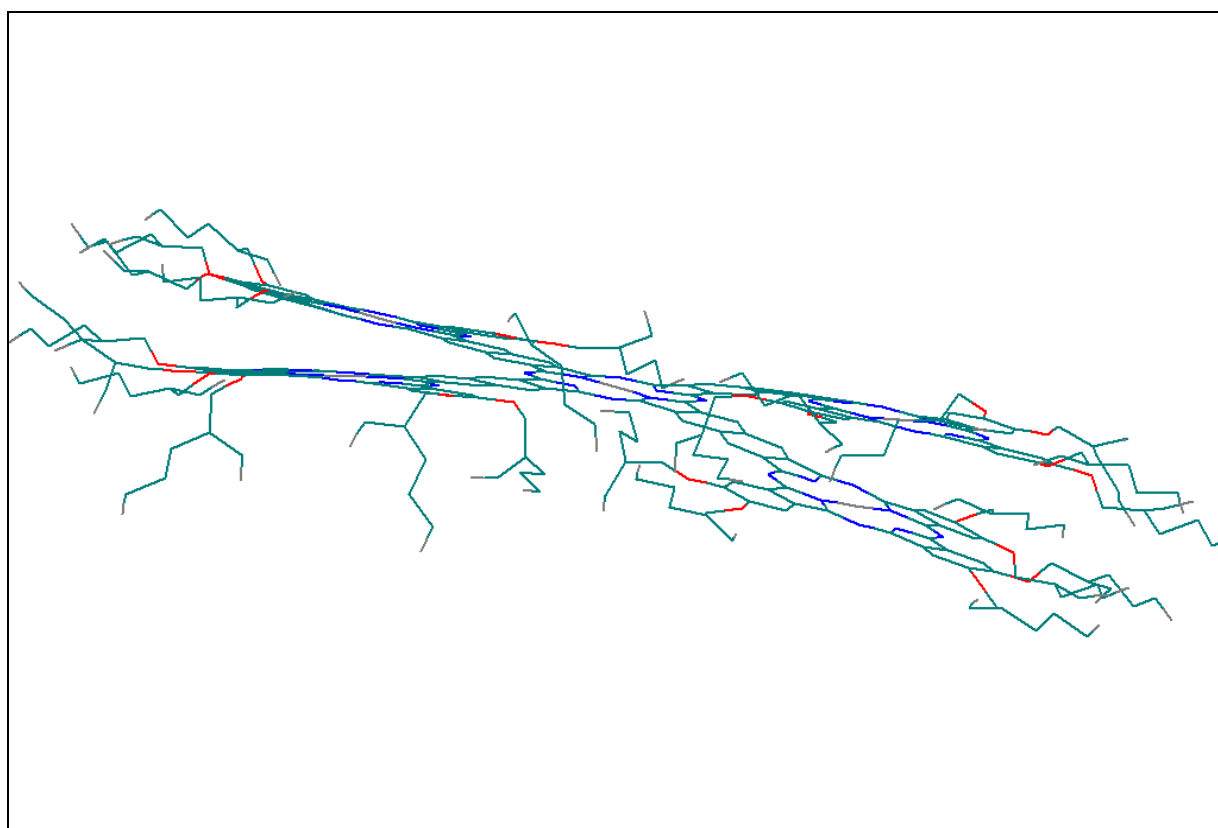
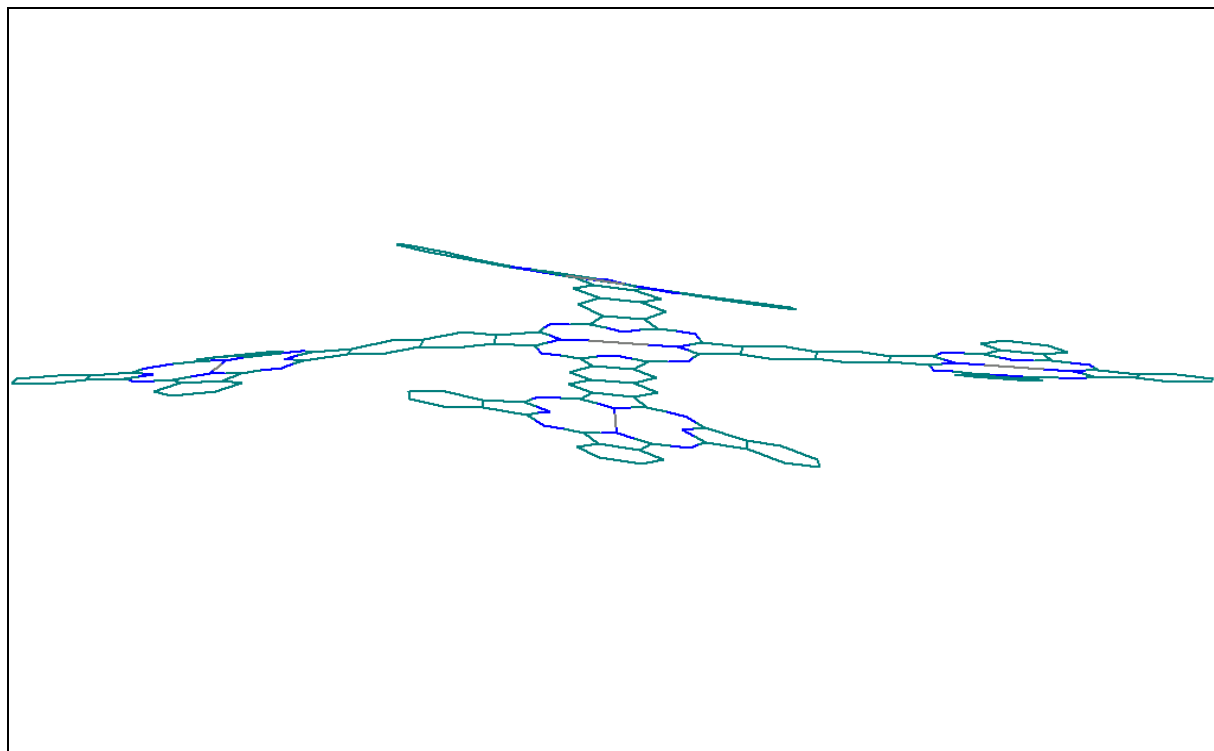
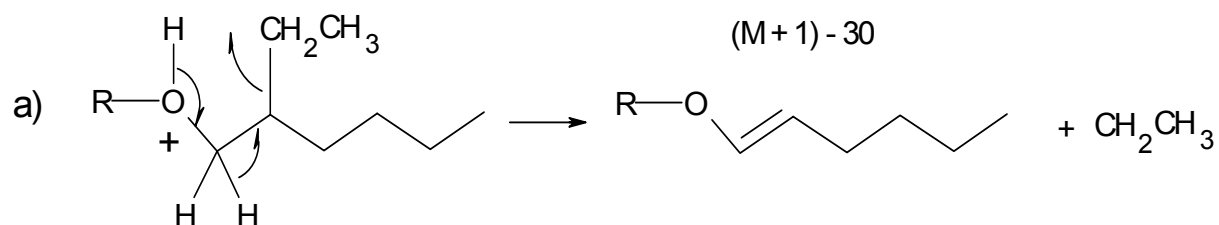


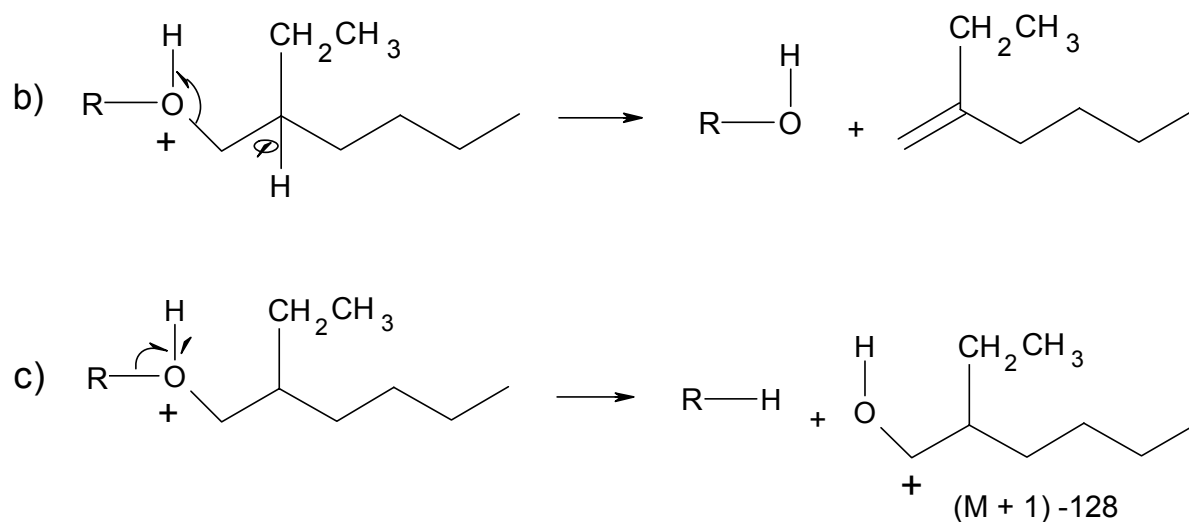
Figure 24: Steric crowding of the **BBBB** isomer.



Figures 25: Rings relative orientation of the **BBBB** isomer (without the 2-ethylhexyloxy substituents).

The binuclear phthalocyanine 2-ethylhexyloxy substituents in **12** and **13** lead to a characteristic fragmentation under the measurement conditions of FAB-MS.^[130] Compounds **12** (unsymmetrically substituted macrocycle) and **13** (symmetrically substituted macrocycle) show the same fragmentation pattern (Scheme 3), corresponding to the molecular peak with loss of two substituents as the highest signal, followed by the loss of other fragments in a common pattern (see experimental, pages 76/77).





Scheme 3: 2-Ethylhexyloxy substituents fragmentation mechanism

The ^1H NMR of **12** and **13** (Ni – Ni binuclear Pc's) exhibit relatively broad peaks of the Pc substituents (2-ethylhexyloxy groups) and broad aromatic signals in the region between 6.80 and 8.80 nm. The broadening is caused by the essentially flat nature of the molecules leading to aggregation. While the ^1H NMR spectrum of **12** shows several merged peaks in the aromatic region mainly due to its aggregation and asymmetry (see experimental, pages 76/77), compound **13** with its symmetric structure, has less aggregated peaks (Figure 26). The protons from C-2 and C-7 carbons are shown at 8.82 ppm (see Scheme 2 for numbering), while the C-10 protons are assigned at 8.53 ppm. The C-15 and C-17 protons are shown at 8.20 ppm. Also the ^{13}C -NMR spectra of the same type of compounds are quite different. The symmetry present in the structure of **13**, leads to less similar peaks, while **12** (Figure 27), in spite of its aggregation, shows the aromatic carbon peaks for C-2, C-7 and C-10 around 104 ppm. Carbons C-15 and C-17 are allocated at 124.7 and 125.1, respectively, while the C-3, C-6, C-11, C-14 and C-16 carbons are assigned between 129.0 and 133.5 ppm. The C-4, C-5, C-12 and C-13 carbons are shown between 136.0 and 142.0, while the alkyloxy substituted aromatic carbons C-23, C-24, C-31 can also be assigned around 153 ppm.

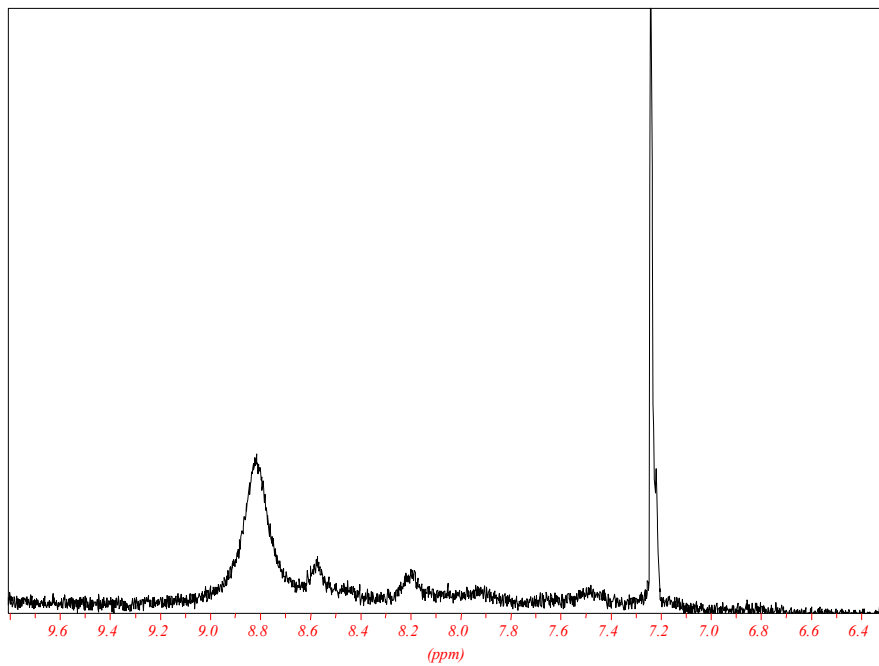


Figure 26: ¹H-NMR spectrum of **13** (aromatic region)

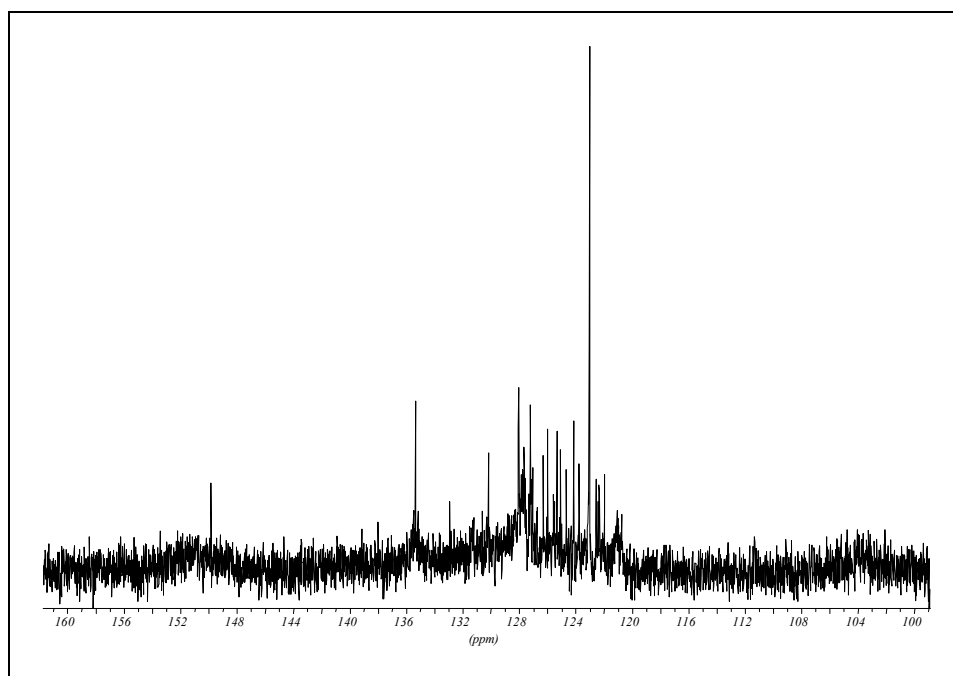


Figure 27: ¹³C-NMR spectrum of **12** (aromatic region)

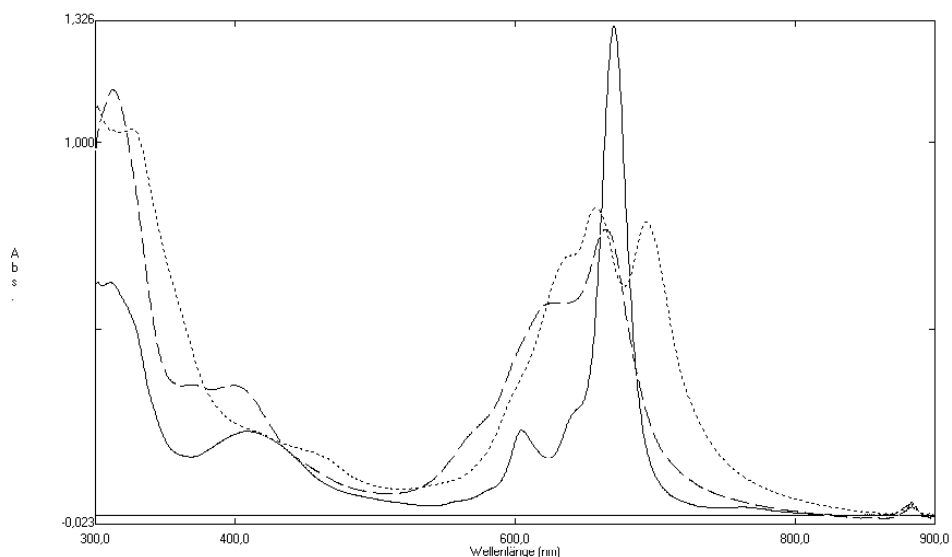


Figure 28: UV/Vis spectra of compounds **12** (·····), **13** (----) and **3** (—) for comparison

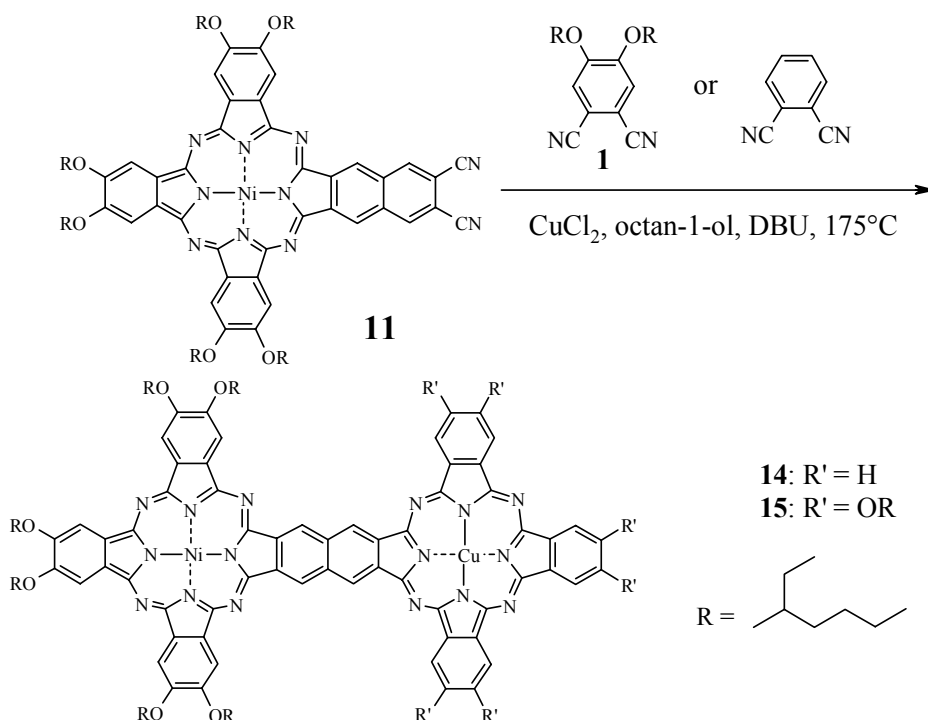
The UV/Vis spectra of **12** and **13** in CH₂Cl₂ show the Q-band maxima at 697.5 and 664.5 nm, respectively (Figure 28). In comparison to the monomeric (RO)₈PcNi (**3**, Figure 23) (AAAA product, R = 2-ethylhexyl), broad absorptions in the Q-band region can be seen in **12** and **13** due to aggregation, which differ characteristically from the sharp peaks of the monomeric phthalocyanine **3**. No or only a small red shift is observed for the Q-bands of **12** and **13**. This points to little π -electron delocalisation in the binuclear systems **12** and **13**, showing an almost independent behaviour of the two Pc-rings, in terms of their UV/Vis spectra. When comparing the spectra of **12**, **13** and (RO)₈PcNi (**3**), a blue shift from the (RO)₈PcNi (670.0 nm) to **13** (664.5 nm), and a red shift going from (RO)₈PcNi (670.0 nm) to **12** (697.5 nm) can be observed.

1.3. Ni/Cu binuclear metal-phthalocyanines **14** and **15**

1.3.1. Synthesis and spectroscopic characterization of binuclear phthalocyanines **14** and **15** (Scheme 4)

The preparation of the binuclear Pc's **14** and **15** was carried out by a similar method to that of **12** and **13**, by reacting one equivalent of **11**, with four equivalents of the corresponding dinitriles [phthalonitrile or 4,5-bis(2-ethylhexyloxy)-phthalonitrile (**1**)] respectively, and CuCl₂ in octanol in the presence of catalytic amounts of DBU (Scheme 4). Separation of the products was performed, as shown previously, by column chromatography on silica gel, and further purification was achieved by extracting the product with methanol several times. The

bimetallic compounds **14** and **15** were isolated in pure form in a yield of 20 and 18%, respectively, based on **11**.



Scheme 4: Binuclear phthalocyanines **14** and **15**

Atomic absorption spectroscopy (AAS) was used for further characterization of **14** and **15**, specially to prove the presence of two different metals in these Pc's.

1.3.1.1. Atomic Absorption Spectroscopy - a simple and effective method for qualitative and quantitative determination of metals^[142,143]

Atomic absorption spectroscopy (AAS) is an analytical method for qualitative and quantitative determination of most of the metals and metalloid elements from the periodic table. It is a technique in which gaseous ground state atoms absorb electromagnetic radiation at a specific wavelength to produce a corresponding measurable signal. The absorption signal corresponds to the concentration of the ground state atoms present in the optical path. The method used by us, flame atomic absorption, is one of the most widely used techniques for trace metal analysis, reflecting its simplicity of use and relative freedom from interferences. The sample, usually in solution is sprayed into the flame by means of a nebulizer with generation of an aerosol.

The type of flame employed was a premixed combustion flame consisting of acetylene as fuel and air as oxidant gas. This premixed flame is stable, simple to operate and produces enough atomisation to enable good sensitivity and freedom from most of interferences. A lamp is used for irradiation of this flame. The radiation lamp used was a demountable hollow-cathode lamp, which is a low-pressure gaseous discharge tube in that only the cathode needs to be changed when going from one element to another.

All light-absorbing methods follow the Lambert-Beer law, which states, in terms of AAS, that a light beam passing through a mass of absorbing gas decreases exponentially in intensity as the number of reacting atoms is summed up arithmetically. The expression of this law is:

$$I_x = I_0 \times 10^{-KC}$$

where I_0 is the intensity of the entering beam, I_x the intensity of the emerging beam, C the concentration of atoms that the beam encounters, and K a constant including such variables as path length and temperature.

Flame Atomic Absorption Spectroscopy (FAAS)^[142,143] was also used for the quantitative determination of the metals Ni and Cu in **14** and **15**.

Three standard solutions of both nickel(II) acetylacetonate and copper chloride at fixed concentrations were prepared, using THF as solvent, in order to calculate a calibration curve. Note that the concentration ($\mu\text{g/l}$) was calculated to the metal in the salt, e.g. $10 \mu\text{g/l}$ of Cu in CuCl_2 solution. Then a solution of respectively **14** and **15** in THF was prepared. The absorbance values for the standard solutions were then measured, followed by measurement of the solutions of **14** and **15**. The calibration curves were then plotted (Figure 29) and the effective concentration of Ni and Cu in **14** and **15** calculated. The values for the absorbance for the respective concentrations of the metal salts are listed also in Table 2, as well as the values recorded for the solutions of **14** and **15** in Table 3.

From the calibration curve equations, which were calculated as the logarithmical approximation curves, (Table 2) the concentration of Ni and Cu in each binuclear Pc (Figure 29) was calculated. For **14** the calculated value was a concentration of $1.9 \mu\text{g/l}$ of Ni and $2.3 \mu\text{g/l}$ of Cu. For **15** the value found was $1.8 \mu\text{g/l}$ for Ni and $2.1 \mu\text{g/l}$ for Cu. This values are in agreement with the difference in molecular weight of Ni ($58,69 \text{ g/mol}$) and Cu (63.55 g/mol), and therefore of the difference of the concentration of both metals.

Table 2: Values of absorbance recorded for the solutions of the metal salts Ni-(II) acetylacetonate and CuCl₂, as well as its respective calibration curve equations

Compound	Concentration ($\mu\text{g/l}$)	Absorbance (a. u.)	Calibration curve
Ni-(II) acetylacetonate	2	0.429	$y = 0.4995\ln(x) + 0.1177$
	10	0.810	
	20	1.098	
CuCl ₂	2	0.357	$y = 0.5532\ln(x) + 0.0052$
	10	1.384	
	20	1.589	

Table 3: Values of absorbance recorded for the solutions of **14 and **15****

Compound	Absorbance value for Ni ion (a. u.)	Absorbance value for Cu ion (a. u.)
14	0.438	0.467
15	0.399	0.410

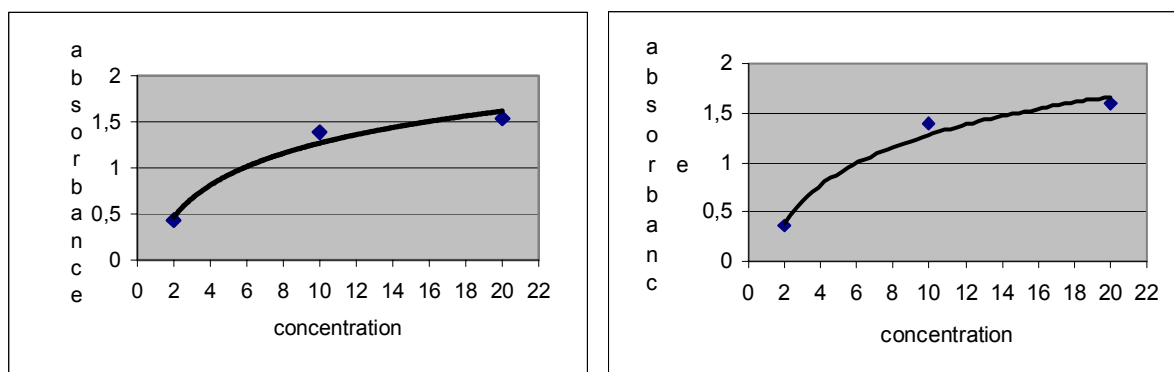


Figure 29: Calibration curve for a) Ni salt solutions and b) Cu salt solutions (absorbance in arbitrary units (a. u.) and concentration in $\mu\text{g/l}$)

The ¹H NMR and ¹³C NMR spectra of **14** and **15** (Ni/Cu binuclear Pc's), show extremely broad and weak resonances, due to the paramagnetism of Cu and aggregation of the molecules. However, the characteristic peaks for **14** and **15** could be detected (see experimental, pages 78/79).

The UV/Vis spectra of all the binuclear phthalocyanines **12–15**, are compared in the following. The UV/Vis maxima of **12–15** measured in CH₂Cl₂ are listed in Table 4. In comparison with the monomeric Pc's (RO)₈PcNi (**3**) and (RO)₈PcCu (R = 2-ethylhexyl),

broad absorptions in the Q-band region are observed for **12–15** due to aggregation, which differ characteristically from the sharp peaks of the monomeric PcMs (RO)₈PcNi (**3**) and (RO)₈PcCu. No or only a small red shift is observed for the Q-bands in PcMs **12–15**, which points to only little π -electron delocalisation in the binuclear systems, as described for the Ni/Ni binuclear Pc's **12** and **13** before. Thereby they show an almost independent behaviour of the two Pc-rings, in terms of the UV/Vis absorption spectra. Only a small shift to lower wavelength of the Q-band is observed going from **14** to **12**, and from **15** to **13**, respectively. This can be explained by the influence of Cu in the binuclear Pc, also supported by the observed shift to lower wavelength when comparing (RO)₈PcCu and (RO)₈PcNi (**3**) (Table 4). In the cases of **12** and **14**, the distance between the first and the second maxima of Q-band, which is characteristic for unsymmetrically substituted phthalocyanines, increases going from **12** to **14**. This is due to the presence of different metals in the binuclear Pc **14**. This shift is more evident comparing **13** with **15**, since these compounds are symmetric, and therefore, the dependence can be assigned to the metal interaction only. A blue shift of the Q-band maxima is observed between (RO)₈PcCu and (RO)₈PcNi (**3**) by 9 nm, the same effect can be seen between **14** and **15**, however to a lesser extent. When we compare the spectra of **14**, **15** and (RO)₈PcCu, a blue shift going from the (RO)₈PcCu to **15**, and a red shift going from (OR)₈PcCu to **14** can be observed. Likewise, the same effect can be detected when comparing (RO)₈PcNi (**3**) with **13** and **12**, respectively.

Table 4: Values of Q and B transition absorption for the list of compounds.

Compound	Q ₀₋₁ (nm)	Q ₀₋₀ (nm)	Q ₁₋₁ (nm)	B ₀₋₀ (nm)	B ₀₋₁ (nm)
12	697.5	669.0	640.0 (sh)	-----	321.0
13	664.5	626.0 (sh)	-----	-----	312.5
14	699.5	661.0	638.0 (sh)	-----	326.0
15	672.5	631.0 (sh)	-----	-----	304.0
(RO)₈PcCu	679.0	611.5 (sh)	-----	418.0	339.5
(RO)₈PcNi	670.0	604.0 (sh)	-----	410.0	310.0

a) All the spectra were recorded in CH₂Cl₂ as solvent. (R = 2-ethylhexyl)

2. Binuclear metal phthalocyanines for optical limiting purposes

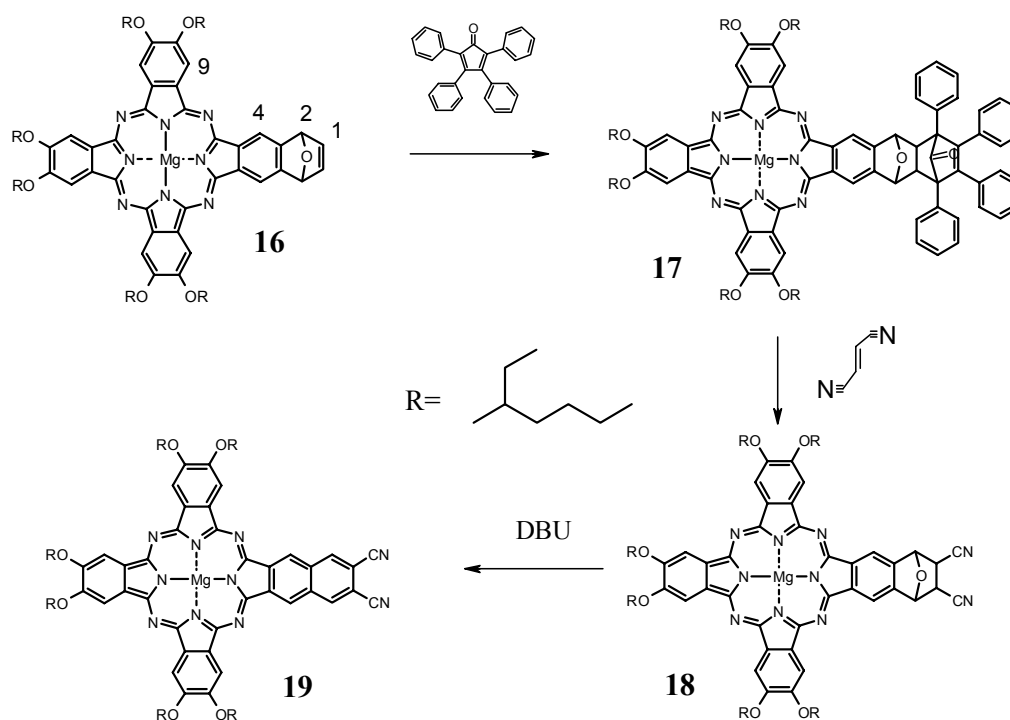
The design of binuclear metal phthalocyanines in order to achieve effective optical limiting materials lead us to the previously discussed methods for the preparation of such materials (page 31 ff). Because phthalocyanines with In or Ga as central metal are known to have good optical limiting performances,^[4,95,101,109] we directed our research now to the

synthesis of this type of binuclear metal phthalocyanines using the same approach as described for the synthesis of Ni/Ni and Ni/Cu binuclear Pc's (**12**, **14**) (c.f. page 31 ff).

To achieve the functionalized dicyano substituted phthalocyanine **19**, (Scheme 5) but with InCl or GaCl as central moieties is expected to be difficult, due to the poor stability of this moieties against the number of steps which are necessary to obtain these corresponding binuclear metal phthalocyanines.

To solve this problem an approach was used in which InCl or GaCl can be inserted in the final step, avoiding the expectable big losses of material throughout all steps shown in Scheme 2. Following the method developed by S. Vagin in our laboratory^[100,144] we synthesized and isolated compound **16**, containing Mg as central metal, in reasonably large amounts using the same method as described before. The further steps were carried out as described for the analogue Ni compounds. Since magnesium (Mg) is a relatively easy metal to remove^[100,144], this step could be done after achieving the Mg/Mg binuclear phthalocyanine (**20**) shown in Scheme 10 on page 49. The metal free binuclear phthalocyanine **21**, is than the starting material for the preparation of suitable optical limiting effective metal binuclear phthalocyanines **22** and **23** containing InCl or GaCl, respectively.

2.1. Synthesis of the unsymmetrically functionalized [2,3,9,10,16,17-hexa-2-ethylhexyloxy-25,26 dicyano phthalocyaninato] magnesium **19**



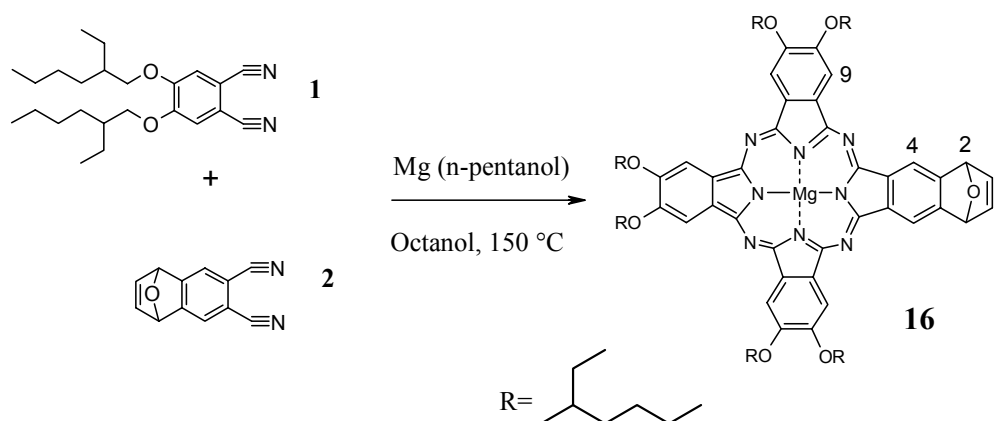
Scheme 5: Overall synthesis to obtain compound **19**

The synthesis of compounds **16–19** (Scheme 5) was accomplished by similar methods used earlier in the case of the binuclear nickel Pc's. The target compounds in each step are structurally similar. Consequently, the spectroscopic characterization of these Pc's is very also similar.

2.1.1. Synthesis and spectroscopic characterization of phthalocyanine 16

A statistical condensation with 3:1 stoichiometry was carried out to obtain phthalocyanine **16**, by reacting 3 equivalents of the dinitrile **1** with 1 equivalent of phthalonitrile **2** with magnesium(II) pentanolate in n-octanol at 150 °C, for 24 hours (Scheme 6). After chromatographic workup **16** was obtained, besides the other statistical products (see page 29).

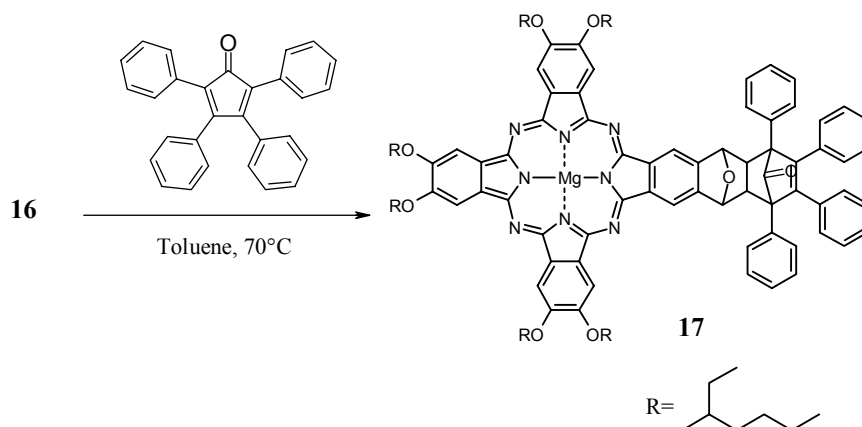
The ¹H-NMR spectrum of phthalocyanine **16** shows, as pointed out before for the corresponding Ni-compound **4**, the predictable aggregation and broadening of the signals. The identification and assignment of the peaks were easier when the ¹H- and ¹³C-NMR spectra were recorded in deuterated THF as solvent, since this solvent forms a complex with the magnesium phthalocyanine, reducing the level of aggregation, as well as the observation of a downfield shifting in NMR (see experimental, page 80). In the ¹H- NMR spectrum the 2-ethylhexyloxy substituents are shown between 0.95 and 2.05 ppm, plus the OCH₂ groups at 4.49 ppm. At 7.83 ppm appear the protons from the epoxide bridge (see Scheme 6 for numbering), while the H-1 protons appear at 8.58 ppm. The H-9 and H-4 protons appear at 9.09 and 10.00 ppm, respectively.



Scheme 6: Synthesis of **16**

2.1.2. Synthesis and spectroscopic characterization of phthalocyanine 17

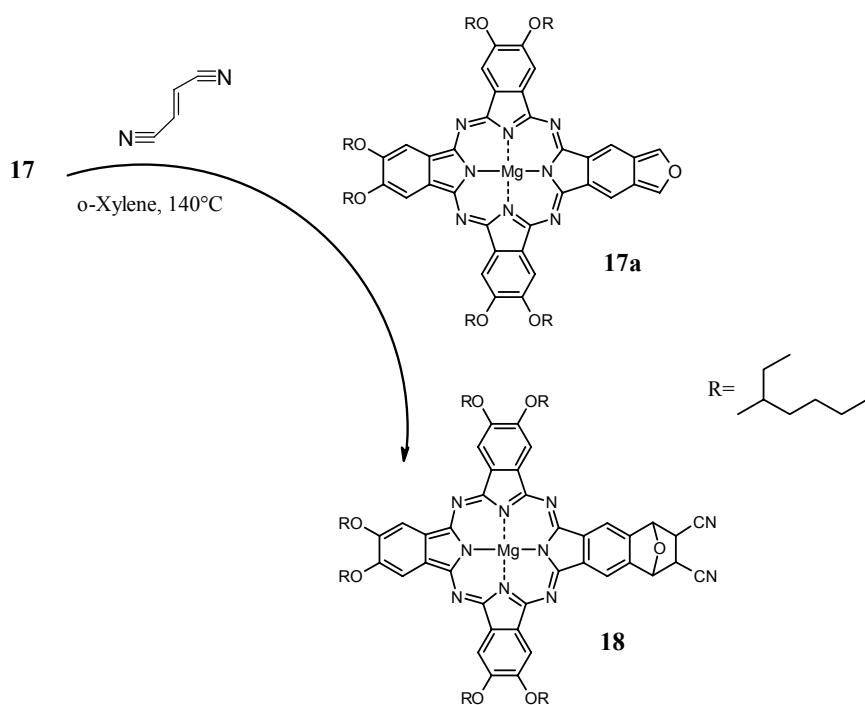
Compound **16** and tetraphenylcyclopentadien-1-one were dissolved in dry toluene and stirred at 70°C for 4 days to obtain **17** in 89% yield (Scheme 7). The $^1\text{H-NMR}$ spectrum of **17** shows the characteristic signals of the phenyl protons in the aromatic region, between 6.94 and 7.67 ppm, as well as the alkyloxy chains in the nonaromatic region, between 0.81 and 2.40 ppm, while the $^{13}\text{C-NMR}$ spectrum presents the characteristic C=O signal at 196.6 ppm, among the other assigned signals (see experimental, page 81). The IR spectrum of **17** also reveal clearly the C=O band at 1780 cm^{-1} . The UV/Vis spectrum shows a two nm red-shift, from 682.5 in **16** to 685.0 nm in **17**.



Scheme 7: Synthesis of **17**

2.1.3. Synthesis and spectroscopic characterization of phthalocyanine 18

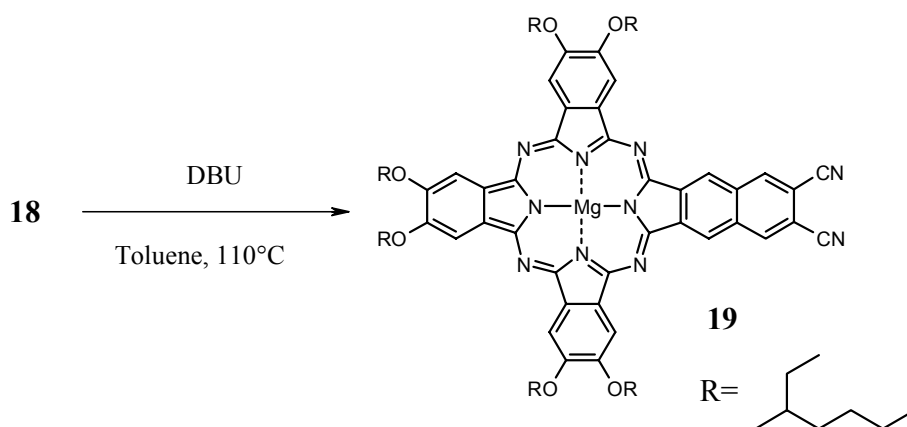
The reaction of **17** with fumaronitrile in *o*-xylene at 140°C via the appropriate intermediate **17a** which is formed from **17**, giving tetraphenylbenzene. Subsequently it reacted with fumaronitrile, (Scheme 8) affording compound **18** in 93% yield. The $^1\text{H-NMR}$ spectrum of **18** shows the loss of the phenyl protons from the previous step, which were replaced by the protons that are adjacent to the cyano groups on the nonaromatic ring, at 3.25 ppm. The $^{13}\text{C-NMR}$ spectrum presents also the characteristic CN signal at 116.7 ppm, among the other assigned signals (see experimental, page 82). The UV/Vis spectrum shows its Q-band maximum at 686.0 nm.



Scheme 8: Synthesis of **18**

2.1.4. Synthesis and spectroscopic characterization of phthalocyanine **19**

Dehydration of **18** with DBU in anhydrous toluene at 110° C (Scheme 9) afforded **19** in 94% yield. A downfield shifted singlet for the protons corresponding to loss of the epoxy bridge is observed at 8.56 nm (see experimental, page 83). The UV/Vis spectrum shows a bathochromic shift of 25 nm for the Q-band, from 686.0 nm in **18** to 710.5 nm in **19**, due to an increased conjugation of **19**, when compared to its precursor, **18**.

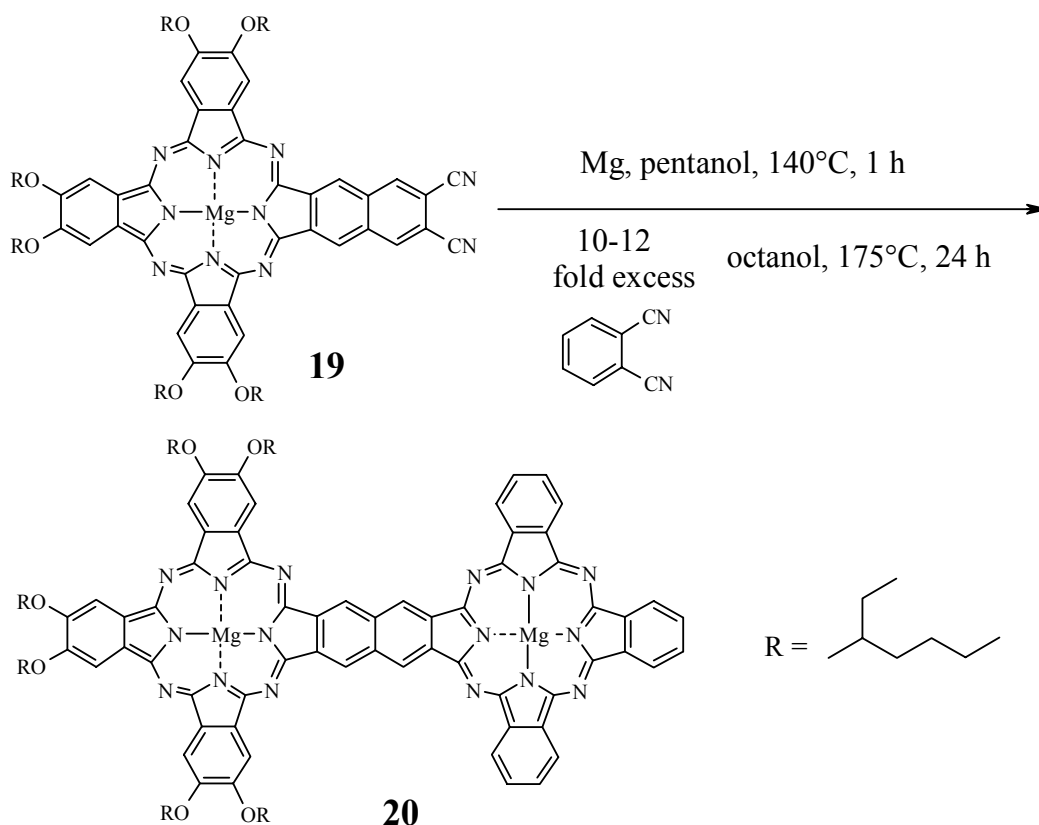


Scheme 9: Synthesis of **19**

2.2. Binuclear metal-phthalocyanines **22** and **23** with InCl and GaCl as central moieties

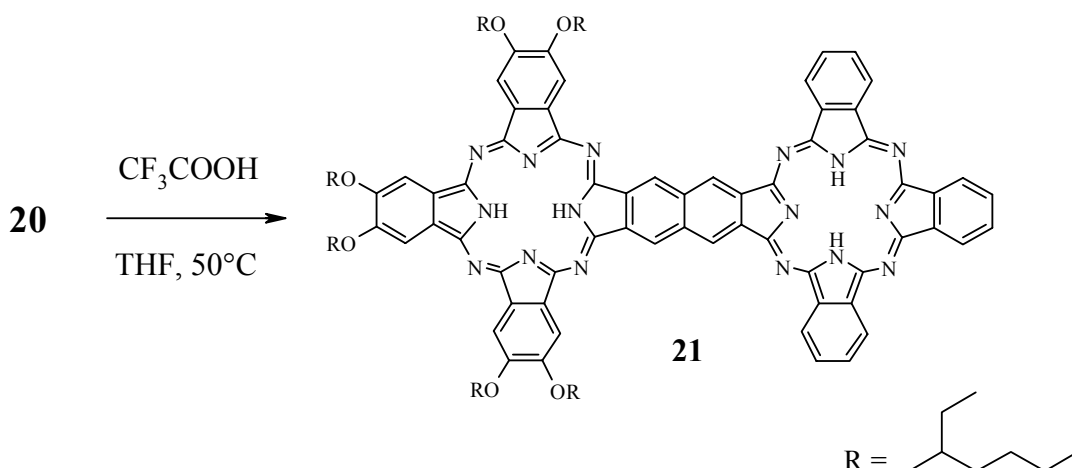
2.2.1. Synthesis of binuclear phthalocyanines **20-23**

A statistical condensation, similar to the one carried out for the formation of the binuclear Ni/Ni and Ni/Cu phthalocyanines **12–15** was used to obtain phthalocyanine **20**, by reacting **19** with a 10-12 fold excess of phthalonitrile **3** and magnesium(II) pentanolate in n-octanol at 175 °C, for 24 hours (Scheme 10). The other main product of this reaction was unsubstituted PcMg, that could be easily separated from **20** by chromatographic workup on silica gel.



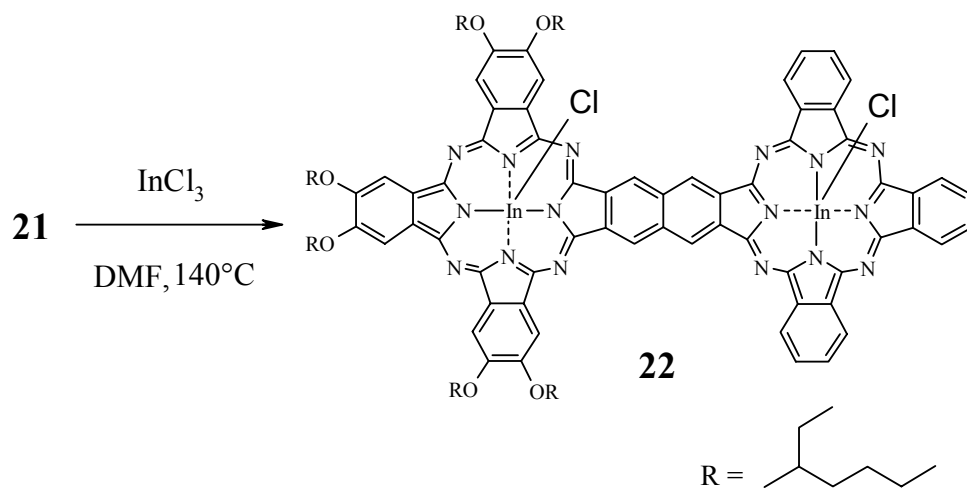
Scheme 10: Binuclear phthalocyanine **20**

The binuclear phthalocyanine **20** was heated with trifluoroacetic acid in THF for 5 hours, to give the metal free compound **21**, which was purified by chromatography on silica gel (Scheme 11). The eluent used to collect the first fraction (**21**) was dichloromethane. The second fraction (unreacted **20**) was eluted afterwards with a mixture dichloromethane–THF (10:1). Compound **21** was then precipitated from methanol/dichloromethane.



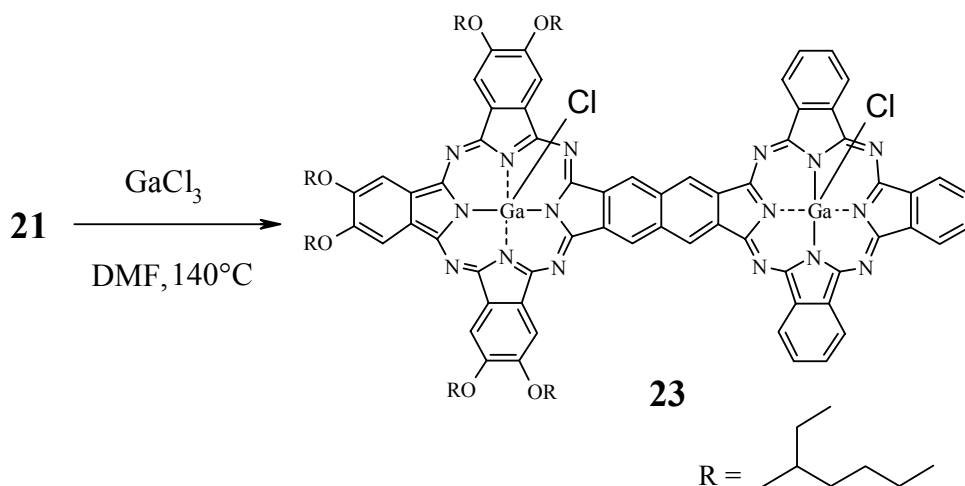
Scheme 11: Binuclear phthalocyanine **21**

A mixture of binuclear Pc **21** and a large excess of InCl_3 in DMF and a small portion of quinoline was heated just below the boiling point of the solvent, in order to obtain compound **22** (Scheme 12). After completion of the reaction (monitored by UV/Vis spectroscopy and thin-layer chromatography) water was added dropwise to the mixture to precipitate the compound. After centrifugation the solid compound was heated in boiling methanol for 1 hour for removal of impurities and collected by filtration.



Scheme 12: Binuclear phthalocyanine **22**

The method used for the preparation of the Ga/Ga compound (**23**) was similar to the one used for preparation of **22**, taking an excess of GaCl_3 (Scheme 13) in this case.



Scheme 13: Binuclear phthalocyanine **23**

2.2.2. Spectroscopic characterization of binuclear phthalocyanines 20–23

The $^1\text{H-NMR}$ spectra of **20**, **22** and **23** are somewhat similar, as expected, since the basic structures of the binuclear Pc's are identical (see Figure 30, for example). The introduction of metals with an axial ligand, (GaCl and InCl, in this case) did not solve the problem of aggregation, typical for this type of compounds, though the Mg/Mg binuclear Pc **20** tends to aggregate even more than the other compounds. This is due to the small size of Mg, and the lack of an axial substituent. Furthermore, since the binuclear Pc's possess one unsubstituted ring, the aggregates can be formed through stacking,^[145] on account of the essentially flat nature of the molecules. The aromatic region of the $^1\text{H-NMR}$ spectra of **20**, **22** and **23** shows merged peaks, due to the aggregation as well as their asymmetry (see experimental, pages 83-87). In Figure 30 it is represented the aromatic region of the $^1\text{H-NMR}$ spectrum of **22**, showing at 6.91 ppm the protons H-25, H-30, H-33 and H-38. At 7.17 and 7.28 ppm the H-17 and H-15 protons can also be seen, respectively. Between 7.40 and 7.90 ppm the H-10, H-9 and H-2 are shown while the H-1 and H-8 protons can be seen around 8.84 ppm.

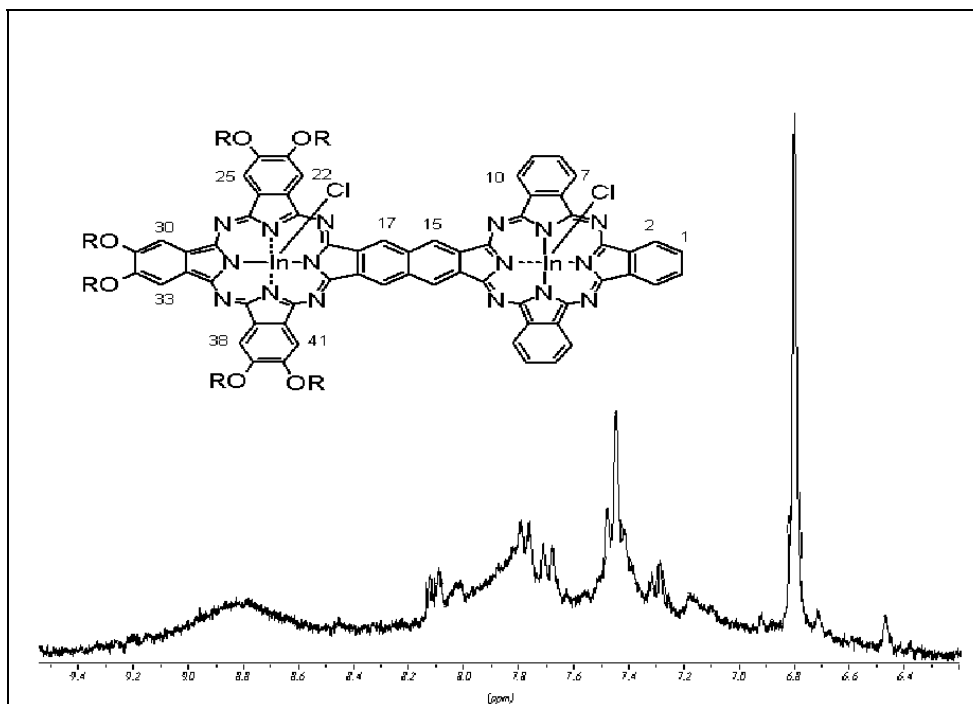


Figure 30: ^1H -NMR spectrum of **22** (aromatic region)

The aggregation is even stronger in the metal free binuclear Pc **21**, especially seen in the aromatic region of its ^1H -NMR spectrum. The characteristic NH peaks can be seen at -0.26 and -0.45 ppm. Since these protons are not equivalent, due to the asymmetry of the molecule, two peaks appear in the referred region.

Also ^{13}C -NMR spectra are very similar for the compounds **20–23**. The assigned carbon peaks appear in the same region for these compounds (see experimental, page 84-87). For instance, the ^{13}C -NMR spectrum of **23** (Figure 31) shows the aromatic carbon peaks for C-22, C-25 and C-30 in the region around 105 ppm. The C-1, C-8, C-9 and C-2, C-7, C-10 carbon atoms of the unsubstituted part of the binuclear Pc can be assigned around 123 ppm and 130 ppm, respectively. Carbons C-15 and C-17 can be allocated at 127.3 and 128.7, respectively. The alkyloxy substituted aromatic carbons C-23, C-24, C-31 can also be assigned around 155 ppm.

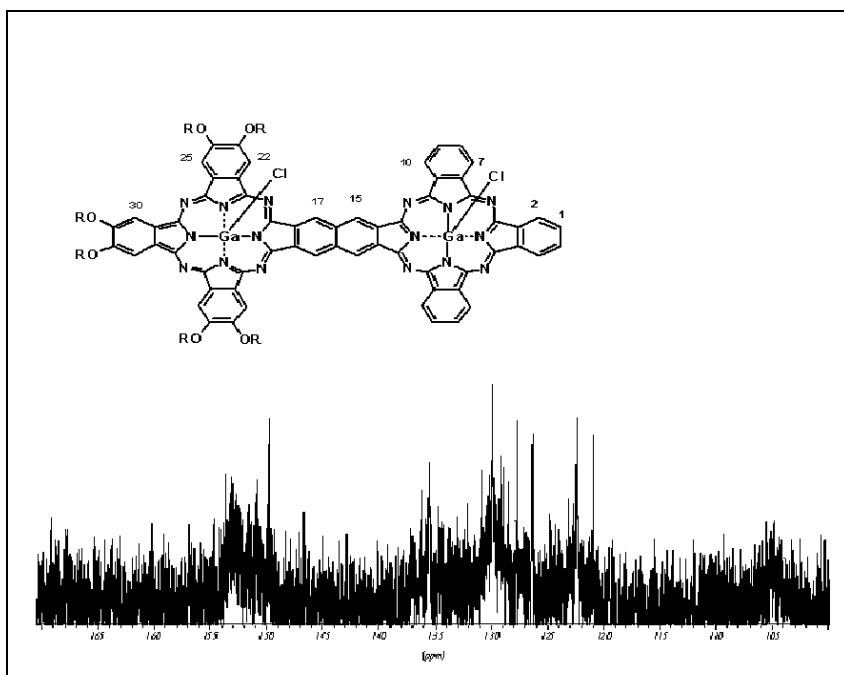


Figure 31: ^{13}C -NMR spectrum of **23** (aromatic region) (R = 2-ethylhexyl)

The IR spectra of compounds **20–23** are resembling to normal phthalocyanines. The important feature is that the IR spectrum of **21** (metal-free binuclear Pc) has the typical NH stretching band at 3298 cm^{-1} , and compounds **22** and **23** show the loss of this band, due to metalation.

In the mass spectra, in spite of the typical fragmentation that occurs when measuring the FAB-MS spectra of these compounds, as discussed before (see pages 36/37), all the peaks could be assigned, as well as the molecular peaks (see experimental).

The formula for **22** and **23** with both axially chlorine in the syn position to each other is arbitrary. We have no information from the spectra whether or not the other isomer with an anti position of the chlorines is also present.

Table 5: Values of Q and B bands in the UV/Vis spectra for **21–27**.

Compound	Q ₀₋₁ (nm)	Q ₀₋₀ (nm)	Q ₁₋₁ (nm)	B ₀₋₀ (nm)	B ₀₋₁ (nm)
20	706.0 (sh)	676.0	652.0 (sh)	432.5	362.0
21	724.0 (sh)	688.0	667.0 (sh)	-----	358.0
22	-----	689.0	663.0	-----	353.0
23	718.5 (sh)	687.0	654.5 (sh)	-----	344.0
24	-----	679.0	613.0 (sh)	-----	360.0
26	-----	698.5	629.5 (sh)	446.0	362.5
27	-----	694.5	625.0 (sh)	441.0	357.5

a) All the spectra were recorded in CH_2Cl_2 as solvent. (R = 2-ethylhexyl)

The UV/Vis maxima of **20-23** measured in CH₂Cl₂ are given in Table 5. Compounds **24** [(RO)₈PcMg], **26** [(RO)₈PcInCl] and **27** [(RO)₈PcGaCl], which will be discussed later, are also included in Table 5. When comparing the binuclear Pc's with the respective monomers (**20** with **24**, **22** with **26** and **23** with **27**), there is no red-shift for the more intense peak of the Q-band for the binuclear Pc's **20-23**. The shoulders show a red-shift of the band of approximately 25 in all cases. As can be seen for the monomers, in which their UV/Vis spectra shows a red-shift when going from **24** to **26**, passing through **27**, the binuclear Pc's also present the same feature, i.e. a red shift can be observed going from the Mg/Mg binuclear Pc, passing through the Ga/Ga binuclear Pc and the In/In binuclear Pc (Figure 32). Comparing these unsymmetrical compounds with the also previously discussed Ni/Ni binuclear Pc **12** and Ni/Cu binuclear Pc **14** (page 43-table 4) we can observe and confirm that the asymmetry in this type of compounds plays an important role in their UV/Vis absorption features. Also the employed type of central moiety in these compounds determines the observed UV/Vis characteristics. Independent of the kind of peripheral substituents present in the Pc ring, (RO)₈PcInCl always shows a red shift of the Q-band, compared to the analogous (RO)₈PcGaCl, and even more pronounced than that of (RO)₈PcMg or (RO)₈PcNi and (RO)₈PcCu. Therefore, the observed red-shift is due to the influence of the different central moieties, but not as shown earlier to an extended delocalization in the ring π-electrons.

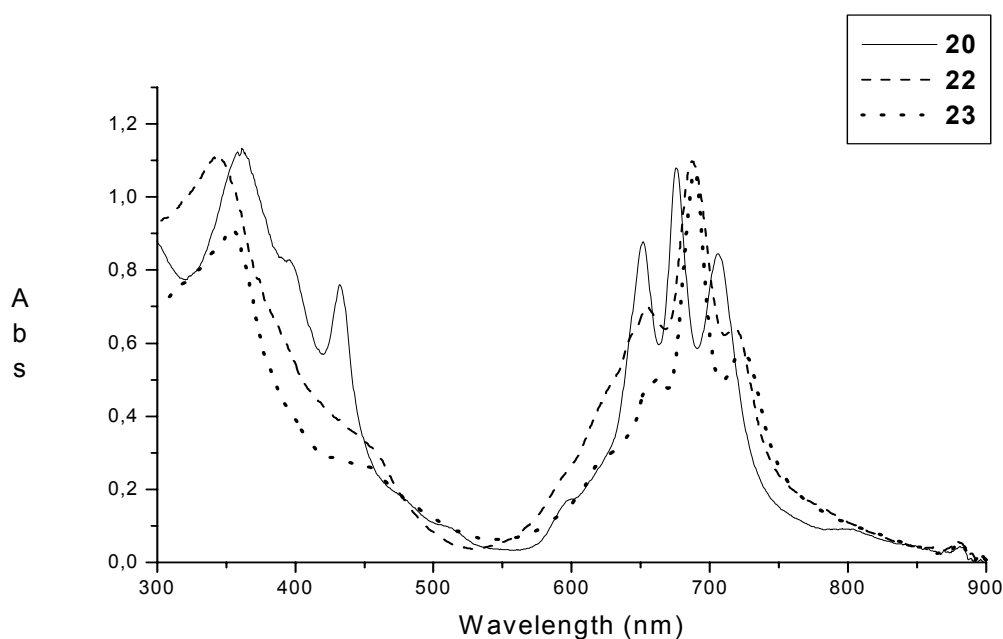


Figure 32: UV/Vis spectra of compounds **20** (—), **22** (----) and **23** (.....) for comparison

The metal-free binuclear Pc **21** also has a very different UV/Vis spectrum, when compared with the mononuclear metal free Pc's. The characteristic double Q-band of the compounds is hardly observable in **21**, as already described by other authors.^[129]

3. Synthesis of octaalkoxy substituted Ga, In and Tl Pc's

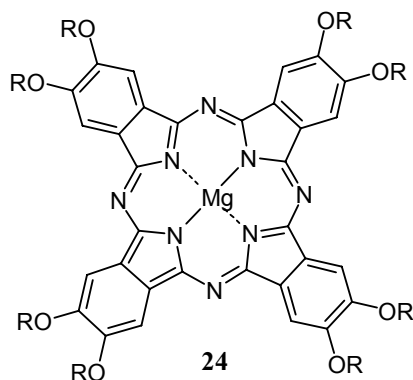
Recently, the substituent effect in several Pc's was studied in our laboratory.^[106] Pc - based materials possessing strong electron withdrawing substituents like fluorine or trifluoromethyl at the peripheral positions show low optical transmission at high levels of irradiation.^[106] To our knowledge, only in few cases previous to this referred work a possible electronic effect of the peripheral substituents features on the optical limiting properties of a Pc macrocycle were taken in consideration.^[146-148] Here we give some additional contribution to this issue. Electron withdrawing groups in conjugated molecules increase their oxidation potential, consequently increasing the chemical stability of these systems against e.g. oxidation due to intense light.^[106]

Octasubstituted Pc's with electron donating substituents and GaCl and InCl as central moieties have not been discussed before. Therefore a comparison of these compounds with the state of art molecule (*t*Bu₄)PcInCl was another scope of this work.

The comparison of the OL properties of Pc's with Ga and In as central moieties has been studied very much in detail by our group. However, due to the synthetic difficulties, the last element of this group, namely Thallium (Tl) has not been studied so far, except in one case.^[149] For the first time we synthesized an octaalkoxy substituted thallium–Pc–compound, namely (RO)₈PcTlX with R = 2-ethylhexyl and X = OCOCF₃.

Octa-(2-ethylhexyloxy)phthalocyaninato magnesium (**24**) is used for obtaining these compounds because treating the alkoxy substituted phthalonitrile directly with GaCl₃, InCl₃ or Tl(CF₃COOH)₃ proceeds only with difficulties. Using a similar approach to the one previously applied for the preparation of the In/In and Ga/Ga binuclear Pc's **22** and **23**, Mg is removed from **24**, yielding **25**. The octa-(2-ethylhexyloxy)phthalocyanine (**25**) is then treated with the corresponding metal salt, in order to obtain the desired metallated Pc's **26**, **27** and **28**.

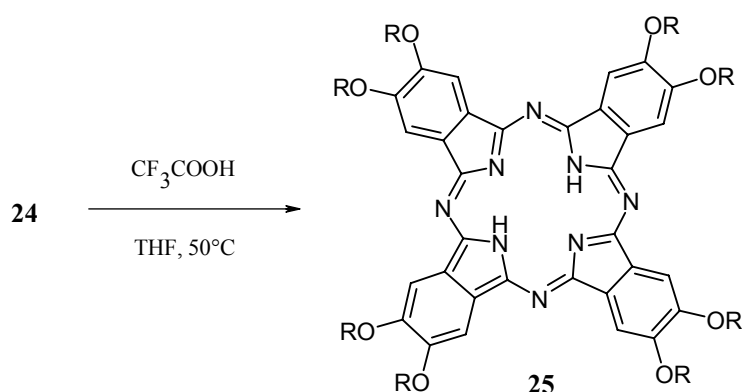
3.1. Isolation and spectroscopic characterization of Mg phthalocyanine 24



[(RO)₈PcMg] (**24**) is collected as the first fraction from the chromatographic separation of the products from the statistical condensation to prepare **16** (see Scheme 6). The collected fraction was precipitated two times with methanol to achieve further purification. The ¹H-NMR of **24** shows, besides the typical non-aromatic signals, a signal (singlet) at 8.50 ppm, assigned to the Pc benzene protons (see experimental, page 87).

3.2. Synthesis and spectroscopic characterization of metal free phthalocyanine 25

The octa-(2-ethylhexyloxy)phthalocyanine (**25**) was obtained by removing the metal from octa-(2-ethylhexyloxy)phthalocyaninato magnesium(II) (**24**) with CF₃COOH yielding 82.5% of metal-free phthalocyanine **25** (Scheme 14).



Scheme 14: Synthesis of **25**

The UV/Vis spectrum shows the two characteristic Q_x and Q_y bands, at 700 and 664.5 nm, respectively for **25**, thereby demonstrating the removal of Mg, while **24** shows a single Q-band at 679.0 nm (Figure 33).

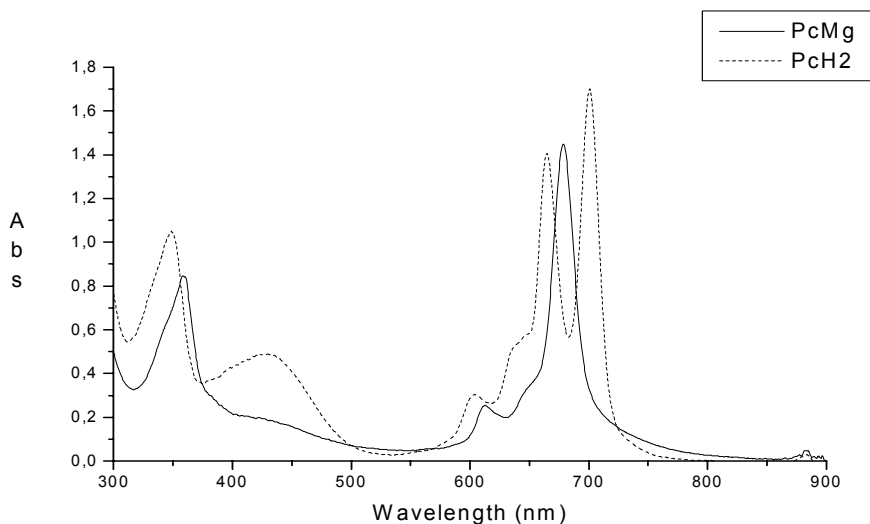


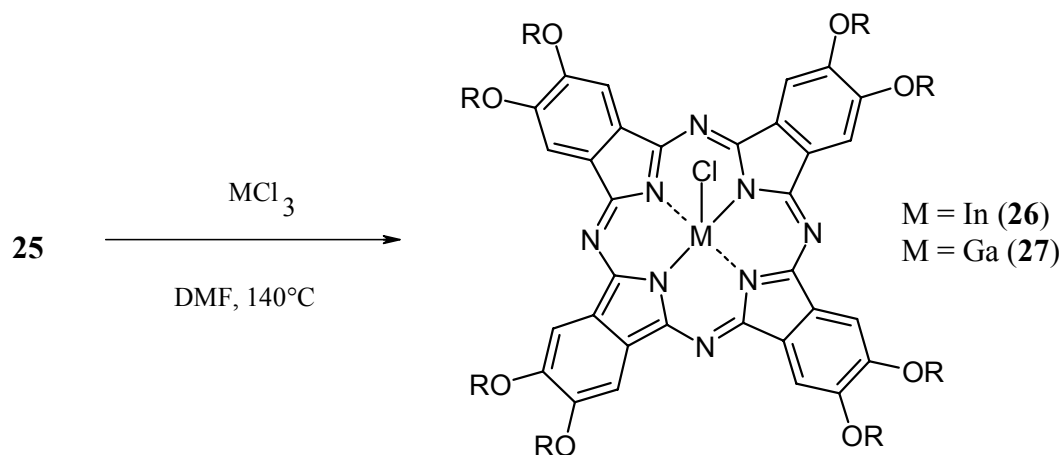
Figure 33: UV/Vis spectra of compounds **24** (—) and **25** (····) for comparison

The $^1\text{H-NMR}$ of **25** is very typical for a metal free phthalocyanine, with the signal corresponding to the protons of NH from the macrocyclic cavity at -0.57 ppm, besides the singlet in the aromatic region at 9.15, from the benzene ring of the phthalocyanine (see experimental, page 88).

3.3. Octasubstituted indium (**26**), gallium (**27**) and thallium (**28**) Pc's

3.3.1. Synthesis and spectroscopic characterization of phthalocyanines **26** and **27**

Indium and gallium were inserted in the cavity of the macrocycle **25** as precursor for these compounds. By reacting **25** with the corresponding metal chloride in DMF as solvent, **26** and **27** were obtained in 88 and 62.5% yields, respectively (Scheme 15).



Scheme 15: Synthesis of **26** and **27**

The ^1H - and ^{13}C -NMR spectra are very similar for both compounds (see experimental, pages 89/90). For example, the ^1H -NMR spectrum of **27** is shown in Figure 34, which presents the characteristic alkyloxy substituents in the region between 0.92 and 2.05 ppm, as well as the $-\text{OCH}_2$ groups at 4.39 ppm. The characteristic singlet assigned to the Pc protons appear at 9.16 ppm.

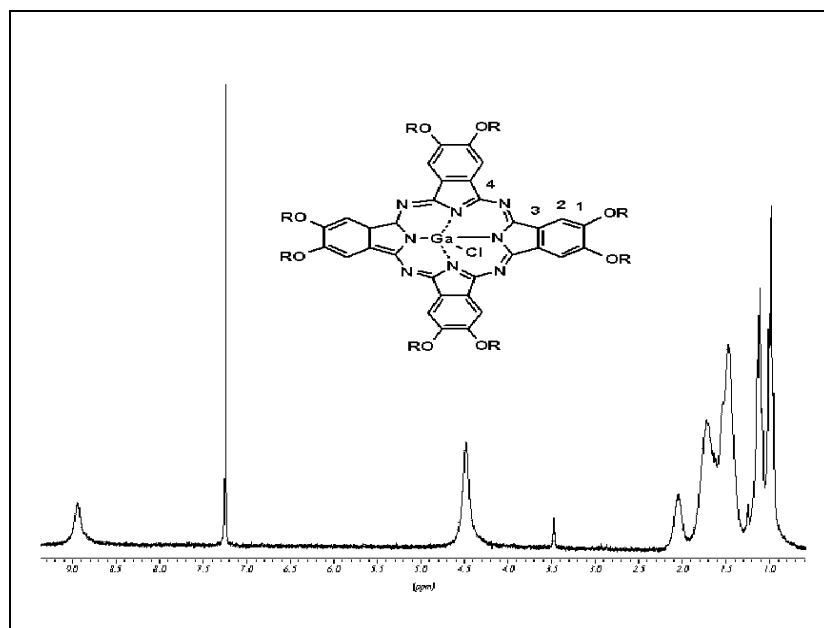


Figure 34: ^1H -NMR spectrum of **27** (R = 2-ethylhexyl)

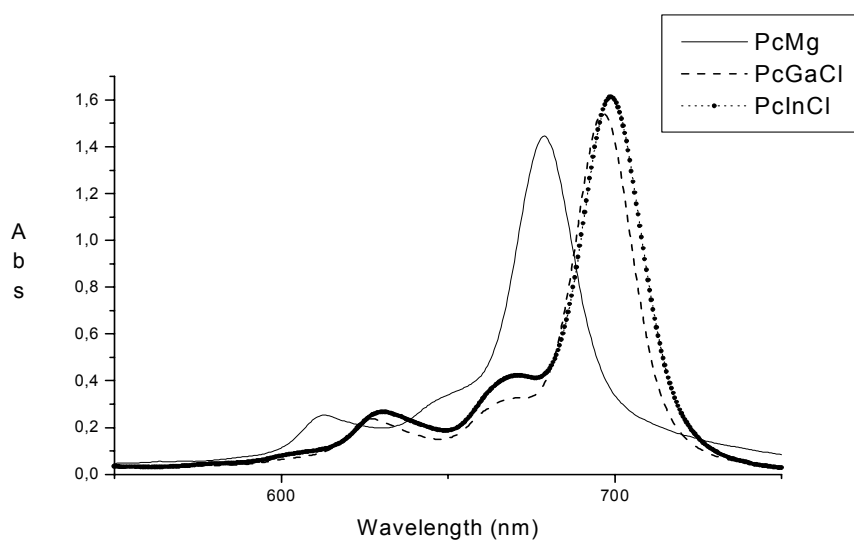


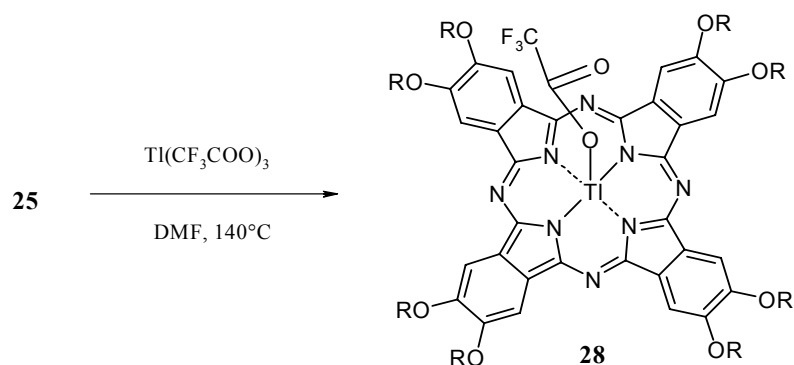
Figure 35: UV/Vis spectra of compounds **24** (—) **26** (····) and **27** (----) for comparison

The UV/Vis spectra of these compounds differ in the position of the Q-band maxima, being 698.5 and 694.5 nm for **26** and **27**, respectively (Figure 35). This shows that, in similar phthalocyanine structures, the metal has some influence on the UV/Vis spectra. From Ga to In, a red shift of the Q-band of approximately 5 nm can be seen (698.5 nm in **26** and 694.5 nm in **27**). This is due to the size of the metal. (RO)₈PcMg (**24**) has a Q-band maximum at 679.0 nm.

3.3.2. Synthesis and spectroscopic characterization of phthalocyanine **28**

Several attempts to reproduce the above discussed method for the introduction with TiCl₃ in the Pc core were unsuccessful. In other words, the corresponding Pc with an axial Cl could not be obtained. Then we used Ti(CF₃COO)₃, as the metal salt, which proved to be successful to synthesize the corresponding (RO)₈PcTiX **28** with R = 2-ethylhexyloxy and X = OCOCF₃.

Octa-(2-ethylhexyloxy)phthalocyanine and Ti(CF₃COO)₃ were dissolved in freshly dried DMF (containing a small portion of quinoline), stirred and boiled at 145 °C for 6 hours (Scheme 16). The product was precipitated with a 10% methanolic solution of NaOH. The precipitation of **28** had to be done under extremely careful conditions. If no base was used, the reaction equilibrium would be changed back with formation of the metal-free Pc **25**. The trifluoroacetic acid, which is formed during the reaction can demetallate **28**. The presence of NaOH leads to the formation of NaOOCF₃, which upon washing is separated from the reaction mixture. The PcTi **28** is not very stable, for instance, in spite of its good solubility in common solvents of medium polarity, e.g. CH₂Cl₂, CHCl₃ or any other chlorinated solvents, it is demetallated (forming the metal-free Pc **25**). However, **28** is stable in solvents such as toluene, xylene, or THF, and poorly soluble in methanol or acetone.



Scheme 16: Synthesis of **28**

When comparing the UV/Vis spectrum of $(\text{RO})_8\text{PcTlX}$ (**28**) with $\text{X} = \text{OCOCF}_3$ with $[(\text{RO})_8\text{PcInCl}]$ (**26**) $\text{R} = 2\text{-ethylhexyl}$ (Figure 36), the Q-band of **28** is red-shifted by 22 nm, from 698.5 nm in **26** to 720.5 nm in **28** (see experimental, page 91). This is due to the fact that Tl is even larger than In, being located outside the plane of the macrocycle. This feature can be also observed in lead phthalocyanine derivatives.^[151] Another factor is the axial ligand, which leads also to a red-shift.^[95]

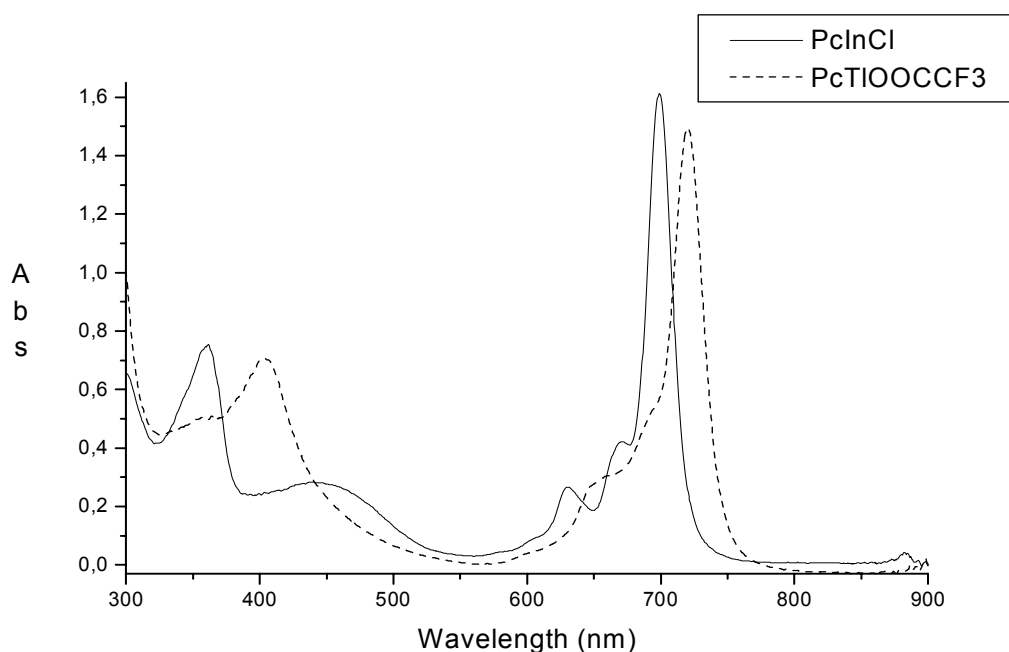


Figure 36: UV/Vis spectra of compounds **26** (—) **28** (-----) for comparison

4. Optical limiting measurements for the In/In binuclear Pc 22

The optical limiting (OL) effect of **22** in toluene has been studied at the wavelength 532 nm with nanosecond laser pulses by means of the Z-scan technique (see page 20 ff). Z-scan profiles of **22** in solution have been determined both in the open (Figure 37) and closed (Figure 38) aperture configurations. In the series of experiments shown in Figures 37 and 38 the optics was $f/5$, i.e. the ratio of the focal length of the lens to the diameter of the laser beam was equal to 5. In the closed aperture configuration the percentage of collection of the transmitted radiation was 40%.

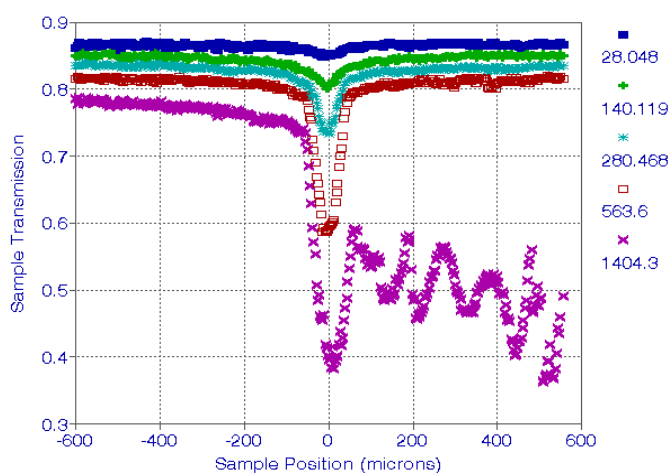


Figure 37: Open aperture Z-scan profiles of a deaerated 5 mM solution of **22** in toluene at 532 nm. The thickness of the sample was 35 μm . Optical windows were made of CaF_2 . The values of the incident energies for the various profiles are given in nJ in the right-side column.

In the series of experiments in Figures 37 and 38 the energy E of the incident beam varied in the range $10 < E < 1500$ nJ. In the open aperture experiments the diminution of sample transmittance in correspondence of the beam focus ($Z = 0$) becomes larger with the increase of the incident energy (Figure 37). Such findings indicate that **22** has a positive nonlinear absorption coefficient. Consequently, **22** behaves as reverse saturable absorber in the adopted range of incident energies and at that value of concentration in toluene solution. At the highest value of incident energies (about 1400 nJ), due to thermal expansion of the liquid solution following the conversion into heat of the absorbed energy, the formation of gas bubbles in the sample could be observed. Such a phenomenon could be associated with the oscillations of the sample optical transmission following the strong absorption of radiation in correspondence of the focus, and it is not indicative of compound degradation.

The Z-scan profiles determined with a closed aperture configuration are shown in Figure 38. The closed aperture curves are characterized by a non symmetrical profile with respect to the focus position. In fact, the profiles have a peak-valley shape, which is indicative of the occurrence of nonlinear refraction. The verification of an increase of transmittance at sample positions preceding the focus is due to a prefocal defocusing effect which is associated with the negative variation of the refractive index upon increase of the incident fluence. This effect becomes apparent at incident energies as low as 14 nJ and dominates the data with the increase of the incident energy. This negative contribution has mostly a thermal origin but an electronic contribution to the nonlinear variation of the refractive index cannot be excluded.

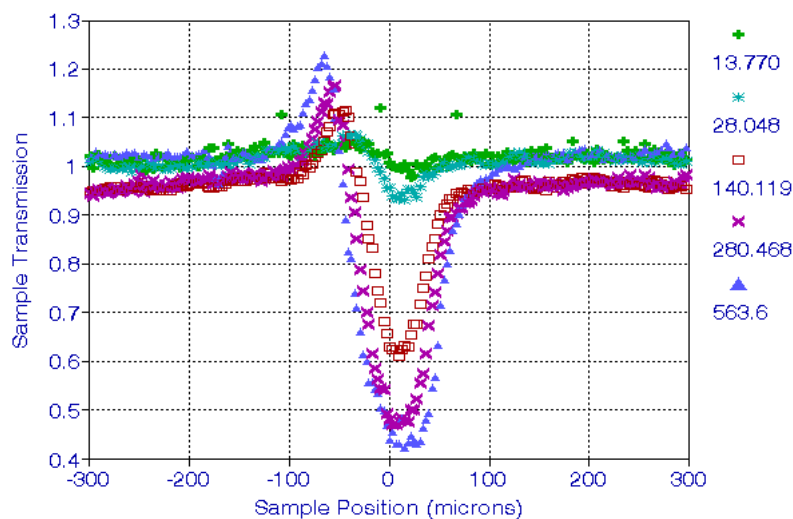


Figure 38: Closed aperture Z-scan profiles of a deaerated 5 mM solution of **22** in toluene at 532 nm. The percentage of collection of the transmitted radiation was 40%. The thickness of the sample was 35 μm . Optical windows were made of CaF_2 . The values of the incident energies for the various profiles are given in nJ in the right-side column.

The transmission variation of the sample of Figure 37 at the focus of a gaussian beam as a function of the incident energy was determined at the wavelength 532 nm and the results are shown in Figure 39.

For binuclear Pc **22** the energy threshold at which the transmittance corresponds to 50% of the linear transmittance value is about 1500 nJ when the concentration of **22** in toluene is 5mM. The OL performance of **22** with that of the "state of the art" molecule *t*Bu₄PcInCl (Figure 40) are compared.^[152] From the comparison of Figures 39 and 40, a larger

decrease of transmittance for $t\text{Bu}_4\text{PcInCl}$ with respect to **22** is observed in the nonlinear regime. In fact, the lowest transmittance of binuclear Pc **22** sample, is below 40% when its linear transmittance is 80 % (Figure 39), whereas the lowest transmittance of $t\text{Bu}_4\text{PcInCl}$ sample, is about 20% when its linear transmittance is 90 % (Figure 40).

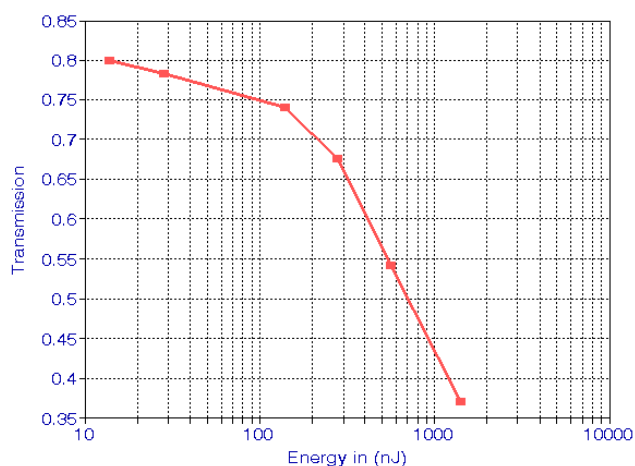


Figure 39: Transmittance variation of a 30 μm thick sample of **22** 5mM in toluene as a function of the incident energy at 532 nm for nanosecond pulses.

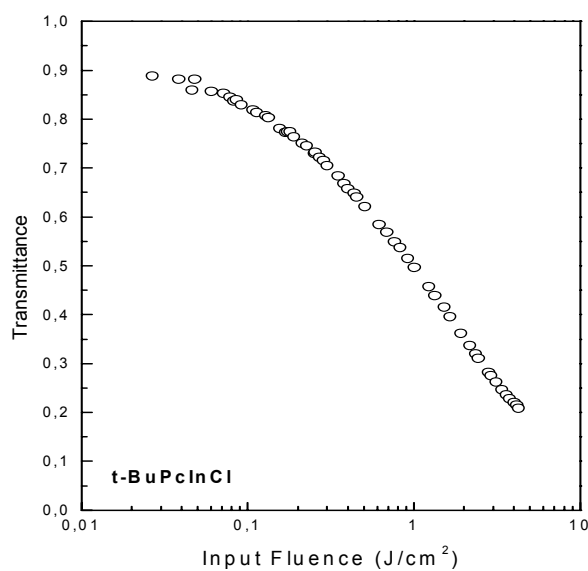


Figure 40: Transmission variation of a solution of $t\text{Bu}_4\text{PcInCl}$ in toluene as a function of the incident fluence at 532 nm.

The better OL performance of *t*Bu₄PcInCl with respect to binuclear phthalocyanine **22** is due to lower aggregation for *t*Bu₄PcInCl in solution, which leads to a longer lifetime of the excited states of *t*Bu₄PcInCl responsible for the absorption of light at high values of incident fluence.

IV - Summary

One objective of this work was the synthesis and full characterization of binuclear metal phthalocyanines **12-15** (c.f. scheme 1, page 31/32)^[120] containing the same metal or different metals e. g. Ni and Cu in the same molecule (**14** and **15**), as well as to obtain unsymmetrically substituted binuclear PcM's **12** and **14**.^[120] Compounds **12** and **13** were synthesized with Ni as central metal in both cavities. Copper and nickel were found to be convenient for the purpose, since both have good chelating and stabilizing properties for the formed phthalocyanines.^[11,120,121]

As shown in scheme 1 (c.f. page 31/32), the starting material for the synthesis of compounds **12-15** was the unsymmetrically substituted phthalocyanine **11**, which was obtained employing a Diels-Alder approach. From the statistical synthesis of phthalonitriles **1** and **2** (c.f. figure 23, page 28) phthalocyanine **4** (among the other statistical products) was obtained. Reaction of **4** with tetracyclone afforded **9**, which was subsequently (via the appropriate intermediate **9a**) transformed into **10** by reaction with fumaronitrile. Then, **11** was obtained through dehydration of **10** with DBU (scheme 1, page 31/32).

Other accomplished objective was the design of binuclear metal phthalocyanines in order to achieve effective optical limiting materials. Because phthalocyanines with In or Ga as central metals are known to have good optical limiting performances,^[4,95,101,109] we directed our research now to the synthesis of this type of binuclear metal phthalocyanines using the same approach as described for the synthesis of Ni/Ni and Ni/Cu binuclear Pc's (**12**, **14**) (c.f. page 31 ff).

To achieve the functionalized dicyano substituted phthalocyanine **19**, (scheme 5) but with InCl or GaCl as central moieties was expected to be difficult, due to the poor stability of these moieties against the number of steps which were necessary to obtain these corresponding binuclear metal phthalocyanines. This problem was solved using an approach in which InCl or GaCl can be inserted in the final step, avoiding the expectable big losses of material throughout all steps shown in scheme 2. We synthesized and isolated compound **16**, containing Mg as central metal, in reasonably large amounts using the same method as described above for the nickel phthalocyanine **4**. The additional steps were also carried out as described for the Ni analogues. Since magnesium is a relatively easy metal to remove^[100,144], this step was done after achieving the Mg/Mg binuclear phthalocyanine (**20**) shown in scheme 10 on page 49. The metal free binuclear phthalocyanine **21** was the starting material for the

preparation and characterization of suitable optical limiting effective metal binuclear phthalocyanines **22** and **23** containing InCl or GaCl, respectively.

Since the use of octasubstituted phthalocyanines with electron donating substituents and GaCl and InCl as central moieties for optical limiting purposes has not been discussed before, the idea of comparison of these type of compounds with the state of art molecule (*t*Bu₄)PcInCl emerged on the course of our work. The comparison of the OL properties of phthalocyanines with Ga and In as central moieties has been studied very much in detail by our group. However, due to the synthetic difficulties, the last element of this group, namely Thallium (Tl) has not been studied so far, except in one case.^[149] For the first time we synthesized an octaalkoxy substituted thallium–Pc–compound, namely (RO)₈PcTlX with R = 2-ethylhexyl and X = OCOCF₃ (**28**), as well as (RO)₈PcInCl (**26**) and (RO)₈PcGaCl (**27**), being also R= 2-ethylhexyl (c.f. page 56 f.f.). Octa-(ethylhexyloxy) magnesium phthalocyanine (**24**) was used for obtaining these compounds because treating the alkoxy substituted phthalonitrile directly with GaCl₃, InCl₃ or Tl(CF₃COOH)₃ proceeds only with difficulties. Using a similar approach to the one previously applied for the preparation of the In/In and Ga/Ga binuclear Pc's **22** and **23**, Mg is removed from **24**, yielding **25** (scheme 14, page 55). The octa-(ethylhexyloxy)phthalocyanine (**25**) is then treated with the corresponding metal salt, in order to obtain the desired metallated Pc's **26**, **27** (scheme 15, page 56) and **28** (scheme 16, page 58).

The optical limiting (OL) properties of In/In binuclear Pc **22** were also studied (cf page 60 f.f.). The OL effect of **22** in toluene has been studied at the wavelength 532 nm with nanosecond laser pulses by means of the Z-scan technique (c.f. page 20 ff). Z-scan profiles of **22** in solution have been determined both in the open (Figure 37, page 60) and closed (Figure 38, page 61) aperture configurations. In the open aperture experiments the diminution of sample transmittance in correspondence of the beam focus (Z = 0) became larger with the increase of the incident energy (Figure 37). Such findings indicated that **22** has a positive nonlinear absorption coefficient. Consequently, **22** behaves as reverse saturable absorber in the adopted range of incident energies and at that value of concentration in toluene solution. The Z-scan profiles determined with a closed aperture configuration (page 61) were characterized by a non symmetrical profile with respect to the focus position. In fact, the profiles showed a peak-valley shape, which was indicative of the occurrence of nonlinear refraction. The verification of an increase of transmittance at sample positions preceding the focus is due to a prefocal defocusing effect which is associated with the negative variation of the refractive index upon increase of the incident fluence. This negative contribution has

mostly a thermal origin but an electronic contribution to the nonlinear variation of the refractive index cannot be excluded.

Comparison of **22** with *t*Bu₄PcInCl (figures 39 and 40, page 62) showed a larger decrease of transmittance for *t*Bu₄PcInCl with respect to **22** in the nonlinear regime. In fact, the lowest transmittance of binuclear Pc **22** sample, was about 40% when its linear transmittance was 80 % (Figure 39), whereas the lowest transmittance of *t*Bu₄PcInCl sample, was about 20% when its linear transmittance was 90 % (Figure 40). The better OL performance of *t*Bu₄PcInCl with respect to binuclear phthalocyanine **22** can be mostly explained in terms of lower aggregation for *t*Bu₄PcInCl in solution, which leads to a longer lifetime of the excited states of *t*Bu₄PcInCl responsible for the absorption of light at high values of incident fluence.

V - EXPERIMENTAL PART

1. General comments

All reactions were carried out in argon atmosphere, unless otherwise stated. The commercial available reagents were used as acquired. Additional purification proceedings are described in the respective synthetic procedures. All solvents were purified and/or dried according to standard methods. The following equipment was used for the analysis and characterization of the compounds:

IR Spectroscopy

Bruker IFS 48 and Bruker Tensor 27: solid substances were grounded with KBr and pressed to pellets, liquid compounds were measured directly in Bruker Tensor 27.

UV/Vis Spectroscopy

Shimadzu UV 2102 PC: The absorption spectra of the compound were recorded as solutions in CH₂Cl₂ (otherwise stated). The path lengths were 1 cm .

¹H-NMR Spectroscopy

Bruker AC250 (250.131 MHz): the deuterated solvent was used as an internal standard. The correlation between the signals was made by using increments and by comparison with known related compounds.

¹³C-NMR Spectroscopy

Bruker AC250 (62.902 MHz): the deuterated solvent was used as an internal standard. The correlation between the signals and the carbon atoms was made by using increments and by comparison with known related compounds.

Mass spectrometry

EI: Finnigan TSQ 70 MAT with direct inlet, temperature of ion source 200°C, electron energy 70 eV.

FD: Finnigan MAT 711A, temperature of ion source: 30°C.

FAB: Finnigan MAT, temperature of ion source: 30°C, electron-energy: NPOE (otherwise stated).

Atomic absorption spectroscopy

Varian Spectra A 20 plus: The type of flame employed was a premixed combustion flame consisting of a fuel and oxidant gas. Air was the oxidant gas and acetylene the fuel gas. The lamp used was a demountable hollow-cathode lamp.

Elemental analysis

Carlo Erba 1104, 1106 and EuroVector EA Elemental Analyzers

2. Synthesis

Note: the numbering which is shown in the compounds figures are solely for ¹H- and ¹³C-NMR assignments, does not follow IUPAC rules.

2.1. Synthesis of precursors

2.1.1. 4,5-Bis(2-ethyl-hexyloxy)-phthalonitrile (1)

2.1.1.1 1,2-Bis(2-ethyl-hexyloxy)benzene

Two different procedures were carried out for the synthesis of this compound:

First method: 55 g of cathecol (0.5 mol) were poured under stirring into 350 ml of acetonitrile in a 1000 ml three-neck flask. 213 ml of 2-ethylhexylbromide (1.2 mol, 231 g) were added, followed by 170 g K₂CO₃ (1.25 mol) and the mixture was heated and stirred at 82°C for 3 days. The solution was allowed to cool down and filtered, to retain the base, washing also with CH₂Cl₂. The solvent was evaporated and the product chromatographed with *n*-hexane to obtain 1,2-bis(2-ethyl-hexyloxy)benzene as a dark yellow viscous oil.

Yield: 1,2-bis(2-ethyl-hexyloxy)benzene, 130 g (67%), dark-yellow viscous oil.

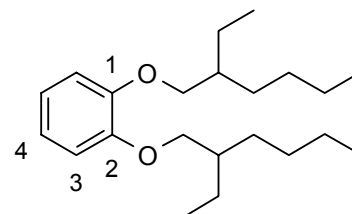
Second method: 0.6 mol of finely powdered KOH (34 g) was added to 23 g cathecol (0.25 mol) and 13 mmol aliquat 336 (phase-transfer catalyst) (4.8 g) in a 500ml round three-neck flask. Then, 0.55 mol of 2-ethylhexylbromide (107 g, 88 ml). was added, with magnetic stirring, and the mixture was heated until 85°C and maintained, with stirring, at that

temperature for 2 hours. After cooling, the only product 1,2-bis(2-ethyl-hexyloxy)benzene (64 g) was recovered after addition of 500 ml CH₂Cl₂ and the solution was filtered through a glass sintered filter to retain the insoluble products. After washing a few times with CH₂Cl₂, the obtained solution was kept and the solvent evaporated, resulting an yellow-brown viscous oil.

Yield: 1,2-bis(2-ethyl-hexyloxy)benzene, 64 g (97%), yellow-brown viscous oil.

MS (EI, 70 eV): 335.5 [M⁺], 222.4 [M⁺ - C₈H₁₆].

¹H NMR (CDCl₃): δ = 0.89, 0.91, 0.99 (s, 12 H, CH₃), 1.16 (br, 2 H, CH), 1.26, 1.46, 1.60 (br, 16 H CH₂), 3.86, 3.93 (d, 4 H, OCH₂), 6.48 (dd, 2 H, H-3), 6.55 (dd, 2 H, H-4).



¹³C NMR (CDCl₃): δ = 10.7, 13.8, (CH₃), 22.5, 23.7, 28.5, 30.2 (CH₂), 41.0 (CH), 72.0 (OCH₂), 116.5 (C-3), 122.0 (C-4), 149.0(C-1).

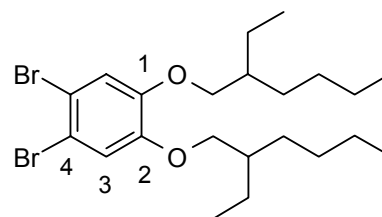
2.1.1.2 1,2-Dibromo-4,5-bis(2-ethyl-hexyloxy)benzene

0.2 mol of 1,2-bis(2-ethylhexyloxy)benzene (67 g) was poured into 300 ml CH₂Cl₂ in a 500 ml three-neck flask and stirred. The solution was cooled till 0°C. Then, a solution of 0.4 mol Br₂ (64 g) in 50 ml CH₂Cl₂ was added dropwise, over 5 hours. The temperature of the reaction mixture was allowed to rise till room-temperature and stirred for 3 hours more. The solution was shaken in a separatory funnel with a 10% solution of NaHSO₃ (150 ml each time) until no more reaction with unreacted bromine could be seen (3 or 4 times). Then, the mixture was extracted with a 10% solution of NaHCO₃. The organic phase was dried with MgSO₄ over 6 hours and the solvent evaporated. Column chromatography was performed with a mixture of n-hexane/CH₂Cl₂ (5/1) in silica-gel (SiO₂) to give a yellow-greenish oil.

Yield: 1,2-dibromo-4,5-bis(2-ethyl-hexyloxy)benzene, 60.3 g, (90%), yellow-greenish oil.

MS (EI, 70 eV): 492.3 [M⁺], 413.4 [M⁺ -Br], 380.0 [M⁺ - C₈H₁₆], 112.9 [C₈H₁₇].

¹H NMR (Aceton-D₆): δ = 0.90, 0.93 (m, 12 H, CH₃), 1.35, 1.49 (m, 16 H, CH₂), 1.72 (m, 2 H, CH), 3.92 (d, 4 H, OCH₂), 7.23 (s, 2 H, H-3).



^{13}C NMR (CDCl_3): $\delta = 11.1, 14.1$ (CH_3), $23.0, 23.8, 29.0, 30.5$ (CH_2), 39.3 (CH), 71.7 (OCH_2), 114.4 (C-4), 117.5 (C-3), 149.3 (C-1).

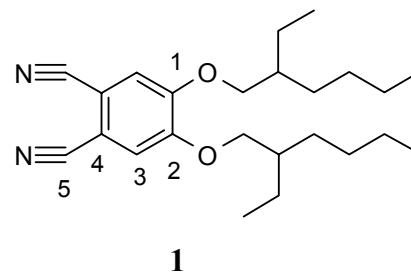
2.1.1.3 4,5-Bis(2-ethylhexyloxy)-phthalonitrile (1)

0.1 mol of 1,2-dibromo-4,5-bis(2-ethylhexyloxy)benzene (49.2 g) was dissolved with 0.3 mol CuCN in 300 ml of freshly dried DMF. A catalytic amount of NaI was added and the mixture stirred and kept under reflux (152°C) for approximately 9 hours. After cooling to room temperature, a solution of 600 ml ammonia was added to the reaction mixture, and aerated for approximately 12 hours or over night. The precipitate was filtrated and washed with neutral water until no ammonia could be found in the solution, and dried in an oven for approximately 24 hours at 80°C . The solid was washed and filtered with hot methanol in a sintered glass filter several times. After evaporating the solvent, the dinitrile was separated by column chromatography on SiO_2 with a mixture of *n*-hexane/ CH_2Cl_2 (3/1). A light green oil, that solidified after few days in the refrigerator, was obtained.

Yield: **1**, 19.5g, (51%), light green solid-oil, m.p.: $40\text{-}42^\circ\text{C}$.

MS (EI, 70 eV): 384.2 [M^+], 359.3 [$\text{M}^+\text{-CN}$], 273.0 [$\text{M}^+\text{-C}_8\text{H}_{16}$].

^1H NMR (CDCl_3): $\delta = 0.85\text{--}0.88$ (m, 12 H, CH_3), 1.29, 1.45 (m, 8 H, CH_2), 1.75 (m, 2 H, CH), 3.89 (d, 4 H, OCH_2), 7.09 (s, 2 H, H-3).



^{13}C NMR (CDCl_3): $11.1, 14.0$ (CH_3), $22.9, 23.8, 28.9, 30.4$ (CH_2), 39.2 (CH), 71.8 (OCH_2), 108.2 (C-4), 115.4 (C-3), 116.0 (C-5), 152.7 (C-1).

2.1.2. 6,7-Dicyano-1,4-Epoxy-1,4-dihydronaphthalene (2)

2.1.2.1 6,7-Dibromo-1,4-epoxy-1,4-dihydronaphthalene

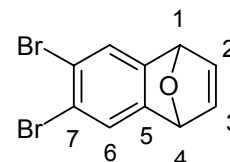
A solution 1.6 M *n*-BuLi in *n*-hexane (53 ml, 85 mmol) was added dropwise to a solution of 31.5 g 1,2,4,5-tetrabromobenzene (80 mmol) and 39 ml furane in 300 ml of dried toluene, for 4 hours, at -23°C . The stirred mixture was allowed to come to room temperature and 3 ml methanol were added. The solution was washed with distilled water, dried with

MgSO₄ and the solvent was evaporated. The resulting yellowish oil was poured into a small quantity of *n*-hexane and recrystallized from methanol.

Yield: 6,7-Dibromo-1,4-epoxy-1,4-dihydronaphthalene, 16.0 g, (66.4%), yellow solid, m.p.: 115-117°C

MS (EI, 70 eV): 301.8 [M⁺], 275.6 [M⁺-C₂H₂]

¹H NMR (CDCl₃): δ = 5.65 (s, 2 H, H-1), 6.98 (s, 2 H, H-2), 7.46 (s, 2 H, H-6),



¹³C NMR (CDCl₃): δ = 81.7 (C-1), 120.6 (C-7), 125.4 (C-6), 142.6 (C-5), 150.3 (C-2).

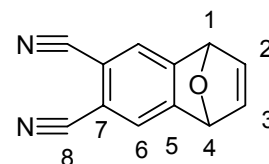
2.1.2.2. 6,7-Dicyano-1,4-Epoxy-1,4-dihydronaphthalene (2)

0.1 mol of 6,7-dibromo-1,4-epoxy-1,4-dihydronaphthalene (30.2 g) was dissolved with 0.3 mol CuCN in 300 ml of freshly dried DMF. A catalytic amount of NaI was added and the mixture stirred and kept under reflux (152°C) for approximately 8 hours. After cooling to room temperature, a solution of 600 ml ammonia was added to the reaction mixture, and aerated for approximately 12 hours or over night. The product was filtrated and washed with water until no ammonia could be found in the solution, and dried in an oven for approximately 24 hours at 80°C. The solid was washed and filtered with hot CH₂Cl₂ in a sintered glass filter several times. After evaporating the solvent, the desired product was recrystallized from CHCl₃. A light yellow solid, was obtained.

Yield: **2**, 7.8 g, (40.0%) yellow solid, m.p.: 200-201°C

MS (EI, 70 eV): 194.1 [M⁺], 167.9 [M⁺-CN].

¹H NMR (CDCl₃): δ = 5.89 (s, 2 H, H-1), 7.04 (s, 2 H, H-2), 7.58 (s, 2 H, H-6).



2

¹³C NMR (CDCl₃): δ = 81.8 (C-1), 113.8 (C-7), 115.6 (C-8), 123.9 (C-6), 142.7 (5), 155.7 (C-2).

2.2. Synthesis of the unsymmetrically substituted nickel phthalocyanine 11

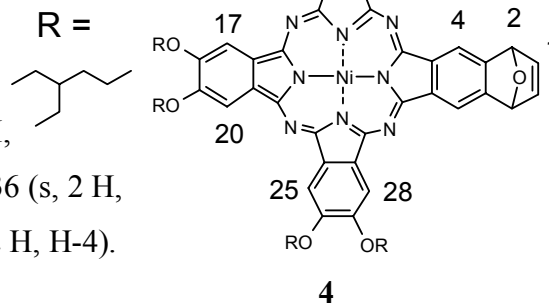
2.2.1. [2,3,9,10,16,17-hexa(2-ethylhexyloxy)-23,26-dihydro-23,26-epoxybenzophthalocyaninato]nickel (4)

780 mg 6,7-Dicyano-1,4-Epoxy-1,4-dihydronaphthalene (4.0 mmol), 4.0 g 4,5-bis(2-ethylhexyloxy)-phthalonitrile (10.4 mmol) and 1.1 g Ni(OAc)₂*4H₂O (4.43 mmol) were suspended in 30 ml pentanol and a catalytic amount of DBU was added. The mixture was heated until 140°C and stirred for 20 hours. After cooling, the mixture was poured in 150 ml methanol, the formed precipitate was isolated using centrifugation and washed several times with methanol. The crude mixture of the PcNi complexes was separated through chromatography on SiO₂ with CH₂Cl₂. After elution of fraction 1 (octa-(2-ethylhexyloxy)PcNi) (3), 4 was obtained as the second fraction. The solvent was removed and the bluish-green solid was recrystallized from methanol to achieve further purification, and dried in vacuum at 90°C. The other products of the statistical condensation were discarded, since they were not necessary for further reactions.

Yield: 4, 900 mg, (18%), bluish-green solid.

MS (FD): 1405.1 [M⁺], 1389, 1293 [M⁺-C₈H₁₆], 1180 [M⁺-2 C₈H₁₆].

¹H NMR (CDCl₃): δ = 1.05, 1.18 (br, 36 H, CH₃), 1.52, 1.79 (br, 48 H, CH₂), 2.08 (br, 6 H, CH), 4.36 (br, 12 H, OCH₂), 6.24 (s, 2 H, H-2), 7.36 (s, 2 H, H-1), 8.23 (3s, br, 6 H, H-9, H-12, H-17), 8.80 (s, 2 H, H-4).



¹³C NMR (CDCl₃): δ = 11.3, 11.5, 14.1, 14.3 (CH₃), 21.6, 23.2, 23.9, 24.2, 29.2, 29.4, 30.3, 30.7, 30.9 (CH₂), 39.7, 39.9 (CH), 71.8 (OCH₂), 82.7 (C-2), 103.8, 104.3, 104.5 (C-9, C-12, C-17), 113.4 (C-4), 130.5, 130.9 (C-8, C-13, C-16), 135.1 (C-5), 143.2, 143.6, 144.7, 146.0 (C-1, C-3, C-7, C-14, C-15), 149.3 (C-6), 151.9, 152.1, 152.5 (C-10, C-11, C-18).

IR (KBr): ν (cm⁻¹): 2958, 2926, 2858, 1607, 1531, 1460, 1381, 1277, 1217, 1105, 1068, 852, 750.

UV/Vis (CH₂Cl₂): λ_{max} = 665, 601, 309 nm.

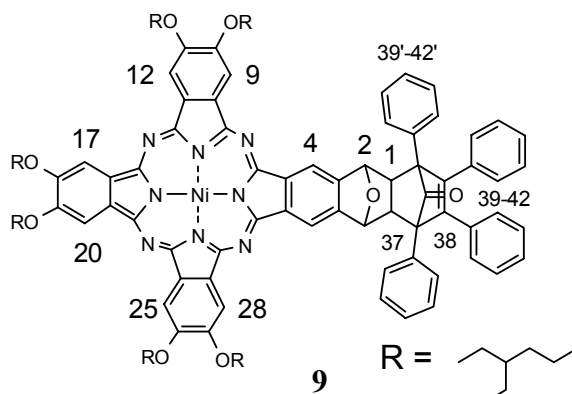
2.2.2. [2,3,9,10,16,17-hexa(2-ethylhexyloxy)-23,26-dihydro-23,26-epoxybenzo-24,25-tetracyclone-phthalocyaninato]nickel adduct **9**

A mixture of 140 mg **4** (~100 μmol) and 40 mg tetraphenylcyclopentadien-1-one (tetracyclone) (103 μmol) was dissolved in 30 ml dried toluene and stirred at 70°C for 4 days. The solvent was evaporated and the residue was separated by flash-chromatography with CH_2Cl_2 (first fraction: tetracyclone, second fraction: product). The solvent was evaporated, the product dried in vacuum at 75°C and reprecipitated from methanol.

Yield: **9**, 160 mg, (89%), bluish-green solid.

MS (FAB): 1790.5 [M^+], 1380.0 [M^+ -isobenzofurane].

^1H NMR (CDCl_3): δ = 1.00, 1.05, 1.18 (br, 36 H, CH_3), 1.52, 1.79 (br, 48 H, CH_2), 2.06 (br, 6 H, CH), 3.39 (s, 2 H, H-1), 4.35 (br, 12 H, OCH_2), 6.33 (s, 2H, H-2), 7.20 (br, 10 H, H-40, H-41, H-42), 7.40-7.68 (br, 10 H, H-40', H-41', H-42'), 8.07, 8.25, 8.41 (3 s, br, 6 H, H-9, H-12, H-17), 9.12 (s, 2 H, H-4).



^{13}C NMR (CDCl_3): δ = 11.3, 11.5, 14.1, 14.3, (CH_3), 23.1, 23.2, 23.9, 29.2, 29.4, 30.7, 30.9, (CH_2), 39.6, 39.8 (CH), 47.1 (C-1), 64.6 (C-37), 68.2, 71.7 (OCH_2), 81.6 C-2), 104.5, 104.6 (C-9, C-12, C-17), 112.2 (C-4), 126.9, 127.5, 128.0, 128.5, 129.3, 129.8, 130.1, 130.8 (C-8, C-13, C-16, C-40-42, C-40'-42'), 135.4, 135.4 (C-39, C-39') 138.7 (C-38), 147.4 (C-3, C-5, C-6, C-7, C-14, C-15), 152.4, 154.5 (C-10, C-11, C-18), 196.6 (CO).

IR (KBr): ν (cm^{-1}): 2959, 2926, 1178 (C=O) 1605, 1481, 1462, 1391, 1358, 1275, 1263, 1234, 1215, 1105, 1061, 851, 802, 696.

UV/Vis (CH_2Cl_2): λ_{max} = 670, 603, 391 nm.

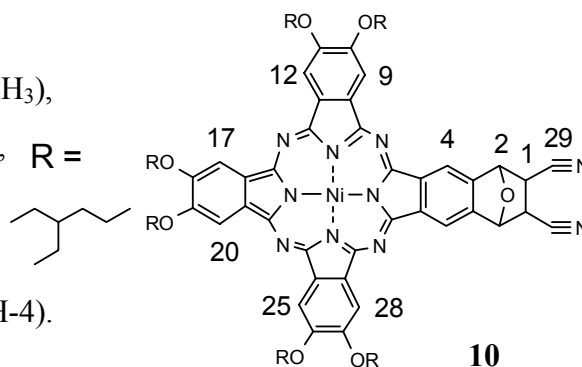
2.2.3. [2,3,9,10,16,17-hexa(2-ethylhexyloxy)-23,26-dihydro-23,26-epoxybenzo-25,26-fumaronitrile-phthalocyaninato]nickel adduct **10**

180 mg **9** (100 μmol) and 63 mg fumaronitrile (800 μmol) were dissolved in 4 ml of *o*-xylene and stirred in a sealed tube at 140 °C for 18 hours. The solvent was evaporated and the residue separated by flash-chromatography in SiO₂. CH₂Cl₂ as eluent gave the first fraction (1,2,3,4-tetraphenylbenzene), a mixture of CH₂Cl₂:ethylacetate (4:1) gave the second fraction (product). After evaporation of the solvent the obtained solid was dried in vacuum and reprecipitated from methanol.

Yield: **10**, 135 mg, (93%), dark green powder.

MS (FD): 1380.5 [M^+ -isobenzofurane].

¹H NMR (CDCl₃): δ = 1.04, 1.20, (br, 36 H, CH₃), 1.51, 1.78 (br, 48 H, CH₂), 2.10 (br, 6 H, CH), 3.02, 3.76 (br, 2 H, H-1), 4.33, 4.40 (br, 12 H, OCH₂), 6.15 (br, 2 H, H-3), 8.09, 8.23, 8.30 (3 s, br, 6 H, H-9, H-12, H-17), 8.41 (br, 2 H, H-4).



¹³C NMR (CDCl₃): δ = 11.4, 11.5, 11.7, 14.2, (CH₃), 23.2, 23.3, 24.1, 29.3, 29.4, 29.6, 30.9, (CH₂), 39.8 (CH), 71.8, 72.1 (OCH₂), 81.1, 83.5 (C-2), 103.7, 104.0, 104.2, 104.5, 104.7 (C-9, C-12, C-17), 112.3, 114.5 (C-4), 116.3 (C-29), 130.3, 130.7, 130.9 (C-3, C-5, C-8, C-13, C-16), 135.9, 139.0, 140.9, 144.0, 146.0, 146.3, 146.4 (C-6, C-7, C-14, C-15), 151.9, 152.2 (C-10, C-11, C-18).

IR (KBr): ν (cm⁻¹): 2959, 2928, 1607, 1529, 1481, 1460, 1389, 1279, 1242, 1200, 1136, 1109, 1090, 1032, 852, 750.

UV/Vis (CH₂Cl₂): λ_{max} = 676, 661, 601, 389 nm.

2.2.4. [2,3,9,10,16,17-hexa(2-ethylhexyloxy)-25,26-dicyano-phthalocyaninato]nickel (**11**)

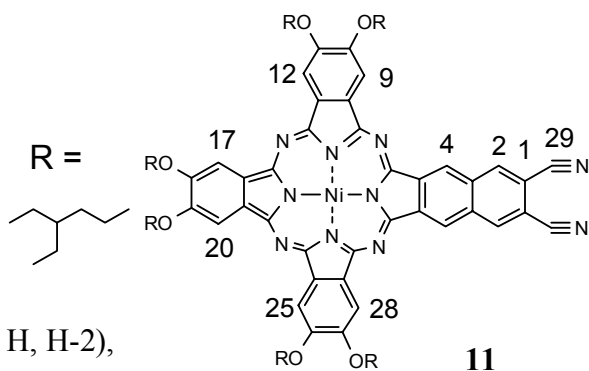
150 mg **10** (102 μmol) were dissolved in freshly distilled anhydrous toluene in an argon purged vessel and 1.2 ml DBU were added. The mixture was stirred for 2 hours at 100°C and then allowed to cool down. The mixture was extracted with distilled water to

remove the unreacted DBU, and the solvent evaporated. Subsequent flash-chromatography (CH_2Cl_2) was performed and the obtained product dried in vacuum.

Yield: **11**, 135 mg, (95%), green-olive powder.

MS (FD): 1440.5 [M^+], 1328.5 [$\text{M}^+ - \text{C}_8\text{H}_{17}$],
1215.0 [$\text{M}^+ - 2 \text{C}_8\text{H}_{17}$].

^1H NMR (CDCl_3): δ = 1.08, 1.20 (br, 36 H, CH_3), 1.46, 1.56, 1.75 (br, 48 H, CH_2), 1.82, 2.03, 2.14 (br, 6 H, CH), 3.68, 4.13, 4.445 (br, 12 H, OCH_2), 6.31 (br, 2 H, H-4), 6.45 (br, 2 H, H-2), 6.97 (br, 2 H, H-17), 7.67, 8.29 (2 s, br, 4 H, H-9, H-12).



^{13}C NMR (CDCl_3): δ = 11.5, 11.7, 14.3 (CH_3), 23.2, 23.7, 23.9, 24.2, 29.4, 29.7, 30.6, 30.8, (CH_2), 39.7, 40.0 (CH), 71.4, 72.1, 17.3, (OCH_2), 102.2, 102.9, 104.4 (C-9, C-12, C-17), 107.7, (C-1), 115.7 (C-29), 118.2 (C-4), 128.7, 128.8, 129.3, 130.4, 132.7, (C-3, C-5, C-8, C-13, C-16), 135.4 (C--2), 139.8, 142.9, 144.9, 145.4 (C-6, C-7, C-14, C-15), 151.3, 151.6, 152.6 (C-10, C-11, C-18).

IR (KBr): ν (cm^{-1}): 2959, 2928, 2230, 1603, 1531, 1460, 1427, 1383, 1281, 1205, 1159, 1109, 1061, 912, 852, 748.

UV/Vis (CH_2Cl_2): λ_{max} = 700.0, 671.5, 633.0, 454, 325.5, 310.5 nm.

2.3. Synthesis of the Ni/Ni and Ni/Cu binuclear metal-phthalocyanines

2.3.1. Unsymmetrically substituted Ni/Ni binuclear metal-phthalocyanine **12**

A mixture of **11** (210 mg, 140 μmol), phthalonitrile (70 mg, 530 μmol) and NiCl_2 (20 mg, 145 μmol) was suspended in octan-1-ol (10 mL) in an argon-purged vessel and DBU (0.05 mL) was added. The mixture was stirred and heated to 175 $^\circ\text{C}$ for 24 h, allowed to cool down, and poured into MeOH (50 mL). The precipitate formed was isolated by centrifugation and was washed several times with MeOH. The crude mixture was separated by flash chromatography on silica gel with dichloromethane as eluent to obtain the desired compound. The first fraction contained mostly unreacted **11** and was discarded. Compound **12** was eluted

as the second fraction. After evaporation of the solvent and drying in vacuum at 100°C, the product was then reprecipitated from methanol. The third fraction was identified as the AAAA-product of the semi-statistical condensation and discarded (poorly soluble PcNi).

Yield: **12**, 60 mg, (23%), dark bluish-green powder.

EA: Theory: C=69.64%; H=6.88%; N=10.17%;

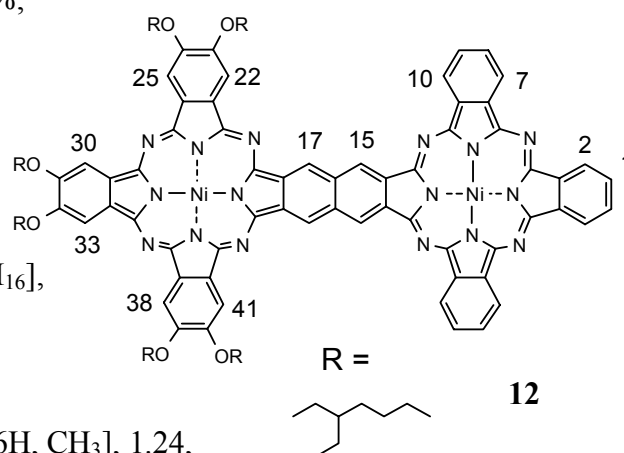
Found: C=69.34%; H=6.28%; N=9.36%.

MS (FAB): m/z (%) = 1686.7 (15)

$[M^+ - C_8H_{16} - OC_8H_{16} + Na]$, 1570.7 (15)

$[M^+ - 3 C_8H_{16} + Na]$, 1327.9 (40) $[M^+ - 5 C_8H_{16}]$,

1214.7 (100) $[M^+ - 6 C_8H_{16}]$.



1H NMR ($CDCl_3$): δ = 0.86, 0.90, 1.09 [br, 36H, CH_3], 1.24,

1.56, 1.66 [br, 48H, CH_2], 1.98, 2.02 [br, 6H, CH], 4.19, 4.29 [br, 12H, OCH_2], 6.80, 6.95, 7.39, 7.52, 7.69, 7.75, 8.04 [br, PcH].

^{13}C NMR ($THF d_8$): δ = 11.0, 11.2, 13.8, 13.9 [CH_3], 19.4, 22.8, 23.5, 23.8, 27.1, 29.3, 29.7, 29.9, 30.4, 31.1, 32.2, 32.9 [CH_2], 37.3, 39.9, 41.2 [CH], 71.4, 71.6, 72.1 [OCH_2], 104.1, 104.3, 104.8 [C-2, C-7, C-8, C-9, C-10, C-22, C-25, C-30], 124.7 [C-15], 125.1 [C-17], 127.7, 128.2, 128.6 [C-22, C-25, C-30], 129.0 – 133.5 [C-3, C-6, C-11, C-14, C-16, C-18, C-21, C-26, C-29], 143.6, 146.1, 147.5, 148.5 [C-4, C-5, C-12, C-13, C-19, C-20, C-27, C-28], 152.0, 152.3, 152.6 [C-1, C-8, C-9, C-23, C-24, C-31].

UV/Vis (CH_2Cl_2): λ_{max} = 697.5, 669.0, 640.0, 321.0 nm.

2.3.2. Symmetrically substituted Ni/Ni binuclear metal-phthalocyanine 13

A mixture of **11** (210 mg, 140 μ mol), 4,5-bis(2-ethylhexyloxy)-phthalonitrile (110 mg, 280 μ mol) and $NiCl_2$ (20 mg, 145 μ mol) was suspended in octan-1-ol (10 mL) in an argon-purged vessel and DBU (0.05 mL) was added. The mixture was stirred and heated to 175 °C for 24 h, allowed to cool down, and poured into MeOH (50 mL). The precipitate formed was isolated by centrifugation and was washed several times with MeOH. The crude mixture was separated by flash chromatography on silica gel with dichloromethane as eluent to obtain the

desired compound. The first fraction from the chromatography contained the **AAAA**-product (compound **3**-discarded) and the second fraction was identified as the desired product. The third fraction was the unreacted **11** and was discarded. After evaporation of the solvent and drying in vacuum at 100°C, the product was then reprecipitated from methanol.

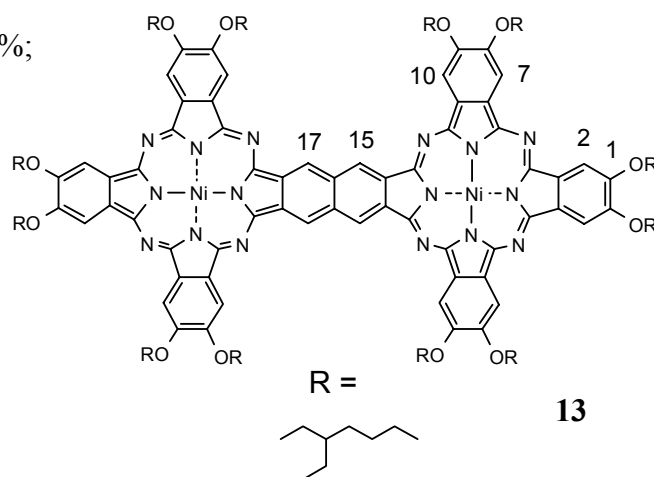
Yield: **13**, 74 mg (20%), bluish-green powder.

EA: Theory: C=72.13%; H=8.06%; N=7.44%;

Found: C=72.05%; H=5.56%; N=7.19%.

MS (FAB): m/z (%) = 2537.4 (30)

$[M^+ - 2 C_8H_{16}]$, 2305.8 (70) $[M^+ - 3 C_8H_{16}]$.



13

¹H NMR (CDCl₃): δ = 0.84, 0.87,

[br, 72H, CH₃], 1.04, 1.24, 1.51, 1.76 [br, 96H, CH₂], 2.02, 2.04,

2.10 [br, 12H, CH], 4.16, 4.32, 4.50 [br, 24H, OCH₂], 7.49, 7.92, 8.53, 8.82 [br, Pch].

¹³C NMR (THF d₈): δ = 10.4, 11.4, 13.6, 14.0 [CH₃], 22.9, 23.1, 23.8, 24.2, 29.0, 29.7, 29.9, 31.1, 31.4, 31.6, 32.1 [CH₂], 38.6, 39.9, 41.3 [CH], 71.3, 71.6, 71.9 [OCH₂], 102.7, 103.6, 104.2 [C-2, C-7, C-10, C-22, C-25, C-30], 117.7 [C-15], 125.2 – 133.9 [C-3, C-6, C-11, C-14, C-16, C-18, C-21, C-26, C-29], 143.2, 143.6, 144.1 [C-4, C-5, C-12, C-13, C-19, C-20, C-27, C-28], 151.1, 151.2, 151.5, 151.9 [C-1, C-8, C-9, C-23, C-24, C-31].

UV/Vis (CH₂Cl₂): λ_{max} = 664.5, 626.0, 398.5, 370.5, 312.5 nm.

2.3.3. Unsymmetrically substituted Ni/Cu binuclear metal-phthalocyanine **14**

A mixture of **11** (210 mg, 140 μ mol), phthalonitrile (70 mg, 530 μ mol) and CuCl₂ (20 mg, 150 μ mol) was suspended in octan-1-ol (10 mL) in an argon-purged vessel and DBU (0.05 mL) was added. The mixture was stirred and heated to 175 °C for 24 h, allowed to cool down, and poured into MeOH (50 mL). The precipitate formed was isolated by centrifugation and was washed several times with MeOH. The crude mixture was separated by flash chromatography on silica gel with dichloromethane as eluent to obtain the desired compound. The first fraction contained mostly unreacted **11** and was discarded. Compound **14** (**AAAB**-product) was eluted as the second fraction. After evaporation of the solvent and drying in

vacuum at 100°C, the product was then reprecipitated from methanol. The third fraction was identified as the **AAAA**-product (PcCu) and discarded.

Yield: **14**, 53 mg, (20%), dark bluish-green powder.

EA: Theory: C=69.66%; H=6.98%; N=10.17%;

Found: C=69.17%; H=7.16%; N=9.33%.

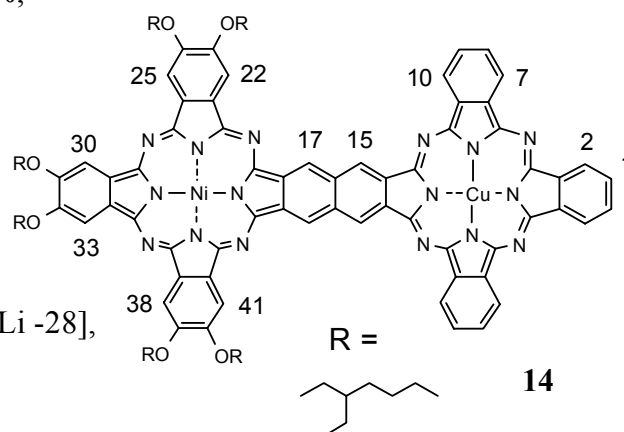
MS (FAB): m/z (%) = 1651.9 (90)

$[M^+ - 2 C_8H_{16} + Li]$, 1602.7 (40)

$[M^+ - 2 OC_8H_{16} - 28]$, 1538.7 (80)

$[M^+ - 3 C_8H_{16} + Li]$, 1511.8 (40) $[M^+ - 3 C_8H_{16} + Li - 28]$,

1440.7 (30) $[M^+ - 4 C_8H_{16}]$.



¹H NMR (CDCl₃): δ = 0.86, 1.07 [br, CH₃], 1.24, 1.41, 1.51, 1.66 [br, CH₂], 2.03 [br, CH], 4.18, 4.26 [br, OCH₂], 6.48 – 9.10 [br, PcH].

¹³C NMR (CDCl₃): δ = 10.6, 11.5, 14.3 [CH₃], 22.7, 23.3, 23.7, 24.1, 24.5, 26.4, 29.3, 29.7, 30.4, 30.8, 31.9 [CH₂], 39.3, 39.4, 39.7, 40.2 [CH], 70.8, 71.7, 73.3 [OCH₂], 102.9 – 103.8 [C-2, C-7, C-8, C-9, C-10, C-22, C-25, C-30], 126.6 – 133.5 [C-22, C-25, C-30, C-3, C-6, C-11, C-14, C-16, C-18, C-21, C-26, C-29], 144.1 – 145.1 [C-4, C-5, C-12, C-13, C-19, C-20, C-27, C-28], 150.7 – 153.0 [C-1, C-8, C-9, C-23, C-24, C-31].

FAAS (Air-Acetylene): 1.9 μ g/L of Ni and 2.3 μ g/L of Cu.

UV/Vis (CH₂Cl₂): λ_{max} = 699.5, 661.0, 638.0, 326.0 nm.

2.3.4. Symmetrically substituted Ni/Cu binuclear metal-phthalocyanine 15

A mixture of **11** (210 mg, 140 μ mol), 4,5-bis(2-ethylhexyloxy)-phthalonitrile (110 mg, 280 μ mol) and CuCl₂ (20 mg, 150 μ mol) was suspended in octan-1-ol (10 mL) in an argon-purged vessel and DBU (0.05 mL) was added. The mixture was stirred and heated to 175 °C for 24 h, allowed to cool down, and poured into MeOH (50 mL). The formed precipitate was isolated by centrifugation and was washed several times with MeOH. The crude mixture was separated by flash chromatography on silica gel with dichloromethane as eluent to obtain the desired compound. The first fraction from the chromatography contained the **AAAA**-product

(octa-(2-ethylhexyloxy)PcCu) and was discarded. The second fraction was identified as the AAAB-product **15**. After evaporation of the solvent and drying in vacuum at 100°C, the product was then reprecipitated from methanol. The third fraction was unreacted **11** and was discarded.

Yield: **15**, 74.5 mg, (18%), bluish-green powder.

EA: Theory: C=72.40%; H=8.34%; N=7.43%;

Found: C=72.59%; H=8.39%; N=7.48%.

MS (FAB): m/z (%) = 2442.8 (20)

$[M^+ - 2 C_8H_{16}]$, 2133.7 (40)

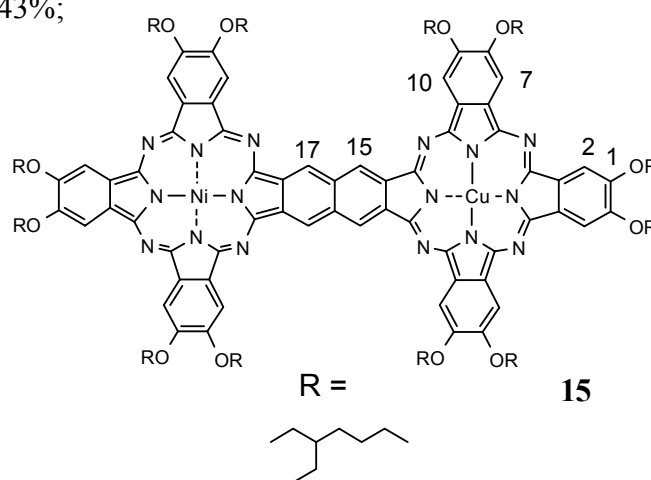
$[M^+ - 3 OC_8H_{16} - C_8H_{16} - 28]$,

1832.7 (60) $[M^+ - OC_8H_{16} - 4 C_8H_{16}]$,

1516.1 (50) $[M^+ - 9 OC_8H_{16}]$, 1357.1 (50)

$[M^+ - 10 OC_8H_{16} - 28]$, 1141.9 (40)

$[M^+ - 12 OC_8H_{16}]$.



¹H NMR (CDCl₃): δ = 0.91, 0.93 [br, CH₃], 1.20, 1.33, 1.50 [br, CH₂], 1.78

[br, CH], 4.01, 4.49 [br, OCH₂], 7.35 – 8.51 [br, Pch].

¹³C NMR (CDCl₃): δ = 11.2, 11.5, 14.1, 14.2 [CH₃], 22.6, 23.0, 23.3, 23.9, 29.1, 29.4, 29.7, 30.6, 30.9, 31.4 [CH₂], 39.3, 39.6, 40.0 [CH], 71.6, 71.8, 72.1 [OCH₂], 104.4 – 108.1 [C-2, C-7, C-8, C-9, C-10, C-22, C-25, C-30], 115.4 [C-15, C-17], 129.2 – 132.9 [C-22, C-25, C-30], 133.1– 136.4 [C-3, C-6, C-11, C-14, C-16, C-18, C-21, C-26, C-29], 143.2 – 146.9 [C-4, C-5, C-12, C-13, C-19, C-20, C-27, C-28], 150.4 – 152.8 [C-1, C-8, C-9, C-23, C-24, C-31].

FAAS (Air:Acetylene): 1.8 μ g/L for Ni and 2.1 μ g/L for Cu.

UV/Vis (CH₂Cl₂): λ_{max} = 672.5, 631.0, 304.0 nm.

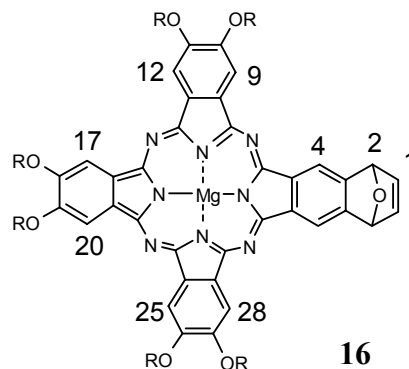
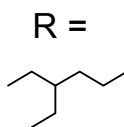
2.4. Synthesis of the unsymmetrically substituted magnesium phthalocyanine 19

2.4.1. [2,3,9,10,16,17-hexa(2-ethylhexyloxy)-23,26-dihydro-23,26-epoxybenzo-phthalocyaninato]magnesium (16)

80 mg magnesium turnings were suspended in ~ 10 ml pentanol. This suspension was heated to 150 °C (reflux) and maintained at that temperature until an amalgam was formed (~1 hour). Octanol was added to this amalgam (20 ml), followed by 780 mg 6,7-dicyano-1,4-epoxy-1,4-dihydronaphthalene (4.0 mmol) and 4.0 g 4,5-bis(2-ethylhexyloxy)-phthalonitrile (10.4 mmol). The suspension was heated till 160°C and stirred for 24 hours. After cooling, the mixture was poured in 150 ml of a mixture methanol/water (5/1). The formed precipitate was isolated by centrifugation and washed several times with methanol. The crude mixture of PcMg complexes was separated through chromatography in silica gel, starting with CH₂Cl₂ as mobile phase. After elution of fraction 1 [octa-(2-ethylhexyloxy)PcMg] (**24**), [2,3,9,10,16,17-hexa(2-ethyl-hexyloxy)-23,26-dihydro-23,26-epoxy-benzophthalocyaninato] magnesium (**16**) was obtained as the second fraction, using a mixture (CH₂Cl₂/THF: 50/1) as eluent. The solvent was removed, the green solids (**16** and **24**) were reprecipitated from methanol to achieve further purification, and dried in vacuum at 100°C. Characterization of **24** is given on pages 87/88. The other products of the statistical condensation were discarded. Yield: **16**, 750 mg, (15%), green solid; **24**, 750 mg (15%), green solid.

MS (FAB): 1372.1 [M⁺], 1258.9 [M⁺-C₈H₁₇],
1146.1 [M⁺- 2 C₈H₁₇].

¹H NMR (THF-d₈): δ = 0.95, 1.00, 1.15 (br, 36 H, CH₃), 1.44 (br, 48 H, CH₂), 2.05 (br, 6 H, CH), 4.39, 4.49 (br, 12 H, OCH₂), 7.83 (s, 2 H, H-2), 8.58 (s, 2 H, H-1), 9.09 (3s, br, 6 H, H-9, H-12, H-17), 10.00 (s, 2 H, H-4).



¹³C NMR (THF-d₈): δ = 11.7, 11.8, 14.6 (CH₃), 23.5, 23.6, 24.1, 24.3, 24.7, 25.1, 25.3, 30.3, 30.5, 31.6, 31.9, 32.8, 32.9 (CH₂), 40.8, 41.1, 42.0 (CH), 72.1 (OCH₂), 78.3 (C-2), 106.3, 106.6, 106.7, 107.0, 107.2 (C-9, C-12, C-17), 117.3 (C-4), 122.1, 122.8, 123.2, (C-8, C-13, C-16), 127.3 (C-5), 130.6, 133.5, 133.8, 134.0, 135.0, (C-1, C-3, C-7, C-14, C-15), 138.0 (C-5), 150.6 (C-6), 152.4, 152.9, 153.1, 154.0, 154.5 (C-10, C-11, C-18).

UV/Vis (CH₂Cl₂): λ_{\max} = 682.5, 620.0, 359.0 nm.

2.4.2. [2,3,9,10,16,17-hexa(2-ethylhexyloxy)-23,26-dihydro-23,26-epoxybenzo-24,25-tetracyclone-phthalocyaninato]magnesium adduct **17**

A mixture of 140 mg **16** (~100 μ mol) and 40 mg tetraphenylcyclopentadien-1-one (103 μ mol) was dissolved in 30 ml dried toluene and stirred at 72°C for 2 days. The solvent was evaporated and the residue was separated by flash-chromatography on SiO₂ using CH₂Cl₂ as eluent (first fraction: tetracyclone, second fraction: **17**). The solvent was evaporated, the product dried in vacuum at 100°C and reprecipitated from methanol.

Yield: **17**, 165 mg, (92%), green solid.

MS (FAB): 1756.9 [M⁺], 1346.3 [M⁺ - C₃₀H₂₂ - CO].

¹H NMR (THF-d₈): δ = 0.81, 1.04, 1.21

(br, 36 H, CH₃), 1.40, 1.62 (br,

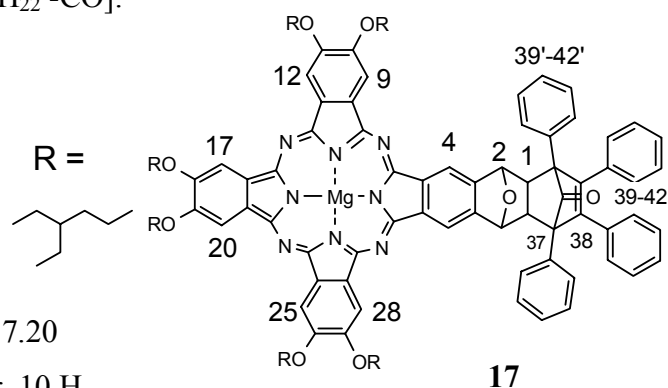
48 H, CH₂), 2.40 (br, 6 H, CH), 3.40

(s, 2 H, H-1), 4.15, 4.38 (br, 12 H,

OCH₂), 6.33 (s, 2H, H-2), 6.94, 7.03, 7.06, 7.20

(br, 10 H, H-40, H-41, H-42), 7.23-7.67 (br, 10 H,

H-40', H-41', H-42'), 8.91, 9.07, (3 s, br, 6 H, H-9, H-12, H-17), 9.51 (s, 2 H, H-4).



¹³C NMR (THF-d₈): δ = 11.6, 11.8, 14.5, 14.6, (CH₃), 23.6, 24.0, 24.2, 24.7, 25.0, 25.3, 26.0, 30.2, 31.8, 32.0, (CH₂), 40.6, 41.0 (CH), 48.6 (C-1), 65.7 (C-37), 68.2, 72.0, 72.2 (OCH₂), 82.7 (C-2), 106.1, 106.3, 106.6 (C-9, C-12, C-17), 114.1 (C-4), 127.3, 127.9, 128.3, 128.9, 130.7, 131.2, (C-8, C-13, C-16, C-40-42, C-40'-42'), 136.8, 137.2, 137.9, (C-39, C-39') 139.6, 139.9 (C-38), 149.2, 150.8, 153.0 (C-3, C-5, C-6, C-7, C-14, C-15), 154.4, 154.9, 155.6, 156.5 (C-10, C-11, C-18), 196.9 (CO).

IR (KBr): ν (cm⁻¹): 2959, 2926, 1178 (C=O) 1605, 1481, 1462, 1391, 1358, 1275, 1263, 1234, 1105, 1061, 802, 696.

UV/Vis (CH₂Cl₂): λ_{\max} = 685.0, 613.0, 359.5 nm.

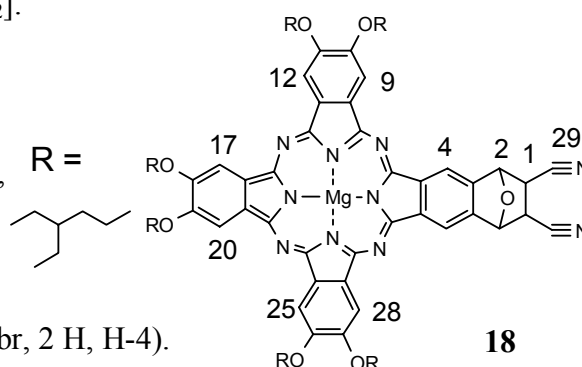
2.4.3. [2,3,9,10,16,17-hexa(2-ethylhexyloxy)-23,26-dihydro-23,26-epoxybenzo-25,26-fumaronitrile-phthalocyaninato]magnesium adduct **18**

180 mg **17** (100 μmol) and 63 mg fumaronitrile (800 μmol) were dissolved in 4 ml of *o*-xylene and stirred in a sealed tube at 140 °C for 16 hours. The solvent was evaporated and the residue separated by flash-chromatography in SiO_2 . Using CH_2Cl_2 as eluent gave the first fraction (1,2,3,4-tetraphenylbenzene) and a mixture of CH_2Cl_2 :THF (5:1) gave the second fraction (**18**). After evaporation of the solvent the obtained solid was dried in vacuum at 100°C and reprecipitated from methanol.

Yield: **18**, 135 mg, (93%), dark green solid.

MS (FAB): 1424.1 [M^+], 1346.1 [$\text{M}^+ - \text{C}_4\text{H}_2\text{N}_2$].

^1H NMR (THF- d_8): $\delta = 1.03, 1.04, 1.16, 1.18$ (br, 36 H, CH_3), 1.31, 1.53, 1.82 (br, 48 H, CH_2), 2.05 (br, 6 H, CH), 3.25, (br, 2 H, H-1), 4.51 (br, 12 H, OCH_2), 6.35 (br, 2 H, H-3), 8.98 (s, br, 6 H, H-9, H-12, H-17), 9.53 (br, 2 H, H-4).



^{13}C NMR (THF- d_8): $\delta = 11.9, 14.6, (\text{CH}_3), 24.1, 30.3, 32.0, (\text{CH}_2), 41.2 (\text{CH}), 72.2 (\text{OCH}_2), 82.2, 84.8 (\text{C}-2), 106.1, 106.3, 106.6, 106.9 (\text{C}-9, \text{C}-12, \text{C}-17), 115.3, 116.7 (\text{C}-29), 119.9, (\text{C}-4), 133.7, 134.2, 134.3 (\text{C}-3, \text{C}-5, \text{C}-8, \text{C}-13, \text{C}-16), 139.9, 140.2, 142.5, 144.1, (\text{C}-6, \text{C}-7, \text{C}-14, \text{C}-15), 151.9, 153.2, 154.0, 155.4 (\text{C}-10, \text{C}-11, \text{C}-18).$

UV/Vis (CH_2Cl_2): $\lambda_{\text{max}} = 686.0, 669.0, 609.5, 426.5, 360.0 \text{ nm}$.

2.4.4. [2,3,9,10,16,17-hexa(2-ethylhexyloxy)-25,26-dicyano-phthalocyaninato]magnesium **19**

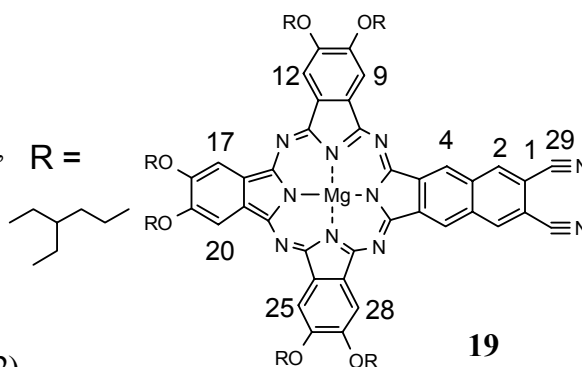
150 mg **18** (102 μmol) were dissolved in freshly distilled anhydrous toluene in an argon purged vessel and 1.2 ml DBU were added. The mixture was stirred for 2 hours at 100°C and then allowed to cool. The mixture was extracted with distilled water to remove the unreacted DBU, and the solvent evaporated. Subsequent flash-chromatography on SiO_2 using CH_2Cl_2 as eluent was performed and **19** dried in vacuum at 100°C.

Yield: **19**, 135 mg, (95%), dark green powder.

MS (FAB): 1406.1 [M^+], 1293.0 [$M^+ - C_8H_{16}$].

1H NMR (THF- d_8): δ = 1.04, 1.07, 1.09

(br, 18 H, CH_3), 1.18, 1.21, 1.24 (br, 18 H, CH_3),
1.57, 1.81, 1.84, 1.87 (br 48 H, CH_2), 2.10 (br,
6 H, CH), 4.53, 4.59 (br, 12 H, OCH_2),
6.36 (br, 2 H, H-4), 8.56 (br, 2 H, H-2),
8.85 (br, 2 H, H-17), 9.02 (2 s, br, 4 H, H-9, H-12).



^{13}C NMR (THF- d_8): δ = 12.0, 14.6 (CH_3), 24.2, 25.3, 30.4, 32.0 (CH_2), 41.1, 41.2 (CH),
72.2, 72.4 (OCH_2), 106.1, 106.5, 106.9 (C-9, C-12, C-17), 109.7, (C-1), 117.3 (C-29), 122.2
(C-4), 132.3, 133.6, 133.9, (C-3, C-5, C-8, C-13, C-16), 134.1, (C--2), 138.2, 138.8, 142.6,
145.3 (C-6, C-7, C-14, C-15), 150.8, 151.7, 152.1, 152.8 (C-10, C-11, C-18).

UV/Vis (CH_2Cl_2): λ_{max} = 710.5, 682.0, 642.0, 544.5, 363.0 nm.

2.4.5. Binuclear Mg/Mg phthalocyanine **20**

80 mg magnesium turnings were suspended in ~ 10 ml pentanol. The suspension was heated to 150 °C (reflux) and maintained at this temperature until an amalgam was formed (~1 hour). After adding 10 ml octanol a mixture of **19** (210 mg, 140 μ mol) and phthalonitrile (210 mg, 1590 μ mol) was suspended in this mixture in an argon-purged vessel. The mixture was stirred and heated to 175 °C for 24 h, allowed to cool and poured into MeOH (50 mL). The precipitate formed was isolated by centrifugation and was washed several times with MeOH. The crude mixture was separated by flash chromatography on silica gel, first with dichloromethane as eluent to remove part of the impurities. The eluent mixture was changed to dichloromethane:THF (50:1) to elute **20**, as second fraction.. The third fraction could only be partially eluted with pure THF and was identified as the **AAAA**-product of the semi-statistical condensation (MgPc) and discarded. After evaporation of the solvent and drying in vacuum, **20** was reprecipitated from methanol.

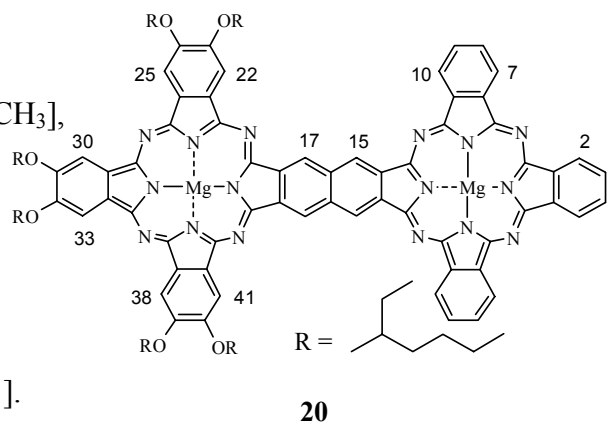
Yield: **20**, 90 mg, (35%), dark green powder.

E.A.: Theory: C=72.64%; H=7.09%; N=11.17%;

Found: C=72.52%; H=7.33%; N=9.95%.

MS (FAB): 1815 [M⁺].

¹H NMR (THF-d₈): δ = 0.90, 1.15 [br, 36H, CH₃],
1.29 [br, 48H, CH₂], 2.12 [br, 6H, CH],
4.39 [br, 12H, OCH₂], 7.47 [s, 4H, H-25,
H-30, H-33, H-38], 7.70 [s,br, 2H, H-17],
7.79 [s,br, 2H, H-15], 7.89, 8.02, 8.25, 8.61
[br, 6H, H-10, H-8, H-9], 8.86, [br, d, 2H, H-1].



¹³C NMR (THF-d₈): δ = 11.9, 14.0, 14.6 [CH₃], 23.7, 24.1, 30.4, 30.6, 31.2, 32.0, 32.9 [CH₂], 40.8, 41.2, 42.2 [CH], 72.3, 72.7 [OCH₂], 105.9, 106.3, 107.0 [C-22, C-25, C-30], 122.6, 123.5, 123.7, 124.3, [C-1, C-8, C-9], 125.5 [C-15], 127.1 [C-17], 128.8, 129.7, 129.9 [C-2, C-7, C-10], 131.0 – 136.7 [C-3, C-6, C-11, C-14, C-16, C-18, C-21, C-26, C-29], 139.4, 140.2, 140.7, 142.0 [C-4, C-5, C-12, C-13, C-19, C-20, C-27, C-28], 151.6, 153.0, 153.9 [C-23, C-24, C-31].

UV/Vis (CH₂Cl₂): λ_{max} = 706.0, 676.0, 652.0, 432.5, 362.0 nm.

2.4.6. Binuclear metal free phthalocyanine 21

50 μmol **20** (90 mg) were dissolved in freshly dried THF. CF₃COOH (5ml) was added dropwise at room temperature in an argon atmosphere and this mixture was heated at 50°C for 5 hours. After cooling, 20 ml of H₂O was added dropwise to the reaction mixture. The formed precipitate was collected and washed several times with methanol. After drying in an oven overnight at 90°C the product was purified by column chromatography on silica gel, in which the eluent used to collect the first fraction (**21**) was dichloromethane. The second fraction (unreacted **20**) was eluted afterwards with a mixture dichloromethane–THF (10:1). Compound **21** was then reprecipitated from methanol/dichloromethane and dried in vacuum at 100°C.

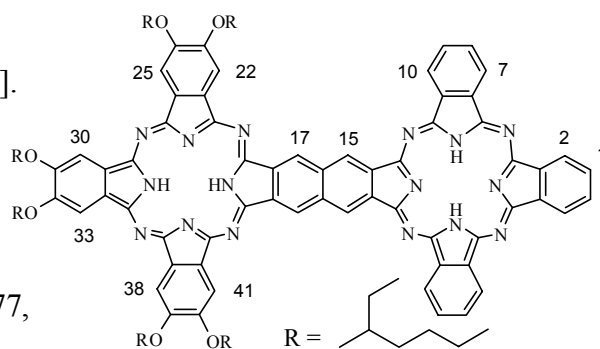
Yield: **21**, 70 mg, (65%), dark bluish-green powder

EA: Theory: C=71.79%; H=7.34%; N=10.28 %;

Found: C= 71.42 %; H= 7.20 %; N= 9.85 %.

MS (FAB): 1770 [M^+], 1346.1 [$M^+ - 4R + Na$],
1120.9 [$M^+ - 6R + Na$], 1006.6 [$M^+ - 6OR + Na$].

1H NMR (THF- d_8): δ = 0.86, [br, 36H, CH_3],
1.15 [br, 48H, CH_2], 2.28 [br, 6H, CH], 4.01,
4.11 [br, 12H, OCH_2], 6.81, 7.08, 7.34, 7.65, 7.77,
8.34 [br, PcH].



21

^{13}C NMR (THF- d_8): 11.1, 11.5, 13.8, 14.2 [CH_3], 22.7, 23.2, 24.2, 26.1, 29.3, 29.7, 30.8,
31.9 [CH_2], 39.8, 40.8, 45.7, 46.3, 47.3 [CH], 71.9 [OCH_2], 103.6, 104.5, 105.7, 108.3 [C-22,
C-25, C-30], 112.2 [C-15], 114.1 [C-17], 121.3, 121.7, 122.7, [C-1, C-8, C-9], 126.5, 127.5,
128.3, 129.3 [C-2, C-7, C-10], 132.5, 133.2, 134.2, 138.7, 139.5 [C-3, C-6, C-11, C-14, C-16,
C-18, C-21, C-26, C-29], 142.0—145.0 [C-4, C-5, C-12, C-13, C-19, C-20, C-27, C-28],
150.6, 151.6, 152.6, 154.4 [C-23, C-24, C-31].

IR (KBr): ν (cm^{-1}): 3298 (NH st), 1607 (NH δ), 801 (NH δ)

UV/Vis (CH_2Cl_2): λ_{max} = 688.0, 673.0, 667.0, 358.0 nm.

2.4.7. Binuclear In/In phthalocyanine 22

Binuclear Pc **21** (70 mg, 40 μ mol) and an excess $InCl_3$ (90 mg, 400 μ mol) were suspended in DMF. After adding 1 ml quinoline, the mixture was heated till 130°C and maintained at this temperature. After completion of the reaction (monitored by UV/Vis spectroscopy and thin-layer chromatography - ~ 4 hours) water was added dropwise to the mixture to precipitate the compound (20 ml). After centrifugation **22** was 3 times reprecipitated from hot methanol and dried in vacuum at 100°C.

Yield: **22**, 68 mg, (82%), dark green powder

EA: Theory: C=64.92%; H=6.05%; N=10.04%;

Found: C= 65.72%; H= 5.57 %; N= 9.19 %.

MS (FAB): 2060.5 [M^+], 1916.0 [$M^+ - OR - CH_3$]

¹H NMR (THF-d₈): δ = 0.87, 0.89, 1.29

[br, 36H, CH₃], 1.40, 1.60, [br, 48H, CH₂], 2.04

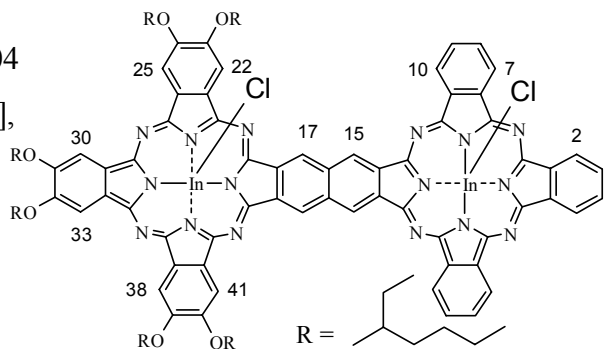
[br, 6H, CH], 4.01, 4.25, 4.50 [br, 12H, OCH₂],

6.91 [s, 4H, H-25, H-30, H-33, H-38], 7.17

[s,br, 2H, H-17], 7.28 [s,br, 2H, H-15], 7.40,

7.78, 7.82, 7.90, [br, 6H, H-10, H-8, H-9],

8.20, 8.24 [br, d, 2H, H-1]



22

¹³C NMR (THF-d₈): δ = 11.5, 11.7, 12.2, 14.6, 14.8 [CH₃], 21.4, 23.0, 23.5, 26.9, 27.7, 28.0, 30.3, 30.6, 32.8, 35.1 [CH₂], 40.0, 40.4, 40.7 [CH], 71.5, 72.2 [OCH₂], 104.9, 105.5, 106.4, 106.9 [C-22, C-25, C-30], 123.6, 123.9, 124.8, 125.9 [C-1, C-8, C-9], 127.5 [C-15], 128.2 [C-17], 128.8, 129.6, 129.9, 130.1, 130.9 [C-2, C-7, C-10], 133.0 – 138.2 [C-3, C-6, C-11, C-14, C-16, C-18, C-21, C-26, C-29], 140.7, 140.9, 142.0 [C-4, C-5, C-12, C-13, C-19, C-20, C-27, C-28], 152.0, 152.7, 153.5 [C-23, C-24, C-31].

IR (KBr): ν (cm⁻¹): 2958, 2927, 2858, 1602, 1494, 1457, 1383, 1276, 1202, 1098, 1049, 892, 740.7, 567.

UV/Vis (CH₂Cl₂): λ_{max} 724.0, 689.0, 663.0, 353.0 nm.

2.4.8. Binuclear Ga/Ga phthalocyanine 23

Binuclear Pc **21** (70 mg, 40 μmol) and an excess of GaCl₃ (90 mg, 500 μmol) were suspended in DMF. Quinoline (1 ml) of was added and the mixture was heated till 130°C and maintained at this temperature. After completion of the reaction (monitored by UV/Vis spectroscopy and thin-layer chromatography - ~ 5 hours) water (20 ml) was added dropwise to the mixture to precipitate the compound. After centrifugation **23** was 3 times reprecipitated from hot methanol and dried in vacuum at 100°C.

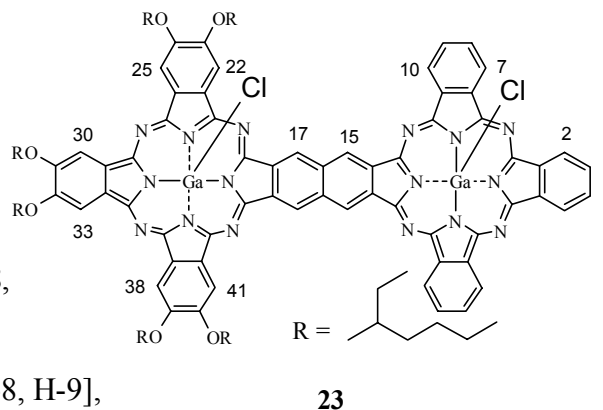
Yield: **23**, 63 mg, (79%), dark green powder

EA: Theory: C=66.84%; H=6.12%; N=10.34%;

Found: C= 66.02 %; H= 5.51 %; N= 9.19 %.

MS (FAB): 1975.7 [M⁺], 1478.2 [M⁺ - 4OR + Na], 1339.1 [M⁺ - 5OR]

¹H NMR (THF-d₈): δ = 0.90, 1.04, 1.17 1.30 [br, 36H, CH₃], 1.54, [br, 48H, CH₂], 2.04 [br, 6H, CH], 4.25, 4.52 [br, 12H, OCH₂], 7.55 [br, 2H, H-17], 7.68 [br, 2H, H-15], 8.13 [br, s, 6H, H-22, H-25, H-30, H-33, H-38, H-41], 8.92, 8.94 [br, d, 2H, H-2], 9.16, 9.19 [br, d, 2H, H-7], 9.42, 9.45 [br, d, 6H, H-1, H-8, H-9], 9.69, 9.71 [br, d, 2H, H-10].



¹³C NMR (THF-d₈): δ = 11.6, 11.9, 12.5, 14.4, 14.8 [CH₃], 23.4, 23.7, 24.1, 26.7, 30.3, 30.6, 31.5, 32.1, 32.9 [CH₂], 40.7, 41.0 [CH], 72.5, 72.7 [OCH₂], 104.2, 105.4, 105.8, 106.6 [C-22, C-25, C-30], 122.0, 123.4, 124.1, [C-1, C-8, C-9], 127.3 [C-15], 128.7 [C-17], 129.9, 130.2, 130.9, [C-2, C-7, C-10], 133.0 – 137.1 [C-3, C-6, C-11, C-14, C-16, C-18, C-21, C-26, C-29], 140.0-150.7 [C-4, C-5, C-12, C-13, C-19, C-20, C-27, C-28], 153.9, 154.6, 155.6 [C-23, C-24, C-31].

IR (KBr): ν (cm⁻¹): 2958, 2927, 2859, 1602, 1495, 1457, 1383, 1276, 1201, 1098, 1048, 892, 857, 740.7, 565.

UV/Vis (CH₂Cl₂): λ_{max} = 718.5, 687.5, 654.5, 344.0 nm.

2.5. Synthesis of In, Ga and Tl octa-substituted phthalocyanines

2.5.1. [2,3,9,10,16,17,24,25-octa-(2-ethylhexyloxy)] Mg phthalocyanine (24)

From step 2.4.1. the first fraction of the performed column previously described (page 80) was collected, the solvent evaporated, twice reprecipitated from methanol and dried in vacuum at 100°C to obtain **24**.

Yield: **24**, 0.75 g, (15%), green solid.

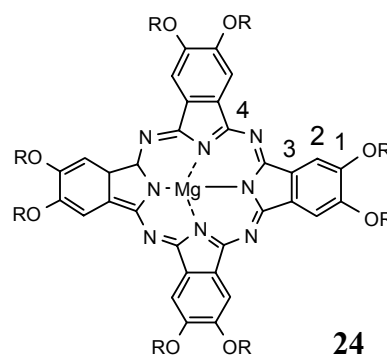
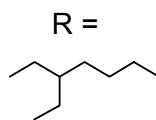
EA: Theory: C=71.13%; H=9.01%; N=7.16%;

Found: C= 70.30 %; H= 8.87 %; N= 7.02 %.

MS (FD): 1564.6 [M⁺], 1451.4 [M⁺-C₈H₁₆⁺].

¹H NMR (CDCl₃): δ = 0.89, 0.99 (br, 48 H, CH₃), 1.25-1.60 (br, 64 H, CH₂), 1.75 (br, 8 H, CH), 4.10 (br, 16 H, OCH₂), 8.50 (s, br, 8 H, H-2).

¹³C NMR (CDCl₃): δ = 11.1, 11.4, 14.0, 14.2 (C-CH₃), 23.0, 23.2, 24.2, 29.0, 29.3, 30.8 (C-CH₂), 39.3, 39.8 (C-CH), 72.2 (C-OCH₂), 105.6, 106.2 (br, C-2), 131.4 (br, C-3), 143.5-149.7 (C-4), 153.0 (br, C-1).



UV/Vis (CH₂Cl₂): λ_{max} = 679.0, 613.0, 360.0 nm.

2.5.2. 2,3,9,10,16,17,24,25-octa-(2-ethylhexyloxy)phthalocyanine (25)

Octa-(2-ethylhexyloxy)phthalocyaninato-magnesium (**24**) (308 mg, 200 μmol) was dissolved in 20 ml of anhydrous THF and 5 ml CF₃COOH were added to the solution. The mixture was stirred at 40°C for 6 hours. After cooling, distilled water (30 ml) was added, in order to precipitate the metal free phthalocyanine. Compound **25** was filtered, washed with aqueous methanol and dried in vacuum at 80°C.

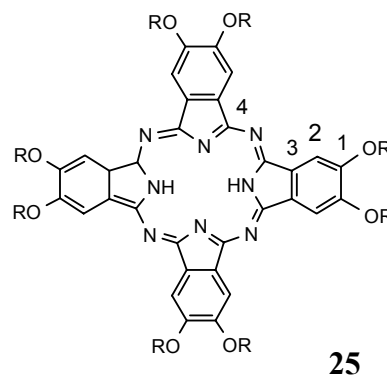
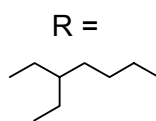
Yield: **25**, 254 mg, (82.5%) greenish-violet powder.

EA: Theory: C=74.96%; H=9.55%; N=7.27%;

Found: C= 75.19 %; H= 9.50%; N= 7.11 %.

MS (FD): 1540.2 [M⁺], 1426.7 [M⁺-C₈H₁₇].

¹H NMR (CDCl₃): δ = -0.57 (s, br, 2 H, H-NH), 0.76 (s, br, 48 H, CH₃), 1.13, 1.32, (br, 64 H, CH₂), 1.63, 2.07 (br, 8 H, CH), 4.15, 4.49 (br, 16 H, OCH₂), 9.15 (br, 8 H, H-2).



¹³C NMR (CDCl₃): δ = 11.1, 14.0 (C-CH₃), 22.9, 23.8, 29.0, 30.5 (C-CH₂), 39.5 (C-CH), 71.7 (C-OCH₂), 104.9, 105.3, 105.7 (br, C-2), 126.0, 127.3, 130.5, 130.7, 131.8 (br, C-3), 143.3, 148.6, 149.7, 150.3 (C-4), 152.6 (br, C-1).

IR (KBr): ν (cm⁻¹): 3297 (NH st), 2958, 2926, 2858, 1607 (NH δ), 1456, 1383, 1276, 1198, 1098, 1023, 856, 801 (NH δ), 746.

UV/Vis (CH₂Cl₂): λ_{max} = 700.0, 664.5, 604.5, 427.0, 346.0 nm.

2.5.3. [2,3,9,10,16,17,24,25-octa-(2-ethylhexyloxy)phthalocyaninato]indium(III)-chloride (26)

100 mg InCl₃ (0.45 mmol) and 140 mg **25** (0.090 mmol) were dissolved in 20 ml freshly distilled DMF (adding 5 ml anhydrous THF), stirred and boiled (145 °C) for 3 hours. After cooling, the product was precipitated upon a dropwise addition of water, filtered, washed through with aqueous methanol and dried in vacuum at 90°C to obtain **26**.

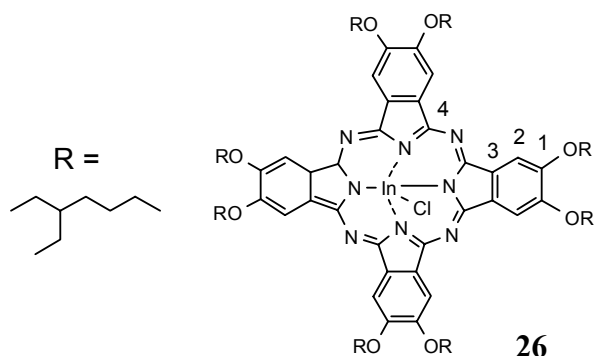
Yield: **26**, 132 mg, (88%), dark green powder.

EA: Theory: C=68.19%; H=8.55%; N=6.64%;

Found: C= 67.95 %; H= 8.50 %; N= 6.58 %.

MS (FD): 1686.1 [M⁺].

¹H NMR (THF-d₈): δ = 0.96 (s, br, 48 H, CH₃), 1.42, 1.63, (br, 64 H, CH₂), 1.97 (br, 8 H, CH), 4.36 (br, 16 H, OCH₂), 8.94 (br, 8 H, H-2).



¹³C NMR (THF-d₈): δ = 11.4, 14.1 (C-CH₃), 23.1, 24.1, 29.2, 30.8 (C-CH₂), 39.7 (C-CH), 72.2(C-OCH₂), 103.7, 105.4, 106.1 (br, C-2), 127.4, 129.8, 131 (br, C-3), 149.7, 150.3 152.8 (C-4), 154.2, 157.1(br, C-1).

UV/Vis (CH₂Cl₂): λ_{max} = 698.50, 671.5, 629.5, 446.0, 401.5, 362.5 nm.

2.5.5. [2,3,9,10,16,17,24,25-octa-(2-ethylhexyloxy)phthalocyaninato]gallium(III)-chloride 27

75 mg GaCl₃ (0.43 mmol) and 125 mg **25** (0.080 mmol) were dissolved in 15 ml freshly distilled DMF (adding 4 ml anhydrous THF), stirred and boiled (145 °C) for 3.5 hours.

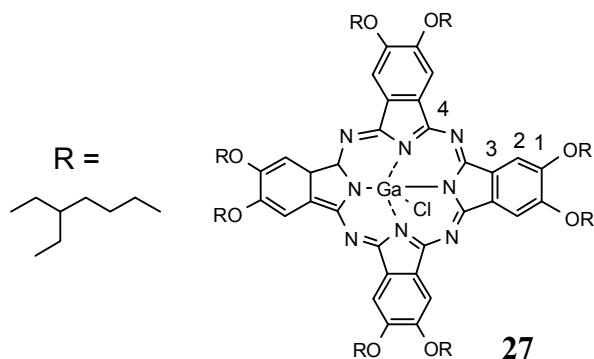
After cooling, the product was precipitated upon a dropwise addition of water, filtered, washed through with aqueous methanol and dried in vacuum at 90°C, obtaining **27**.

Yield: **27**, 80.4 mg, (62.5%), dark green powder.

EA: Theory: C=70.16%; H=8.83%; N=6.82%;

Found: C= 70.09 %; H= 8.84 %; N= 6.90 %.

MS (FD): 1642.0 [M⁺].



¹H NMR (THF-d₈): δ = 0.92 (s, br, 48 H,

CH₃), 1.33, 1.53 (br, 64 H, CH₂), 2.05

(br, 8 H, CH), 4.24, 4.39 (br, 16 H, OCH₂), 9.16 (br, 8 H, H-2).

¹³C NMR (CDCl₃): 11.1, 14.2 (C-CH₃), 23.0, 23.2, 29.0, 30.8 (C-CH₂), 39.3, 39.8 (C-CH), 72.0 (C-OCH₂), 105.6, 106.2 (br, C-2), 131.4 (br, C-3), 143.5-149.7 (C-4), 153.0 (br, C-1).

UV/Vis (CH₂Cl₂): λ_{max} = 694.5, 625.0, 441.0, 357.5 nm.

2.5.6. [2,3,9,10,16,17,24,25-octa-(2-ethylhexyloxy)phthalocyaninato]thallium(III)-trifluoroacetate (**28**)

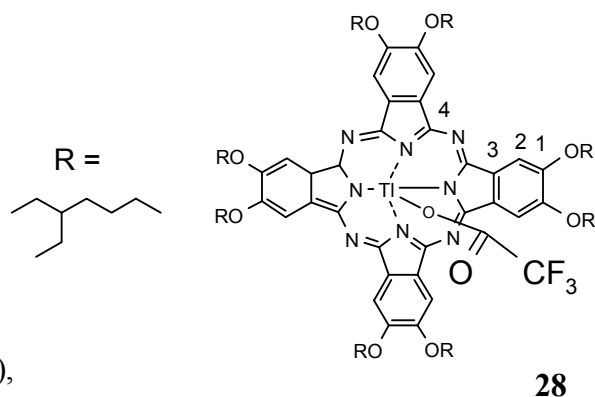
120 mg Tl(CF₃COO)₃ (0.2 mmol) and 125 mg **25** (0.080 mmol) were dissolved in 15 ml freshly distilled DMF (adding 4 ml quinoline), stirred and boiled (145 °C) for 6 hours. After cooling, the product was precipitated upon a dropwise addition of a 10% methanolic solution of NaOH, filtered, washed through several times with aqueous methanol and dried in vacuum at 70°C.

Yield: **28**, 100 mg, (60.0%), dark green powder.

EA: Theory: C=62.93%; H=6.82%; N=6.04%;

Found: C= 61.96 %; H= 5.65 %; N= 5.97 %.

MS (FD): 1855.6 [M⁺].



¹H NMR (THF-d₈): δ = 1.00 (s, br, 24 H, CH₃),

1.12 (s, br, 24 H, CH₃) 1.33, 1.49 (br, 64 H, CH₂),

1.98 (br, 8 H, CH), 4.48 (br, 16 H, OCH₂), 8.95 (br, 8 H, H-2).

¹³C NMR (THF-d₈): 12.2, 12.5, 15.0, 15.2 (C-CH₃), 24.7, 25.8, 30.7, 30.9, 32.2, 33.2 (C-CH₂), 41.4, 41.7 (C-CH), 73.0 (C-OCH₂), 107.0 (br, C-2), 135.2 (br, C-3), 143.5-149.7 (C-4), 151.3–153.8(br, C-1), 157.1 (C=O).

IR (KBr): ν (cm⁻¹): 2958, 2926, 2858, 1700 (C=O), 1601, 1455, 1376, 1268, 1199. 1041, 878, 842, 746 (C—F), 718 (C—F), 673.

UV/Vis (CH₂Cl₂): λ_{max} = 720.5, 647.5, 403.5, 364.5 nm.

V - Literature

- [1] Y.R. Shen, *The Principles of Nonlinear Optics*, John Wiley and Sons: New York, **1984**
- [2] B. Sheehy, L.F. Di Mauro, *Ann. Rev. Phys. Chem.*, **1996**, 47, 463
- [3] M. Hanack, H. Heckmann, R. Polley, in *Methoden der Organischen Chemie (Houben-Weyl)*, vol. E9d; 4th Ed.; Thieme Verlag :Stuttgart, **1997**
- [4] H. S. Nalwa, J. S. Shirk, in *Phthalocyanines, Properties and Applications* Eds: (C. C. Leznoff, A. B. P. Lever), VCH, New York, **1996**, vol. 4, pp 79-182, and cited therein
- [5] E. Orti, J. L. Bredas, C. Clarisse, *J. Chem. Phys.*, **1990**, 92, 1228
- [6] D. R. Coulter, A. Miskowski, J. W. Perry, T. Wei, E. W. van Stryland, D. J. Hagan, *SPIE Proc.*, **1989**, 1105, 42
- [7] L.W. Tutt, T.F. Boggess, *Progr. Quant. Electr.*, **1993**, 17, 299.
- [8] *Phthalocyanines, Properties and Applications*, (Eds: C. C. Leznoff, A. B. P. Lever), VCH, New York, **1989 – 1996**, vol 1–4
- [9] F. H. Moser, A. L. Thomas, *The Phthalocyanines*, CRC: Boca Raton, FL, **1983**
- [10] F. Baumann, B. Bienert, G. Rösch, H. Vollmann, W. Wolf, *Angew. Chem.*, **1956**, 68, 133
- [11] M. Hanack, M. Lang, *Adv. Mater.*, **1994**, 6, 819
- [12] M. Hanack, M. Lang, *Chemtracts*, **1995**, 8, 131
- [13] M. Hanack, A. Datz, R. Fay, K. Fischer, U. Kepeler, J. Koch, J. Metz, M. Metzger, O. Schneider, H.-J. Schulze, in *Handbook of Conducting Polymers*, vol 1 (Ed.: T. A. Skotheim) M. Dekker Inc., New York, **1986**, pp 133
- [14] H. Schultz, H. Lehman, M. Rein, M. Hanack, *Structure and Bonding* 74, Springer-Verlag, Heidelberg, **1991**, pp 41
- [15] U. Drechsler, M. Hanack, in *Comprehensive Supramolecular Chemistry*, J. L. Atwood, J. E. D. Davies, D. D. McNicol, F. Vögtle Eds., Pergamon: Oxford, **1996**, Vol 9, pp 283
- [16] J. F. van der Pol, E. Neelman, J. W. Zwikker, R. J. M. Nolte, W. Drenth, J. Aerts, R. Visser, S. J. Picken, *Liq. Cryst.*, **1989**, 6, 577;
- [17] J. Simon, C. Sirlin, *Pure Appl. Chem.*, **1989**, 61, 1625
- [18] M. K. Engel, P. Bassoul, L. Bossio, H. Lehmann, M. Hanack, J. Simon, *Liq. Cryst.*, **1993**, 15, 709
- [19] G. G. Roberts, M. C. Petty, S. Baker, M. T. Fowler, N. J. Thomas, *Thin Solid Films* **1985**, 132,113;

- [20] M. J. Cook, A. J. Dunn, F. M. Daniel, R. C. O. Hart, R. M. Richardson, S. J. Roser, *Thin Solid Films*, **1988**, 159, 395;
- [21] S. Palacin, P. Lesieur, I. Stefanelli, A. Barraud, *Thin Solid Films*, **1988**, 159, 83;
- [22] M. Burghard, M. Schmelzer, S. Roth, P. Haisch, M. Hanack, *Langmuir*, **1994**, 10, 4265
- [23] M. J. Cook, *J. Mater. Chem.*, **1996**, 6, 677
- [24] J. Simon, J.-J. André, in *Molecular Semiconductors*, J. M. Lehn, C. W. Rees, Eds., Springer: Berlin, **1985**, pp 73
- [25] P. Gregory, *High-Technology Applications of Organic Colorants*, Plenum: New York, **1991**, pp 59
- [26] S. Takano, T. Enokida, A. Kambata, *Chem. Lett.*, **1984**, 2037
- [27] R. O. Loutfy, C. K. Hsiao, A. M. Hor, G. J. Di Paola-Baranyl, *Imaging Sci.*, **1985**, 29, 148
- [28] K.-Y. Law, *Chem. Rev.*, **1993**, 93, 449
- [29] J. E. Kuder, *Imaging Sci.*, **1988**, 32, 51
- [30] S. Kobayashi, K. Iwasaki, H. Sasaki, S. Oh-Hara, M. Nishizawa, M. Katayose, *Jpn. J. Appl. Phys.*, **1991**, 30, 114
- [31] R. Ao, L. Kümmert, D. Haarer, *Adv. Mater.*, **1995**, 5, 495
- [32] D. Wöhrle, M. Shopova, S. Müller, A. D. Milev, V. N. Mantareva, K. K. Krastev, *J. Photochem. Photobiol. B*, **1993**, 21, 155
- [33] R. Bonnett, *Chem. Soc. Rev.*, **1995**, 95, 19
- [34] S. B. Brown, T. G. Truscott, *Chem. Ber.*, **1993**, 29, 955
- [35] A. B. P. Lever, M. R. Hempstead, C. C. Leznoff, W. Liu, M. Melnik, W. A. Nevin, P. Seymour, *Pure Appl. Chem.*, **1986**, 58, 1467
- [36] D. Schlettwein, M. Kaneko, A. Yamada, D. Wöhrle, N. I. Jaeger, *J. Phys. Chem.*, **1991**, 95, 1748;
- [37] D. Wöhrle, D. Meissner, *Adv. Mater.*, **1991**, 3, 129
- [38] A. Battenberg, V. F. Breidt, H. Vahrenkamp, *Sensor and Actuators B*, **1996**, 30, 29
- [39] R. A. Collins, K. A. Mohamed, *J. Phys. D*, **1988**, 21, 154;
- [40] T. A. Temofonte, K. F. Schoch, *J. Appl. Phys.*, **1989**, 65, 1350;
- [41] Y. Sadaoka, T. A. Jones, W. Göpel, *Sensors and Actuators B*, **1990**, 1, 148;
- [42] J. D. Wright, *Prog. Surf. Sci.*, **1989**, 31, 1
- [43] S. Dogo, J.-P. Germani, C. Maleysson, A. Pauly, *Thin Solid Films*, **1992**, 219, 244
- [44] S. Mukhopadhyay, C. A. Hogarth, S. C. Thorpe, M. J. Cook, *J. Mater. Sci., Mater. Electron*, **1994**, 5, 321

- [45] K.-D. Schierbaum, R. Zhou, S. Knecht, R. Dieing, M. Hanack, W. Göpel, *Sensors and Actuators B*, **1995**, 24/25, 69
- [46] T. J. Marks, *Science*, **1985**, 227, 881
- [47] T. J. Marks, *Angew. Chem. Int. Ed. Engl.*, **1990**, 29, 857
- [48] M. Kato, Y. Nishioka, K. Kaifu, K. Kawamura, S. Ohno, *Appl. Phys Lett.*, **1985**, 86, 196
- [49] M. K. Casstevens, M. Samoc, J. Pflieger, P. N. Prasad, *J. Chem. Phys.*, **1990**, 92, 2019
- [50] J. Simon, P. Bassoul, S. Norvez, *New J. Chem.*, **1989**, 13, 13
- [51] A. Braun, J. Tcherniac, *Ber. Dtsch. Chem. Ges.*, **1907**, 40, 2709
- [52] H. de Diesbach, E. von der Weid, *Helv. Chim. Acta*, **1927**, 10, 886
- [53] R. P. Linstead, *Br. Ass. Adv. Sci. Rep.*, **1933**, 465
- [54] R. P. Linstead, *J. Chem. Soc.*, **1934**, 1016
- [55] G. T. Byrne, R. P. Linstead, A. R. Lowe, *J. Chem. Soc.*, **1934**, 1017
- [56] R. P. Linstead, A. R. Lowe, *J. Chem. Soc.*, **1934**, 1022
- [57] C. E. Dent, R. P. Linstead, *J. Chem. Soc.*, **1934**, 1027
- [58] C. E. Dent, R. P. Linstead, R. Lowe, *J. Chem. Soc.*, **1934**, 1033
- [59] P. A. Barret, C. E. Dent, R. P. Linstead, *J. Chem. Soc.*, **1936**, 1719
- [60] P. A. Barret, D. A. Frye, R. P. Linstead, *J. Chem. Soc.*, 1938, 1157
- [61] J. S. Anderson, E. F. Bradbrook, A. H. Cook, R. P. Linstead, *J. Chem. Soc.*, **1938**, 1151
- [62] R. P. Linstead, *Ber. Dtsch. Chem. Ges. A*, **1939**, 72, 93
- [63] A. B. P. Lever, *Adv. Inorg. Radiochem.*, **1965**, 7, 27
- [64] a) M. Gouterman, G. H. Wagnière, L. C. Synder, *J. Mol. Spectrosc.*, **1963**, 11, 108
 b) C. Weiss, H. Kobayashi, M. Gouterman, *J. Mol. Spectrosc.*, **1965**, 16, 415
 c) A. J. McHugh, M. Gouterman, *Theor. Chim. Acta*, **1972**, 24, 346
- [65] C. C. Leznoff, in *Phthalocyanines, Properties and Applications*, (Eds: C. C. Leznoff, A. B. P. Lever), VCH, New York, **1989**, vol 1, pp1
- [66] W. Kalz, H. Homborg, H. Küppers, B. J. Kennedy, M. S. Murray, *Z. Naturforsch., Teil B*, **1984**, 39, 1478
- [67] B. J. Kennedy, K. S. Murray, P. R. Zwack, H. Homborg, W. Kalz, *Inorg. Chem.*, **1986**, 25, 2539
- [68] U. Kepeler, M. Hanack, *Chem. Ber.*, **1986**, 119, 3636
- [69] G. Pawlowski, M. Hanack, *Synthesis*, **1980**, 287
- [70] W. Eberhardt, M. Hanack, *Synthesis*, **1997**, 95
- [71] M. Sommerauer, C. Rager, M. Hanack, *J. Am. Chem. Soc.*, **1996**, 118, 10085

- [72] M. Hanack, G. Schmid, M. Sommerauer, *Angew. Chem.*, 1993, 105, 1540; Intl. Ed. Engl., **1993**, 32, 1422
- [73] G. Schmid, M. Sommerauer, M. Geyer, M. Hanack, in *Phthalocyanines, Properties and Applications*, (Eds: C. C. Leznoff, A. B. P. Lever), VCH, New York, **1996**, vol 4, pp1
- [74] a) N. Kobayashi, S. Nakajima, T. Osa, *Inorg. Chim. Acta*, 1993, 210, 131
 b) N. Kobayashi, in *Phthalocyanines, Properties and Applications*, (Eds: C. C. Leznoff, A. B. P. Lever), VCH, New York, **1993**, vol 2, pp97
- [75] a) E. Ortí, J. L. Brédas, in *Conjugated Polymeric Materials: Opportunities in Electronics, Optoelectronics and Molecular Electronics*; J. L. Brédas, R. R. Chance, Eds.; Kluwer Academic Publisher: The Netherlands, **1990**, pp 517;
 b) E. Ortí, M. C. Piqueras, R. Crespo, J. L. Brédas, *Chem. Mater.* **1990**, 2, 110;
 c) E. Ortí, J. L. Brédas, *J. Chem. Phys.* **1990**, 92, 1228;
 d) E. Ortí, J. L. Brédas., *J. Am. Chem. Soc.* **1992**, 114, 8669
 e) E. Ortí, R. Crespo, M. C. Piqueras, F. Tomás, *J. Mater. Chem.*, **1996**, 6, 1751
- [76] M. Hanack, G. Renz, J. Strähle, S. Schmid, *J. Org. Chem.*, **1991**, 56, 3501
- [77] P. A. Franken, A. E Hill, C. W. Peters, G. Weinreich, *Phys. Rev. Lett.*, **1961**, 7, 118
- [78] S. R. Vigil, in PhD Thesis, Washington State University, **2000**
- [79] P. A. Miles, *Appl. Opt.* **1994**, 33, 6965
- [80] T. Xia, D. J. Hagan, A. Dogariu, A. A. Said, and E. W. Van Stryland, *Appl. Opt.* **1997**, 36, 4110
- [81] b) P. Chen, I. V. Tomov, A. S. Dvornikov, M. Nakashima, J. F. Roach, D. M. Alabran, P. M. Rentzepis, *J. Phys. Chem.*, **1996**, 100, 1750
- [82] B. L. Justus, A. J. Campillo, A. L. Huston, *Opt. Lett.*, **1994**, 19, 673
- [83] J. Robertson, P. Milsom, J. Duignan, G. Bourhill, *Opt. Lett.*, **2000**, 25, 1258
- [84] K. Mansour, M. J. Soileau, E. W. Van Stryland, *J. Opt. Soc. Am. B*, **1992**, 9, 1100
- [85] K. M. Nashold, D. P. Walter, *J. Opt. Soc. Am. B*, **1995**, 12, 1228
- [86] B. P. Singh, P. N. Prasad, F. E. Karasz, *Polymer*, **1988**, 29, 1940
- [87] F. Kajzar, J. Messier, C. Rosilio, *J. Appl. Phys.*, **1986**, 60, 3040
- [88] K. D. Belfield, D. J. Hagan, E. W. Van Stryland, K. J. Schafer, R. A. Negres, *Org. Lett.*, **1999**, 1, 1575
- [89] M. A. Kramer, W. R. Tompkin, R. W. Boyd, *Phys. Rev. A*, **1986**, 34, 2026
- [90] J. S. Shirk, R. G. S. Pong, S. R. Flom, H. Heckmann, M. Hanack, *J. Phys. Chem. A*, **2000**, 104, 1438

- [91] a) F. Z. Henari, J. Callaghan, W. J. Blau, P. Haisch, M. Hanack. *Pure Appl. Opt.* 1997, 6, 741
 b) H. S. Nalwa, A. Kakuta *Thin Sol. Films* **1995**, 254, 218
 c) H. S. Nalwa, M. Hanack, G. Pawlowski, M. K. Engel *Chem. Phys.* **1999**, 245, 17
 d) D. Schlettwein, D. Wöhrle, E. Karmann, U. Melville *Chem. Mater.* **1994**, 6, 3
 e) J. S. Shirk, R. G. S. Pong, F. J. Bartoli, A.W. Snow *Appl. Phys. Lett.* **1993**, 63, 1880
 f) J. S. Shirk, R. G. S. Pong, S. R. Flom, F. J. Bartoli, M. E. Boyle, A. W. Snow *Pure Appl. Opt.* **1996**, 5, 701
 g) J. S. Shirk, J. R. Lindle, F. J. Bartoli, Z. H. Kafafi *Int. J. Nonlinear Opt.* **1992**, 1, 699
 h) J. S. Shirk, J. R. Linde, F. J. Bartoli, Z. H. Kafafi, A. W. Snow in *Materials for Nonlinear Optics – Chemical Perspectives* (Eds : S. R. Marder, J. E. Sohn, G. D. Stucky), ACS Symposium series 455 **1991**, 626
- [92] a) M. Hanack, T. Schneider, M. Barthel, J. S. Shirk, S. R. Flom, R. G. S. Pong, *Coord. Chem. Rev.* **2001**, 219-221, 235
 b) J.W. Perry in *Nonlinear Optics of Organic Molecules and Polymers* (H.S. Nalwa; S. Miyata Eds.), CRC Press: Boca Raton (FL), **1997**, p 813
 c) M. Barthel, D. Dini, S. Vagin, M. Hanack *Eur. J. Org. Chem.* **2002**, 3756
- [93] a) M. Barthel, M. Hanack, *J. Porphyrines Phthalocyanines* **2000**,4, 635
 b) G. De la Torre, P. Vásquez, F. Agulló-López, T. Torres *J. Mat. Chem.* **1998**, 8, 1671
- [94] a) C. Claessens, W. Blau, M. Cook, M. Hanack, R. Nolte, T. Torres, D. Wöhrle *Monatsh. f. Chemie* **2001**, 132(1), 3
 b) M. Hanack *Abstracts of Papers, 222nd ACS National Meeting*, Chicago, IL, United States, August 26-30, **2001**, POLY-006.
- [95] D. Dini, M. Barthel, M. Hanack, *Eur. J. Org. Chem.*, **2001**, 3759; and references cited therein.
- [96] M. Hanack, D. Dini, M. Barthel, S. Vagin, *Chem. Record*, **2002**, 2(3), 129
- [97] Y. Chen, L.R. Subramanian, M. Fujitsuka, O. Ito, S. O’Flaherty, W.J. Blau, T. Schneider, D. Dini, M. Hanack, *Chem. Eur. J.* **2002**, 8, 4248
- [98] Y. Chen, S. O’Flaherty, M. Fujitsuka, M. Hanack, L. R. Subramanian, O. Ito, W. J. Blau, *Chem. Mater.* **2002**, 14(12), 5163
- [99] S. M. O’Flaherty, S. V. Hold, M. J. Cook, T. Torres, Y. Chen, M. Hanack, W. J. Blau, *Adv. Mat.* **2003**, 15(1), 19
- [100] S. Vagin, M. Barthel, D. Dini, M. Hanack, *Inorg. Chem.* **2003**, 42, 2683

- [101] D. Dini, M. Hanack, Physical Properties of Phthalocyanine-based Materials, *The Porphyrin Handbook*, vol 17, 107, 1 (Eds.: K. A. Kadish, K. M. Smith, R. Guilard) Academic Press, New York, **2003**
- [102] Y. Chen, S. O'Flaherty, M. Fujitsuka, L.R. Subramanian, O. Ito, W.J Blau, M. Hanack, *Adv. Mat.*, **2003**; *15* (11), 899
- [103] G. Y. Yang, M. Hanack, Y. W. Lee, M. K. Y. Lee, D. Dini, *Chem. Eur. J.* **2003**, *9*(12), 2758
- [104] M. Hanack, D. Dini, M. Barthel, S Vagin, *Adv. Col. Sci. Tech.* **2003**, *6*(2), 47
- [105] S. Vagin, M. Hanack, *Eur. J. Org. Chem.* **2003**, (14), 2661
- [106] D. Dini, G. Y. Yang, M. Hanack, *J. Chem. Phys.* **2003**, *119*, 9, 4857
- [107] C. G. Claessens, A. Gouloumis, M. Barthel, Y. Chen, G. Martin, F. Agullo-Lopez, I. Ledoux-Rak, J. Zyss, M. Hanack, T. Torres, *J. Porphyrins Phthalocyanines* **2003**, *7*(4 & 5), 291
- [108] Y. Chen, M. Hanack, D. Dini, M. Fujitsuka, O. Ito, *J. Mat. Chem.* **2003**, *13*(10), 2405
- [109] a) K.P. Unnikrishnan, J. Thomas, V.P.N. Nampoori, C.P.G. Vallabhan, *Opt. Comm.* **2003**, *217*, 269
- b) C.R. Mendonca, L.Gaffo, L. Misoguti, W.C. Moreira, O.N. Oliveira, S.C. Zilio, *Chem. Phys. Lett.* **2000**, *323*, 300
- c) T.C.Wen, I.D. Lian, I. D. *Synth. Met.* **1996**, *83*, 111
- d) E.S. Manas, F.C. Spano, L.X. Chen, *J. Chem. Phys.* **1997**, *107*, 707-719.
- e) X. Wang, C.-L. Liu, Q.-H. Gong, Y.-Y. Huanh, C.-H. Huang, J.-Z. Jiang, *Appl. Phys. A* **2002**, 497.
- f) J.S. Shirk, J.R. Lindle, F.J. Bartoli, M.E. Boyle *J. Phys. Chem.* **1992**, *96*, 5847.
- g) R. Philip, M. Ravikanth, G. Ravindra Kumar, *Opt. Comm.* **1999**, *165*, 91
- h) Y. Chen, M. Barthel, M. Seiler, L.R. Subramanian, S. Vagin, M. Hanack, *Angew. Chem.* **2002**, *114*, 3373; *Angew. Chem. Int. Ed.* **2002**, *41*, 3239
- [110] T. Schneider, H. Heckmann, M. Barthel, M. Hanack, *Eur. J. Org. Chem.*, **2001**, 3055
- [111] a) G. Assanto, *J. Mod. Opt.*, **1990**, *37*, 855
- b) J. F. Reintjes, in *Nonlinear Optic Parametric Processes in Liquids and Gases*, Academic Press: New York, **1984**, pp 327
- [112] *Optical Phase Conjugation* (Ed.: R. A. Fischer), Academic Press: New York, **1984**
- [113] R. C. Lind, D. G. Steel, G. J. Dunning, *Opt. Eng.*, **1982**, *21*, 190
- [114] A. Yariv, *IEEE J. Quant. Electr.*, **1978**, QE-14, 650
- [115] B. F. Levine, C. G. Bethea, *Appl. Phys. Lett.*, **1974**, *24*, 445

- [116] E. W. van Stryland, M. Sheik-Bahae, A. A. Said, D. J. Hagan, *Prog. Cryst. Growth Charact.*, **1993**, 27, 279
- [117] M. Sheik-Bahae, A. A. Said, T. Wei, D. J. Hagan, E. W. Van Stryland, *IEEE J. Quantum Electron.*, **1990**, 26, 760.
- [118] M. Sheik-Bahae, A. A. Said, D. J. Hagan and E. W. Van Stryland, *Opt. Lett.*, **1989**, 14, 955
- [119] L. Yang, R. Dorsinville, Q. Z. Wang, P. X. Ye, R. R. Alfano, R. Zamboli and C. Taliani, *Opt. Lett.*, **1992**, 17, 323.
- [120] M. Calvete, M. Hanack, *Eur. J. Org. Chem.*, **2003**, 2080
- [121] C. Rager, G. Schmid, M. Hanack, *Chem. Eur. J.* **1999**, 5, 280
- [122] M. J. Stillman, T. Nyokong, *Phthalocyanines, Properties and Applications*, vol. 1 (Eds.: C. C. Leznoff; A. B. P. Lever), VCH, New York, **1989**
- [123] G. Torre, M. V. Martinez-Diaz, P. R. Ashton, T. Torres, *J. Org. Chem.* **1998**, 63, 8888
- [124] G. Torre, M. V. Martinez-Diaz, T. Torres, *J. Porphyrins Phthalocyanines*, **1999**, 3, 560
- [125] M. J. Cook, M. J. Heeney, *Chem Commun.* **2000**, 969
- [126] a) R. Jung, K.-H. Schweikart, M. Hanack, *Synth. Met.* **2000**, 111, 453
 b) R. Jung, K.-H. Schweikart, M. Hanack, *Eur. J. Org. Chem.* **1999**, 11, 646
- [127] B. Behnisch, P. Martinez-Ruiz, K.-H. Schweikart, M. Hanack, *Eur. J. Org. Chem.* **2000**, 14, 2541
- [128] N. Kobayashi, *Coord. Chem. Rev.* **2002**, 227, 129
- [129] J. Yang, M. R. van de Mark, *Tetrahedron Lett.* **1993**, 34, 5223
- [130] D. Lelièvre, L. Bosio, J. Simon, J.-J. Andre, F. Bensebaa, *J. Am. Chem. Soc.* **1992**, 114, 4475
- [131] C. C. Leznoff, H. Lam, S. M. Marcuccio, W. A. Nevin, P. Janda, N. Kobayashi, A. B. P. Lever, *J. Chem Soc. Chem. Commun.* **1987**, 699
- [132] D. Lelièvre, O. Damette, J. Simon, *J. Chem. Soc. Chem. Commun.* **1993**, 939
- [133] N. Kobayashi, A. Muranaka, V. Nemykin, *Tetrahedron Lett.* **2001**, 42, 913
- [134] E. M. Garcia-Frutos, F. Fernández-Lázaro, E. M. Maya, P. Vásquez, T. Torres, *J. Org. Chem.* **2000**, 65, 6841
- [135] B. Hauschel, R. Jung, M. Hanack, *Eur. J. Inorg. Chem.* **1999**, 693; and references cited therein
- [136] N. McKeown, I. Chambrier, M. Cook, *J. Chem. Soc. Perkin Trans.*, **1990**, 1, 1169
- [137] R. Jung, PhD Thesis, Univ. Tübingen, Germany **2000**
- [138] R. Jung, M. Hanack, *Synthesis*, **2001**, 9, 1386

- [139] P. Haisch, M. Hanack, *Synthesis*, **1995**, 1251
- [140] A. M. Schaffer, M. Gouterman, *Theor. Chim. Acta* 1972, 25, 62
- [141] A. M. Schaffer, M. Gouterman, E. R. Davidson *Theor. Chim. Acta* 1973, 30, 9
- [142] M. Slavin, *Chemical Analysis, Atomic Absorption Spectroscopy*, vol. 25 (Eds.: P. J. Elving, J. D. Winefordner, I. M. Kolthoff) John Wiley & Sons, New York, **1979**
- [143] a) *Encyclopedia of Analytical Science*, vol. 1 (Ed.: A. Townshend) Academic Press, London, **1995**; c) *Encyclopedia of Analytical Chemistry, Applications, Theory and Instrumentation*, vol. 11 (Ed.: R. A. Meyers) RamTech Ltd, Tarzana, CA, U.S.A., John Wiley & Sons, New York, **2000**
- [144] S. Vagin, M. Hanack, *Eur. J. Org. Chem.* **2002**, 2859;
- [145] A. W. Snow, Phthalocyanine aggregation, *The Porphyrin Handbook*, vol 17, 109, p.129 (Eds.: K. A. Kadish, K. M. Smith, R. Guilard) Academic Press, New York, **2003**
- [146] M Drobizhev, A. Karotki, M. Kruk, N. Zh. Mamardashvili, A. Rebane, *Chem. Phys. Lett.* **2002**, 361, 54
- [147] A. B. P. Lever, S. R. Pickens, P. C. Minor, S. Licoccia, B. S. Ramaswamy, K. Magnell, *J. Am. Chem. Soc.* **1981**, 103, 6800
- [148] P. J. Hood, B. P. Edmonds, P. G. MacLean, D. M. Brandelik, *Proc. SPIE-Int. Soc. Opt. Eng.* **1994**, 2229, 91
- [149] P. D. Huffman, J. P. Fitzgerald, J. S. Shirk, *Abstracts of Papers, 223rd ACS National Meeting*, **2002**
- [150] N. B. McKeown, I. Chambrier, M. J. Cook, *J. Chem. Soc. Perk. Trans. 1*, **1990**, 1169
- [151] P. Brochard, V. Grolier-Mazza, R. Cabanel, *J. Opt. Sci. Am. B* **1997**, 14, 405
- [152] D. Dini, G. Y. Yang, J. Wei, M. Hanack, unpublished results

Meine akademischen Lehrer waren die Professoren und Dozenten:

Maria José Almeida, Luís Arnaut, Fernando Bernardo, Hugh Burrows, Correia Cardoso, M. Graça Carvalho, J. Caridade Costa, M. Margarida Costa, Ana Paula Egas, M. Ermelinda Eusébio, Abel Ferreira, Sebastião Formosinho, Fernando Garcia, A. M. Rocha Gonçalves, M. Hanack, G. Häfelinger, M. Luisa Leitão, R. Fausto Lourenço, Décio Martins, T. Pinho e Melo, J. Sérgio Melo, M. Graça Miguel, A. Canelas Pais, Carlos Paliteiro, M. Miguéns Pereira, M. Graça Rasteiro, J. S. Redinha, Jorge Rocha, M. Elisa Serra, M. Isilda Silva, Abilio Sobral, J. Strähle, A. J. Varandas, K.-P. Zeller

Lebenslauf

Persönliche Daten

Name Mario Calvete
geboren am 24. Juli 1975 in Figueira da Foz, Portugal
Eltern José Calvete und Rosa Freitas
Familienstand ledig

Schule

1981 - 1985 Grundschule in Paiao-Figueira da Foz
1985 - 1990 Gymnasium in Paiao-Figueira da Foz
1990 - 1993 Gymnasium in Figueira da Foz, spezifisch Uni Bewerbung

Studium

10/1993 - 11/2000 Studium der Industriellen Chemie an der Universidade de Coimbra
02/2000 Monographie unter der Anleitung von Prof. Dr. *cat.* S. Formosinho mit dem Thema: "Use of co-incineration methods for solid waste treatment-advantages and disadvantages"
09/1999 - 11/2000 Diplomarbeit unter der Anleitung von Dra M. Isilda Silva am Departamento de Química da Faculdade de Ciências e Tecnologia da Universidade de Coimbra mit dem Thema : "Photodegradation of organochloro-compounds using ruthenium catalysts"

Promotion

02/2001 - 01/2004 Anfertigung der vorliegenden Arbeit unter Anleitung von Prof. Dr. Dr. h. c. M. Hanack am Institut für Organische Chemie der Universität Tübingen, Deutschland